SURROGATE BRIDGE FREEZING SENSORS

by

SRDJAN JANKOVIC

Bachelor of Science

University of Belgrade

Belgrade, Yugoslavia

1996

Submitted to the Faculty of the
Graduate College of the
Oklahoma State University
in partial fulfillment of
the requirements for
the Degree of
MASTER OF SCIENCE
December, 2000

SURROGATE BRIDGE FREEZING

SENSORS

Thesis Approved:

Thesis Adviser

Dean of the Graduate College

ACKNOWLEDGEMENTS

This thesis is the result of a team effort, which includes the combined talents of many great people. A combination of humbleness and pride are behind my expression of gratitude and appreciation to those who merit special recognition.

Foremost, my utmost appreciation goes to my Committee Chairman and Adviser, Dr. Jeffrey D. Spitler for his intellectual prowess, guidance, encouragement, assistance, friendship, and above all, unending patience throughout my graduate program. I consider it a privilege to have worked under your supervision. Thank you for providing me with this research opportunity and generous financial support. I also wish to thank Oklahoma Department of Transportation and the Federal Highway Administration for funding this project.

I also extend appreciation to my other committee members, Dr. David G. Lilley and Dr. Daniel E. Fisher for valuable suggestions regarding this work. I convey my sincere gratitude to those who provided suggestions and assistance during the early stages of this study including Dr. R.L. Dougherty and Dr. R.L. Lowery. I gratefully acknowledge the contributions of my fellow students, Dustin Hamill and Rajesh Hedge, for their help in the system design and their time spent at the field experimental sites under "the worst weather conditions imaginable".

Perhaps the greatest importance has been the love, support and patience of family and friends back home. I would like to thank my parents, Sinisa and Varvara Jankovic,

and my brother Stevan, for their continued support and patience throughout my life that has enabled me to be where I am.

Thanks are extended to my friends here for their constant understanding and patience. Especially, I want to recognize Amer Celjo and Senad Divanovic, for their encouragement and friendship every step of the way. Also, thanks to Zeljko Nikolic for his support, much needed help, and most of all, friendship.

Finally, I want to thank all faculty members and staff of the School of Mechanical and Aerospace Engineering for their empathy and support.

TABLE OF CONTENTS

LIST OF TABLES

LIST OF FIGURES

CHAPTER I

INTRODUCTION

1.1 Background

For a long time it has been known that many accidents on high-speed highways occur as a result of motorists encountering situations and conditions that they had not anticipated. In recognition of this problem, state and federal transportation authorities have tried to aid motorists by the use of signing and warning lights. Some hazards may arise as a product of certain environmental conditions. A good example of such conditions is preferential icing of bridge decks and highway overpasses. As a result, motorists may find themselves unprepared for the slippery bridge surface. Often times motorists may be traveling at a rate that does not allow them to regain control of their vehicle, once lost due to icy conditions.

Frost, ice and snow on a bridge deck accumulates faster than on the roadway due to the fact that the surface is not in contact with the ground, thus it has significantly less thermal mass. If a fast transition from warm to colder weather occurs, the temperature of the bridge will decrease faster than that of the ground since there is not as much "stored energy" to dampen sudden temperature change on the surface. In addition, the bridge

deck loses heat more rapidly then the roadway because it is exposed to the atmosphere on both the top and bottom surfaces. Conditions when the bridge deck freezes before the rest of the roadway are referred to as "preferential icing".

One of the most common and widespread techniques used to warn motorists of such situations is the use of traffic signs, stating the possibility of a hazardous condition which may occur (for example, "Watch for ice on bridge"). In some states, a passing maintenance crew or a highway patrolman activates the signs. However, the main disadvantage of static traffic signs is that a vast majority of the time, the conditions they describe do not exist. A driver still must determine on his own when warning is meaningful, and thus they do not encourage cautious behavior (drivers are "conditioned" to ignore the warnings).

Maintenance crews can use deicing chemicals to significantly reduce the frequency of frozen bridge decks. This reduces the number of accidents, but there are two major problems associated with the use of deicing chemicals. The first is that the least expensive and most commonly used chemicals (i.e. salt) have an adverse effect on the bridge structure itself, reducing the life of the bridge. Secondly, the effectiveness of deicing chemicals is limited since they cannot prevent icing below a certain temperature. The first problem suggests that chemical treatment should be as infrequent as possible. This requires accurate prediction of a hazardous situation for chemical application. Maintenance crews are forced to take a somewhat conservative approach and apply chemicals more often than absolutely necessary. The main drawback of extra treatments is that they increase expenses in both labor and materials and necessitate bridge deck replacement in a shorter time period.

Over the years, awareness of these problems initiated the development of the "Smart Bridge"- an informal name arising from the automatic nature of its control system (Chiasson and Spitler, 2000). The goal is to develop a bridge deck heating system to eliminate preferential icing. This system is hydronic, and makes use of a ground source heat pump system, which recovers energy stored in the ground to heat the fluid that circulates throughout tubes embedded in the bridge deck. It is automatically controlled and uses local and remote weather stations to forecast potential icing conditions. The geothermal smart bridge project is expected to improve both safety, by eliminating hazardous icing conditions, and bridge deck life, by eliminating the application of deicing chemicals. In addition, significant savings can be made when there are no expenses for maintenance crew and materials.

In order to develop the "smart" control system, some data are necessary to "train" stochastic control algorithms, such as neural networks. These data should provide information regarding the occurrence of icing on bridge decks. Since operating bridge decks are not allowed to freeze, it was deemed necessary to develop a surrogate for an actual bridge deck.

The objectives of this study are to (1) develop the surrogate bridge freezing sensors, i.e. reasonably inexpensive instrumented concrete slabs that can determine whether or not the surrogate surface is dry, wet, ice-coated, frost-coated, or snow-coated, and (2) to provide training data for the advanced control strategies as a part of automatic nature of the smart bridge project.

1.2. Literature Survey

Detection of ice and snow is a topic that has generated a lot of interest among different department of transportation agencies, aviation industry, HVAC&R industry and researchers in recent decades. Consequently, this has lead to a number of ideas for ice sensors presented in various publications. This survey will concentrate on the commercial sensors, their principles of operation and efficacy during various testing procedures reported in technical papers and interim reports.

Brinkman (1977) suggested that the most obvious way to recognize dry, wet or icing conditions is to observe and measure some physical property that is distinct in behavior for different conditions of the surface. Most likely it is necessary to measure more than one property to differentiate among dry, wet or frozen surfaces.

Some of the properties used to detect different conditions are electrical conductivity, electrical capacitance, vibration frequency, humidity, surface and air temperature, and electrical voltage.

Prediction of preferential ice formation based on data obtained as weather characteristics, such as humidity and air temperature have been unsuccessful because weather changes occur suddenly, going from freezing to nonfreezing and vice versa quickly. An additional problem is the influence of deicing chemicals and traffic, which cannot be easily accounted for.

In the past decades, ice detection devices have been developed for two major applications:(1) sensors for ice detection on aircrafts, and (2) sensors for ice detection on the pavement surface.

1.2.1. Aircraft Ice Sensors

1.2.1.1. Pruzan (1993)

Pruzan (1993) reported an experimental study on an ice detector that is based on the principle that electrical capacitance changes as the ice layer increases. The sensor itself is a probe that must be placed in areas of the airframe of an aircraft where ice is most likely to form.

The ice detector design described in the NASA Langley patent, # 4,766,369 consists of three major parts, a Type 1 and Type 2 capacitance electrodes and a thermistor probe as shown in Figure 1-1. The Type 1 electrodes have fingers with gaps between them, being sensitive only to very thin layers of ice, while, the Type 2 electrodes are simple metal plates that can response to ice thickness of a broader range. The geometry of capacitance electrodes is such that the voltage output should be proportional to the ice thickness, regardless of ice temperature and composition. The temperature sensor is used to determine whether the increase in the capacitance sensor signal is due to ice or water on the sensors.

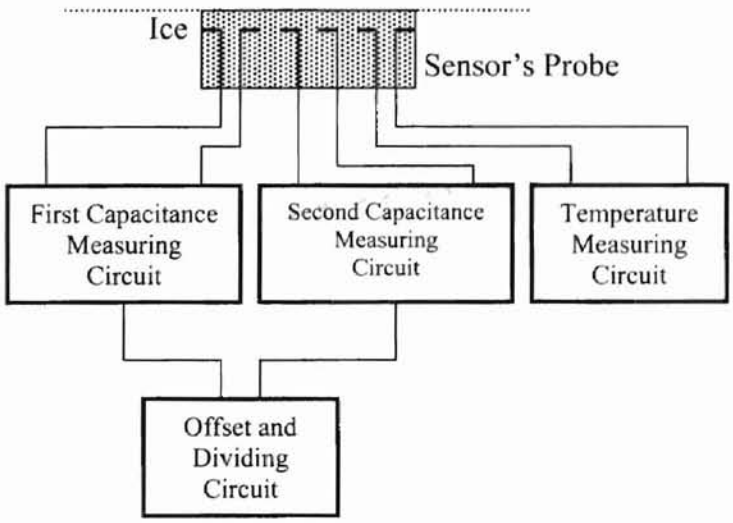

Figure 1-1. Capacitance Ice Sensor Configuration (NASA Patent #4,766,369)

The capacitance sensor is based on the electromagnetic relationship between two flat plates separated by a dielectric, described by the following equation,

$$C = \frac{\varepsilon \cdot A}{t} \tag{1-1}$$

where,

C = system capacitance, [F]

ε = permittivity of the dielectric material, [F/m]

A = surface area of the electrodes, [m^2]

t = gap between two electrodes, [m]

As can be seen, the capacitance over electrodes is directly proportional to the dielectric constant of the medium between the electrodes. The dielectric constant of ice is different from that of water, both of which are different from the dielectric constant of air. As ice or water accumulates over the sensor, the capacitance increases relative to the average thickness of the accumulating layer. To determine the sensors' behavior, a laboratory analysis was conducted, and repeated several times. The change in capacitance per dielectric used in experiment versus ice layer increase is shown in Figure 1-2.

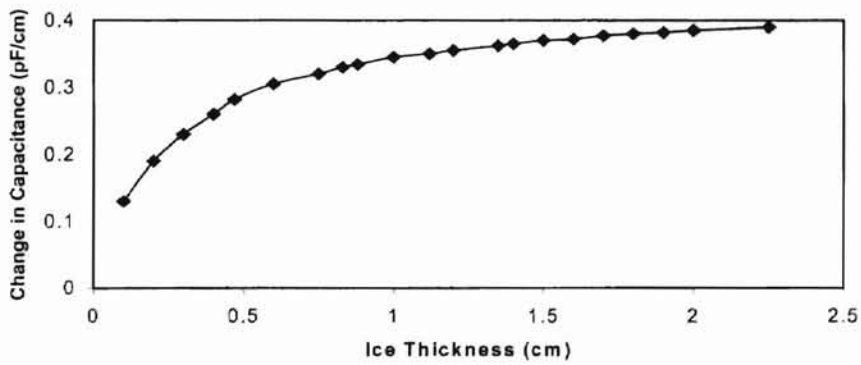

Figure 1-2. Response of the Sensor as Ice Thickness Increases (Pruzan, 1993)

These sensors were not tested with frost formation nor with snow-coating, thus no information whatsoever was obtained from this report on two weather characteristics that are of a great interest in this project.

1.2.1.2. Feely (1994)

Feely (1994) described primary ice detection sensor developed by Rosemount Aerospace, Inc. The system can detect icing conditions on the surface of an aircraft during flight.

The sensor consists of an ultrasonic vibrating probe that uses the response to a vibration input to estimate actual ice accretions. The probe is an axially vibrating, magnetostrictive cylinder coupled to a rigid diaphragm. The diaphragm is driven magnetostrictively to vibrate at its resonant frequency well into the ultrasonic range. The adhesive properties of ice produce an effect on the probe's vibration different of that produced by some other media, such as water or oil. Accordingly, icing signals are generated only by presence of ice.

As ice collects on the probe, the added mass stiffens the diaphragm and causes the vibrational frequency to decrease. When the value of frequency corresponds to a certain amount of ice, the sensor is deiced by internal heating elements. The deiced probe cools swiftly, and it is ready to sense ice presence again. The cycle process is repeated as long as detector is exposed to an icy surrounding. An example with the reference point of 0.02 in. of ice thickness for a repeated cycle is given in Figure 1-3.

The study with this sensor was never expanded to investigate possibility of detecting different surface conditions except icy ones.

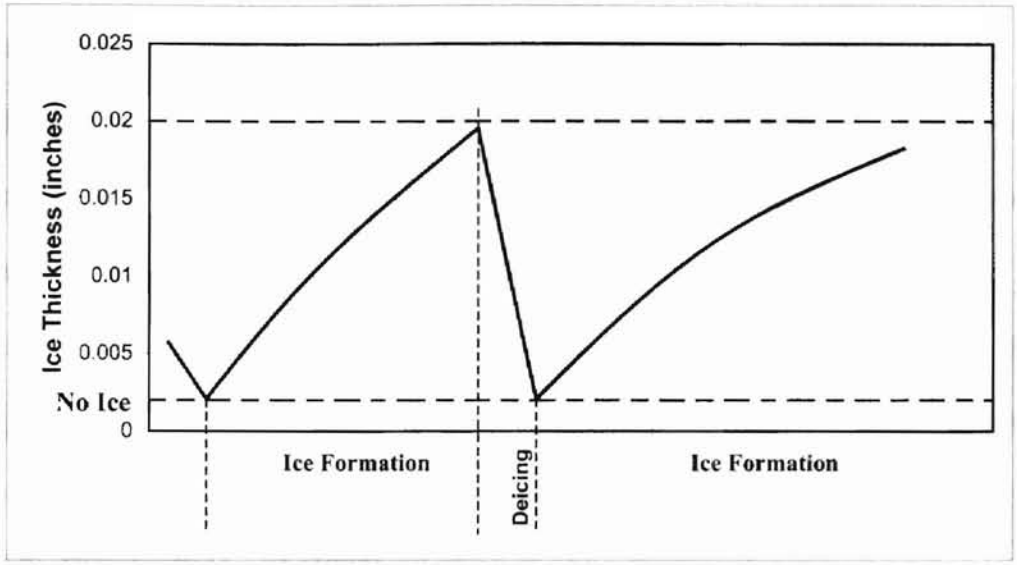

Figure 1-3. Cycle Counting System Operation (Feely, 1994)

1.2.1.3. Ringer and Stallabrass (1978)

Ringer and Stallabrass (1978) described application of an electro-optical sensing system as a part for ice detection on a helicopter. The sensor itself uses the voltage output from the electro-optical sensing system in order to detect ice presence. The voltage output is proportional to the accumulated ice thickness. The system is also capable of detecting the presence of water using the same principle.

1.2.2. Pavement and Road Surface Ice Detection Sensors

1.2.2.1. Finkele (1997)

Finkele (1997) discussed a road surface classification concept based on a bistatic, fully polarimetric millimeter-wave sensor. It is designed to analyze the change in polarization of an electromagnetic wave that is reflected from a road surface, allowing

detection of different surface conditions. Depolarization is primarily a consequence of two surface parameters, the dielectric constant of the surface material, and the surface roughness. For testing purposes, an asphalt road was scanned by the millimeter-wave sensor in the dry condition, and after the icing of a thin water film. As expected, the projections of the polarization of the reflected waves due to dry and icy surface conditions were different. However, with moderate surface icing, the polarization hardly changes, and thus the distinction between a bare, dry road surface, and ice-coated one creates a major problem for a millimeter-wave sensor.

1.2.2.2. Ciamberlini, et al (1995)

Ciamberlini, et al. (1995) described an optoelectronic system suitable for road surface tests. The detector system is based on the different scattering properties of road in different conditions. The experimental version of the system consisted of a 20mW continuous infrared wave semiconductor laser, a solid-state photodetector and a multimeter (Figure 1-4).

The laser illuminates a 5mm diameter spot on the sample surface. A photodiode measures the angular distribution of scattered light reflected from the examined surface. The detector optics were installed in such a way that only the reflectance pattern from the inspected surface can be observed. Both the photodiode and the laser are mounted on a semicircular structure, placed in the plane perpendicular to the tested surface. The asphalt road samples were placed on the table driven by remotely controlled motors.

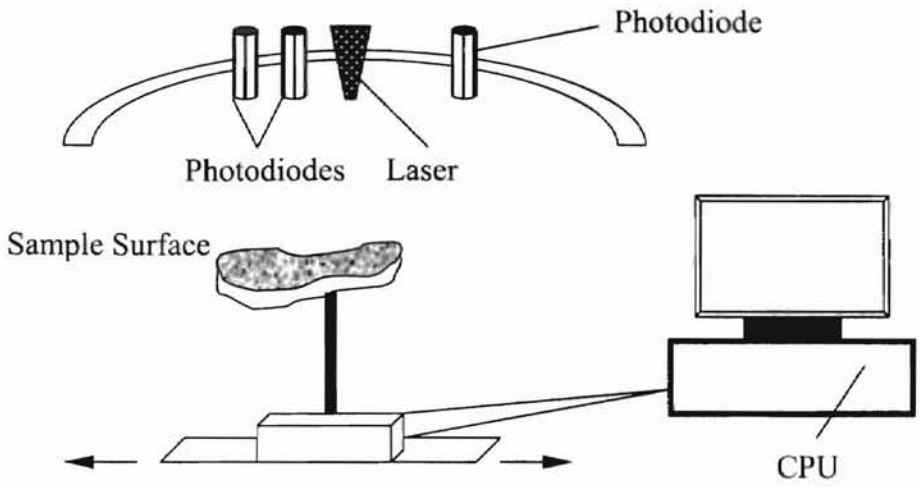

Figure 1-4. Experimental Version of the System (Ciamberlini, et al.1995)

During the experiment the angle of incidence of the laser beam was varied. Output voltage was measured on detector's side for different surface conditions and different positions of the photosensors with the fixed angle of the light source.

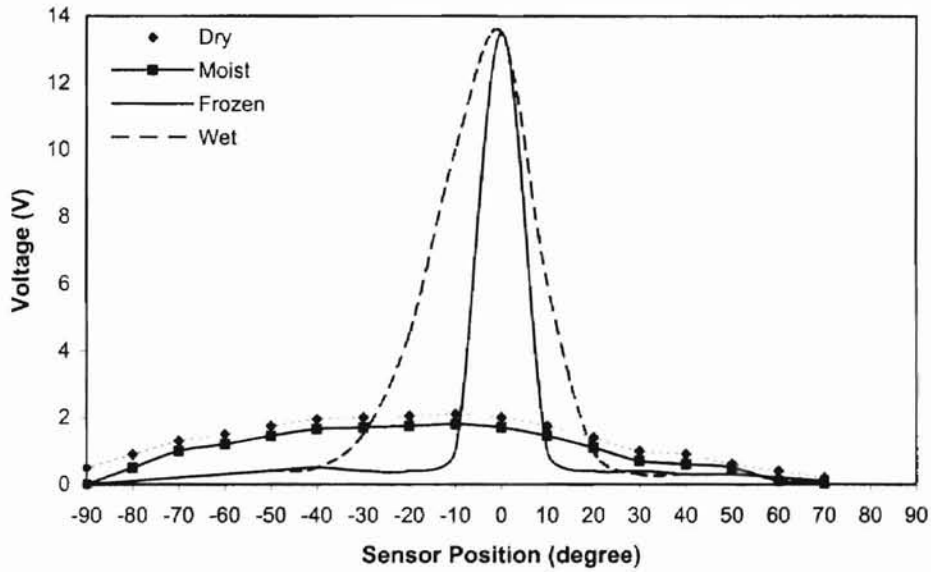

Figure 1-5. Photodiode Output Voltage vs. Angular Photosensor Position

(Ciamberlini, et al.1995)

Figure 1-5 represents one set of scans, and shows the photosensor output patterns for the four different surface conditions. The best results in determining surface condition were obtained for the sensor positioned between –40 to 40 degrees. Due to the roughness of the inspected surface, results for the same angular position of the sensor but in different direction (positive or negative) does not exactly match. The detection of water or ice on the surface involves the reflection effect, where surface under both conditions behaves as a highly specular. Three photodiodes were set at different reflection angles (Figure 1-4). Ratio was taken between the output from three photodiodes in order to obtain data related to asphalt surface conditions. Results for four distinct surface conditions are shown in Table 1-1.

Table 1-1. Values of Output Ratios for Different Surface States, With Angular Position of Photodiodes at 100°, 110° and 120°, Respectively

Surface Condition	**Out_1/Out_2**	**Out_1/Out_3**	**Out_2/Out_3**
Dry	1.0	1.5	1.4
Moist	1.2	3.3	2.8
Wet	30	65	2.2
Frozen	4.5	46	10

With the ratio method an instantaneous measurement of surface conditions is obtained, and different values correspond to different conditions on inspected surface.

1.2.2.3. Besant, et al. (1994)

Besant, et al. (1994) presented a method of frost thickness measurement using a laser beam. The physical nature of frost formation makes the measurement of its thickness very difficult. Due to its crystalline structure, frost on a surface is rough, readily breakable in the outer region, but tough near the surface where its density is close to that of ice.

The experimental apparatus consisted of a 5mW helium-neon laser as a beam source, a light attenuating filter and a precision light meter. The laser beam was directed in such way that it passes parallel to the frosted surface in so that part of the beam is occluded by the frost crystals. Frost on the surface scattered the laser beam into wide irregular bend. Light intensity of the reflected laser beam was measured and with accretions of crystalline frost different values had been read. This procedure required very precise calibration in order to obtain good results.

1.2.2.4. Ciemochowski (1969)

One of the most typical ice detectors for highway use is a conductivity/temperature device. Ciemochowski (1969) explained the design of such a sensor manufactured by Holley Carburetor Co. The basic unit consists of two deck probes for moisture and surface temperature detection, a relative humidity sensor, an air temperature sensor, and an electronic control unit. The system was initially designed for two modes of operation, namely (1) the anticipatory mode that predicts frost formation and initiates an "early warning" signal, and (2) ice detection mode where the deck sensors detect frozen precipitation and initiate an "ice" output. In this installation the

early warning device was a flashing amber light mounted on the top of the electric warning signs that flash a "Bridge Icy Ahead" signal to the motorist.

Theoretically, if the bridge deck temperature is at or below the dew point temperature of the air, condensation of water vapor will occur. If the surface temperature is at or below 0°C, frost crystals will form. The dew point temperature (the equivalent of 85% relative humidity) used as a reference for the anticipatory part of the system was assumed to be 2°C below the ambient temperature. However, the basis of this assumption remains unclear.

To anticipate frost formation, the system needs three inputs, with the following levels:

1. Bridge deck temperature of 0°C or lower
2. Temperature differential between bridge surface and ambient air of at least 2° C, and
3. High relative humidity (>85%)

To detect ice formation two inputs signals are combined in the control unit:

1. Bridge deck temperature of 0° C or below, and
2. Conductive imbalance between two surface probes.

The conductive imbalance is obtained by using two deck moisture sensors. Physically the sensors are concentric stainless steel cylinders, forming an outer and an inner electrode, with a small gap between them. Imbedded in one sensor is thermistor-controlled heating element. The sensor relies on the difference in electrical conductivity between water and ice. Ice has a low electrical conductivity, while water has a high one. Since one sensor is not heated, if the temperature is below freezing point, ice forms

between electrodes resulting in a low electrical conductivity. Any precipitation on the heated sensor will be maintained as, or converted to water, resulting in high conductance. When a conductive imbalance is sensed and surface temperature is below 0° C, the control unit will activate warning signal for ice. If deicing chemicals are used, conductive balance is restored, and ice output will turn off. A system schematic is given in Figure 1-6.

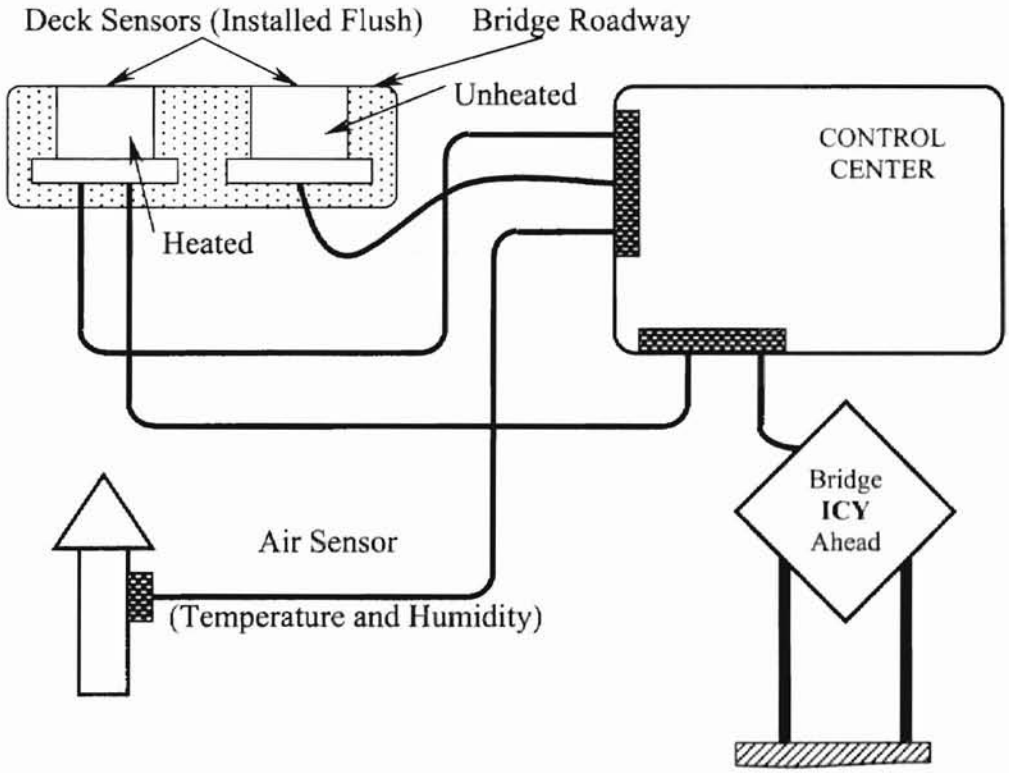

Figure 1-6. Schematic Diagram of the System (Ciemochowski, 1969)

Snow precipitation is recognized by the system in the same way as ice. However, treatment of the bridge deck with deicing chemicals can cause unreliability in ice detection, because when the salt content is increased, ice may have the same electrical

conductivity as liquid water. Later, an improved system was proposed, where the change in AC impedance was measured on both electrodes in order to detect presence of deicing chemicals.

1.2.2.5. Mawhinney and McCone (1974)

Mawhinney and McCone (1974) reported activity to evaluate reliability of commercially available snow and ice detection systems. For the evaluation, five different detection systems were chosen, based upon four different principles of operation: electrical conductance, capacitance, spectral temperature and latent heat of fusion. The first two principles have been previously explained.

Systems using latent heat of fusion detect frost and ice by applying a thermal pulse to a witness plate, and noticing a delay in temperature change due to the absorption of latent heat of melting.

The device based on a radiometer measures spectral temperature at 1.6cm wavelength. Spectral temperature is the product of actual temperature and surface emissivity. For dry pavement the surface emissivity is around 0.8, that of water 0.1, and that of ice around 0.4, thus different spectral temperatures should be obtained for different surface conditions.

Final detector selection for evaluation included the conductivity/temperature sensor, capacitance sensor and one that uses latent heat of fusion. The two other sensors were not chosen because the unit price was found to be excessively high and beyond the funds available. Site selection for testing purposes needed to fulfill some basic requirements: (a) high frequency of ice, snow, and frost, (b) moderate traffic flow, (c) moderate maintenance by snow removal crew, and (d) reasonable accessibility. The

bridge that corresponded to these requirements was on State Highway 89N, in Truckee, California.

Two sets of each of the three different types of sensors were installed flush with the surface in the bridge deck. Evaluation was conducted in winter 1974, and the detector performance was most disappointing. One of the detectors that used the latent heat of fusion failed immediately due to malfunction in one of its components. The capacitance sensor did not faithfully track the bridge deck conditions. The conductivity/temperature sensor proved to be most reliable, but it was changed a few times during the winter due to mechanical damage caused by tire chains. This unit showed the best overall performance, with reliability of 80% to be in accord with the following formula:

Reliability Percentage=100 - (number of detector errors)·100/(number of "slippery" conditions) (1-2)

The conductivity/temperature sensor occasionally gave a false positive alarm for frost. Namely, the alarm came on too early as the conditions approached those necessary for frost formation.

In general, the conclusions they reached were that (1) different surface conditions could be detected, (2) reliability of prediction was unsatisfactory and (3) a moderate, but not exhaustive, effort has been made to design reasonably inexpensive sensors that can distinctly determine whether or not the bridge is dry, wet, frozen or snow-coated. The shortcomings of their studies are summarized as follows:

- Sensors were able to determine whether or not surface is frozen, but significant difference of sensors' operation under snow, ice, frost and moisture was never outlined and investigated.
- With the exception of Ciemochowski (1969) design, which was later proved in Mawhinney and McCone (1974) report, the majority of highway sensors failed to show satisfactory operation over longer periods during winter season.
- Price range for the systems mentioned above varied from $1,600 to $25,000.

Systematic and quantitative experiments are required to develop sensor that can give desirable response for the successful surface condition detection. The variety of distinct surface conditions detected, as shown in previous studies, had not been accounted for in a single device.

1.3. Research Objectives

Many accidents on highway bridges and overpasses are caused by unexpected road conditions. This has created demand for prediction of hazardous conditions. Although research in this field has been intensified over the past few decades, it is far from complete. The objectives are outlined to provide the role of this present study and its anticipated contributions to this area.

The research objectives are as follows:

1) Design and test surrogate bridge freezing sensors

2) Fabricate between three to five surrogate bridge freezing sensors, i.e. instrumented concrete slabs, that are reasonably inexpensive and relatively simple. They should be able to determine whether or not slab's surface is dry, wet, icy, frost-coated or snow-coated. The sensors will be designed in such manner that they can be deployed at locations around the state of Oklahoma.

3) Develop of suitable data acquisition system.

4) Install surrogate bridge freezing sensors at Mesonet weather station sites, at different locations throughout the state. Sensors will not be connected to Mesonet.

5) Monitor surrogate bridge freezing sensors over several winters.

6) Provide training data for the development of advanced control strategies for stochastic control algorithms as a part of "smart" control system.

As specified above, we will hopefully extend our current knowledge and experience on bridge deck conditions prediction, thus increasing our ability to address some of the questions in this area.

Chapter 2 will provide information on the optical sensor initially used for the experiment. Also, results will be presented that will show why the optical sensor did not meet requirements for this project. A new approach was considered, where a temperature/resistance sensor was introduced. Chapter 3 will explain the principles behind the system, its design and development. Experimental results of the laboratory tests and field tests are given in Chapter 4. Conclusions and recommendations for future work on this subject are given in Chapter 5.

CHAPTER II

OPTICAL SENSOR

For the initial experiments, an infrared optical sensor was chosen because of its simplicity and very low price. The sensor projects a beam of infrared light onto the object, hitting one specific point called the reference point. The detector is a phototransistor. The output signal is a voltage and it changes depending on the intensity of reflected infrared light, and/or deviation from the targeted spot position on the detector's side. If the transmitter moves closer to or farther from the reference point, the spot position of the reflected light on the detector changes (Figure 2-1, Holzwarth, 1993). Therefore an ice buildup might be expected to make the distance between transmitter and inspected surface shorter, resulting in different voltage output, than that of a dry surface. Also, the scattered pattern of the infrared beam is different for different materials and surface conditions, which results in change of the reflectance of projected light even if the transmitter's position does not change. Therefore the difference between dry and wet conditions might be detected. The transmitter is a source of infrared light, and, physically, the detector is a phototransistor.

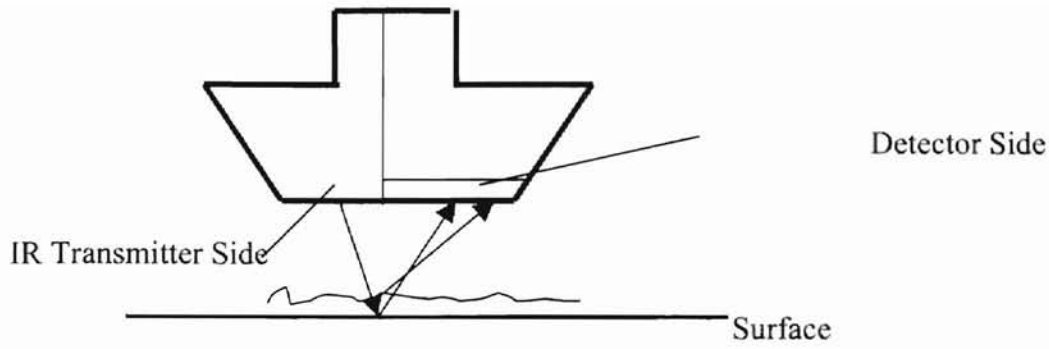

Figure 2-1. Infrared Beam Sensor

2.1 Measurements With Infrared Sensor Under Laboratory Conditions

The sensor was an "Optek Technologies, Inc." product, type Reflective Object Sensor-OPB701. The operating temperature range for this model is from -40°C to 100°C. The electric circuit used for the lab measurements is shown in Figure 2-2. The output voltage will be measured, for different surface conditions. Photodiodes were connected to the wires and enclosed in the plastic housing. On the emitter's side the red wire goes to the positive of the power supply, while the black wire goes to the negative of the power supply. For the detector's side, the white wire was connected to the positive of the power supply, while the green wire was attached to the negative of the power supply. An AC to DC voltage converter is used as a power source. Output DC voltage from the source can vary from 0 to 30 VDC.

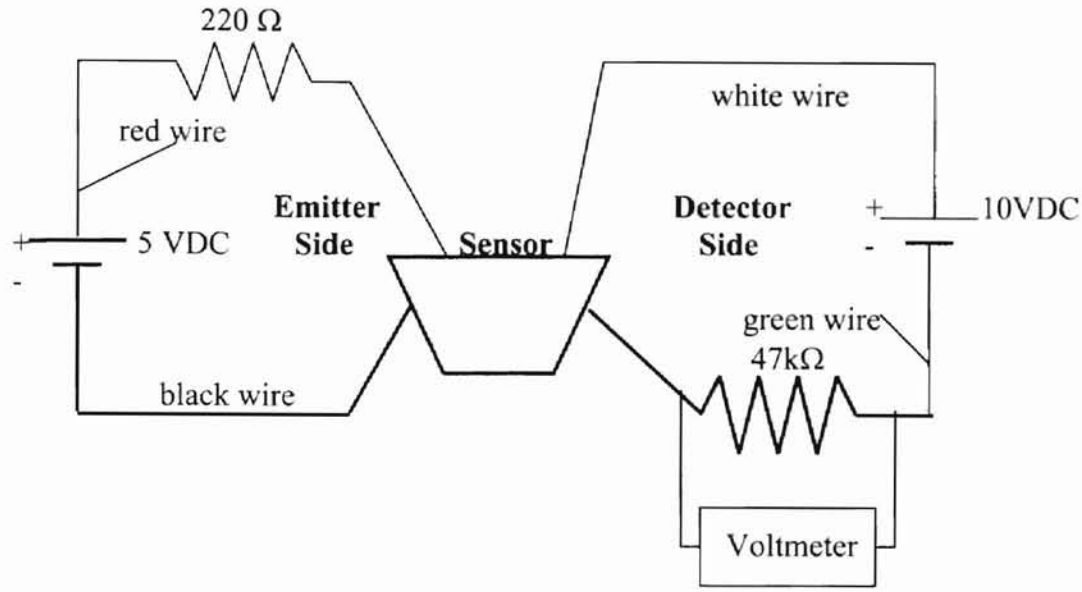

Figure 2-2. Electric Circuit

2.1.1. Moisture Detection Experiments

The goal of these experiments is to see whether moisture can be detected on a particular surface by application of this sensor.

First, the infrared beam was directed onto dry surface. The most common materials that are in use to cover bridge decks are asphalt and concrete. Thus, concrete and asphalt were used in this experiment. The sensor was mounted above surface at the approximate distance of 5mm. Both, dry concrete and asphalt surfaces were exposed to the infrared beams (Figure 2-3). More than one point on the examined surfaces was irradiated, since both surfaces were very rough. The output results did not change only with the different materials, but also differed with the distance of sensor from inspected surface. The results for the dry conditions are shown in the second column of Table 2-1.

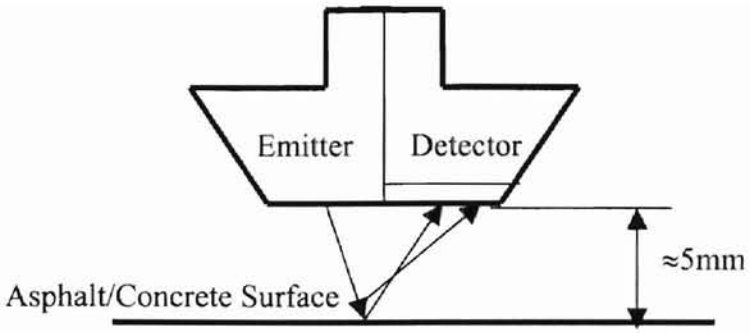

Figure 2-3. Experimental Setting for the Dry Surface Measurements

In the second part of experiment, both pieces, one by one, were placed in a transparent plastic water container. The surfaces were sprayed with water, and water layer was increased to approximately 2mm in thickness over each surface. Results for the initially wetted surfaces, the surfaces with 1mm of water, the surfaces with 2mm of water and the dry surfaces are seen in Table 2-1.

Measurements were recorded over several hours and the output response was randomly noted. As it can be seen both surfaces had a significant difference in the output response. Also, for the same surface, difference in the output value exists when it is dry or wet. This means that the presence of moisture can be detected on certain surfaces using this device.

Table 2-1. Output Voltage in Detection of Moisture Presence on the Surface

	Condition			
Material	Dry	Wet	1 mm of Water Over Surface	2 mm of Water Over Surface
Concrete	1.29 to 1.45 Vdc	0.92 to 1.03 Vdc	0.74 to 0.83 Vdc	0.52 to 0.59 Vdc
Asphalt	0.49 to 0.57 Vdc	0.17 to 0.26 Vdc	0.79 to 0.93 Vdc	0.37 to 0.42 Vdc

2.1.2. Ice Detection Experiments

The third part of the experiment was intended to show whether or not there is change in the reflectance during phase change from water to ice. The same conditions were present as in part two of the experiment but with the water in the container being frozen. Samples of concrete and asphalt were placed in the plastic container in such manner that water layer above surfaces is approximately (due to roughness of the surfaces) 1 mm in thickness. The container was exposed to a temperature of –10°C causing the water to freeze. After the freezing process the sample is obtained for the experiment that has a layer (1 mm) of ice above the concrete and asphalt sample.

First, an infrared beam was directed at the ice layer over the asphalt surface, then over the concrete surface. The output voltage obtained was in the range of 0.29 to 0.41 VDC for the ice over the asphalt surface. In the second case, output was in the range of 0.53 to 0.59 VDC.

If we compare these results with those of the previous experiment conducted over the water layer it can be deduced that the formation of ice layers over both surfaces can be detected. It must be emphasized that these results are obtained under well maintained laboratory conditions. However, the question remains whether or not similar results can be obtained outdoors.

Based on the experimental results, the formation of ice over asphalt and concrete surfaces will cause the output voltage to decrease, when compared to dry conditions. A dry rough surface scatters light in a diffuse way. An increasing quantity of ice over surface scatters light in a more specular way, and changes the reflectance to being more and more specular. If a water or ice layer is present over the surface the light reflected is

superposed of light scattered diffusely from the asphalt or concrete surface and of light reflected at the surface of the ice layer or the water film (Holzwarth, 1993).

Further investigation was done to conduct measurements over a thick layer of ice. For the entire test, the sensor was kept at a 5mm distance from the ice surface. If we freeze a container with water in order to obtain ice of approximately 7 mm in thickness over both the asphalt and concrete surfaces, the output response will range from 0.47 to 0.60 VDC. For an ice thickness of 10mm, the output voltage will increase and it will be in the range of 0.80 to 1.12 VDC. As the ice layer thickness increases, surfaces become less diffusely reflective, resulting in the change of output response. The output voltage for different conditions mentioned above is shown in Table 2-2.

Table 2-2. Output Voltage for Comparison of Moisture and Ice Presence

Condition on the Surface/Thickness	**Output Voltage (VDC)**
Asphalt- ice layer (1mm)	0.29-0.41
Asphalt- water layer (1mm)	0.43-0.51
Concrete- ice layer (1mm)	0.53-0.59
Concrete- water layer (1mm)	0.63-0.78
Concrete/Asphalt- ice layer (7mm)	0.47-0.60
Concrete/Asphalt- ice layer (10mm)	0.80-1.12

In both cases, change in phase can be detected due to significant change in the output response. As can be seen from Figure 2-4, different surface conditions give separable voltage responses: 1) dry surface with voltage being in the range from 1.2 to 1.4 VDC, 2) wet surface with voltage ranges from 0.8 to 1.0 VDC and 3) icy surface with voltage values ranging from 0.6 to 0.7 VDC. The data were obtained as a sequence of scans from the data logger with the scanning interval of 20 minutes.

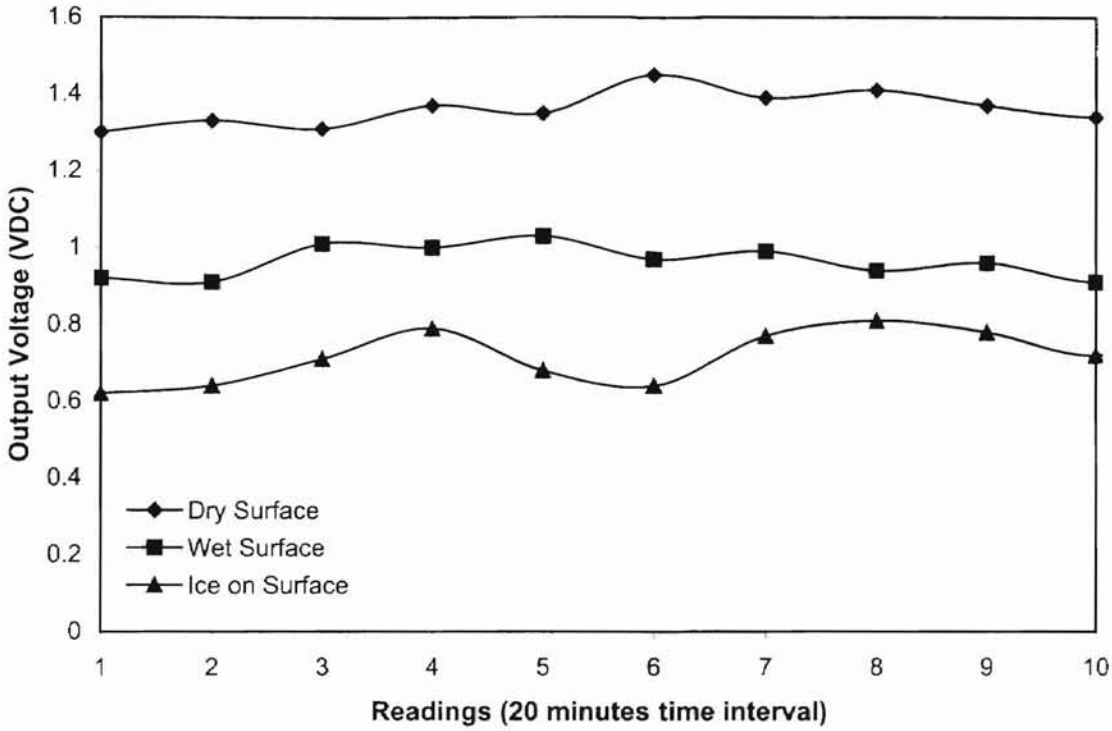

Figure 2-4. Output Response for Different Surface Conditions of Concrete Sample

2.1.3. Frost Detection Experiments

In the first part of the experiment, a sample of concrete was placed on a four-pound block of dry ice. In order to maintain the temperature of the concrete and prevent the evaporation of the dry ice, both were placed in the thermally insulated chamber, with the storage size of the chamber being approximately 60x60x60 cm. In order to increase convective heat transfer, the chamber was supplied with an adjustable-speed fan (Figure 2-5.).

The sample was left in the chamber for a certain period of time in order to adjust its temperature to the temperature of the dry ice below. An infrared sensor is placed above the ice layer at the approximate distance of 5mm.

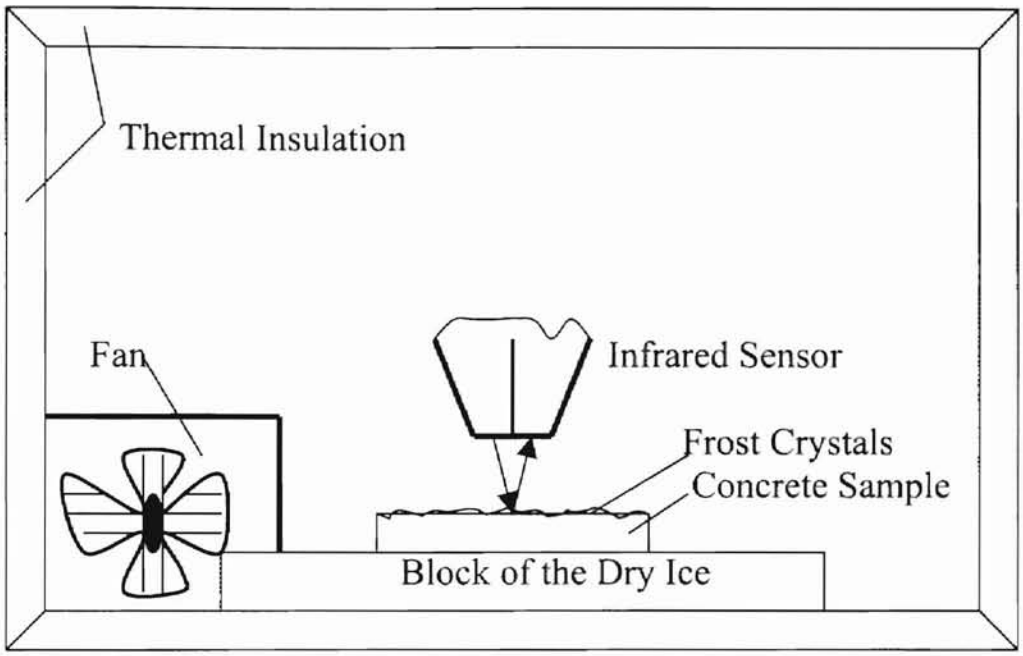

Figure 2-5. Apparatus and Experiment Sample Setting

The general idea of simulating frost formation on the surface was to spray a mist over the surface that would result in giving the surrounding air with a high relative humidity. This will cause surface to become wet due to condensation of the moisture from the ambient air. Since water is exposed to the low temperature of the surface, the droplets will freeze and become frost crystals. The experiment showed that the wet surface does not change phase instantly, but gradually over a period of 3 to 4 seconds. For the second part of the experiment conditions are maintained but the asphalt sample is used instead of concrete. Measurements are repeated several times, and recorded for both materials.

During the process the output voltage was monitored. For the concrete sample results are shown in Table 2-3, including results previously observed for the ice on the

surface. Temperature variation for examined concrete sample varied from -11.7 to -12.2°C.

Table 2-3. Frost Formation Over the Concrete Surface Compared to Different Surface Conditions

Condition on the Concrete Surface	Range of the Output Results (VDC)
Dry-precooled	1.30-1.40
Wet	0.95-1.07
Frost	1.17-1.20
Ice	0.60-0.78

The variation found in the results is due to the roughness of the surface as well as the size variations of the frost crystals throughout the surface. As can be seen for the different conditions, an infrared sensor can detect forming of ice and frost. However, several limitations must be taken into consideration. These are as follows:

- Since this detector is very sensitive to change in distance from the observed sample, the examined surface must be fairly flat.
- All results are obtained in well maintained laboratory conditions, which means that if this sensor should be applied outdoors, under natural conditions, it must be protected from "mechanical influences" such as dirt, dust, strong rain, etc.

The following section describes system behavior during in-situ measurements.

2.2. In-Situ Measurements With Infrared Sensor

Here the sensor itself was mounted above the concrete slab (approximately 2' in diameter, 8" thick). The circuitry is similar as previously shown, where AC to DC transformer is used, connected to an AC power supply. Transformer has an adjustable, stable voltage range, thus there is no need for voltage regulator. Input voltages of the emitter and detector were set to be 6 VDC and 9 VDC respectively. The sensor arrangement is shown in Figure 2-6.

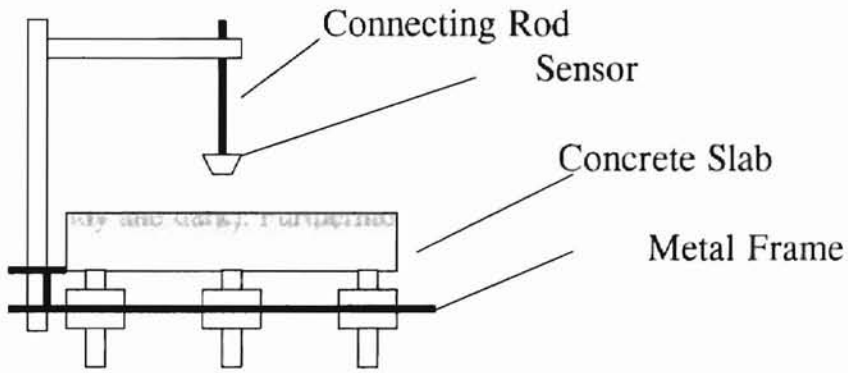

Figure 2-6. System Schematic for In-Situ Measurements

A thermocouple was embedded into the concrete slab in order for the temperature to be monitored and stored in a data logger. Also, the output voltage on the detector's side of the sensor was stored in the data logger's memory.

Measurements were conducted under different weather conditions over the course of several weeks, from the March 7th, 1999 to the April 29th, 1999. Air temperatures ranged from 1 to 20°C. It rained several times during the test, and spraying water over the slab created "artificial" precipitation. Weather conditions with ice and frost formation on the concrete slab did not occur during this course of time.

The overall range of the output for the dry surface in different temperatures (from 1°C to 20°C) and solar radiation levels (sunny, cloudy, dark) was from 0.14 to 0.21 VDC. The overall range of the results for the wet (sprayed) surface under the same weather conditions was from 0.07 to 0.12 VDC. The overall range of the results for the wet surface under the influence of rain of various intensity was from 0.05 to 0.12 VDC.

The surface conditions (dry, wet) were monitored for several days and were recorded to be compared with the data stored in the data logger's memory. Results concerning measurements of the dry surface showed that they were not affected with the intensity of the solar radiation. The same range of results is obtained for different solar radiation levels (sunny, cloudy and dark). Furthermore, there is a significant difference in the results that correspond to the dry and wet surface. If the water layer over surface is increased, output voltage showed a tendency to decrease.

Results obtained from the data logger match very well with the results mentioned above, but they give somewhat of a broader range of output voltage for the wet and dry surfaces. Sample readings from data logger are shown in Table 2-4.

Table 2-4. Sample Readings From Data Logger for Dry/Wet Conditions

(wet conditions are shaded gray)

Date/Time	Output Voltage (VDC)	Surface Temperature (° C)
03/10/1999 9:40	0.102	4.218
03/10/1999 9:55	0.103	4.727
03/10/1999 10:10	0.107	5.027
03/10/1999 10:25	0.107	5.318
03/10/1999 10:40	0.130	6.049
03/10/1999 10:55	0.125	6.386
03/10/1999 11:10	0.124	6.807
03/10/1999 11:25	0.160	7.497
03/10/1999 11:40	0.173	8.545
03/10/1999 11:55	0.185	8.800
03/10/1999 12:10	0.201	9.873
03/10/1999 12:25	0.187	10.612
03/10/1999 12:40	0.141	10.243
03/10/1999 12:55	0.160	10.560
03/10/1999 13:10	0.223	11.622
03/10/1999 13:25	0.219	12.717
03/10/1999 13:40	0.161	12.393
03/10/1999 13:55	0.186	12.844
03/10/1999 14:10	0.193	13.576
03/10/1999 14:25	0.184	13.999
03/10/1999 14:40	0.146	13.602
03/10/1999 14:55	0.253	14.741
03/10/1999 15:10	0.162	14.194
03/10/1999 15:25	0.180	15.558

Figure 2-7 shows results from a three-day period. As can be seen wet conditions can be well detected, where the output voltage had a significantly lower value. Readings obtained from the data logger are consistent with spot observations.

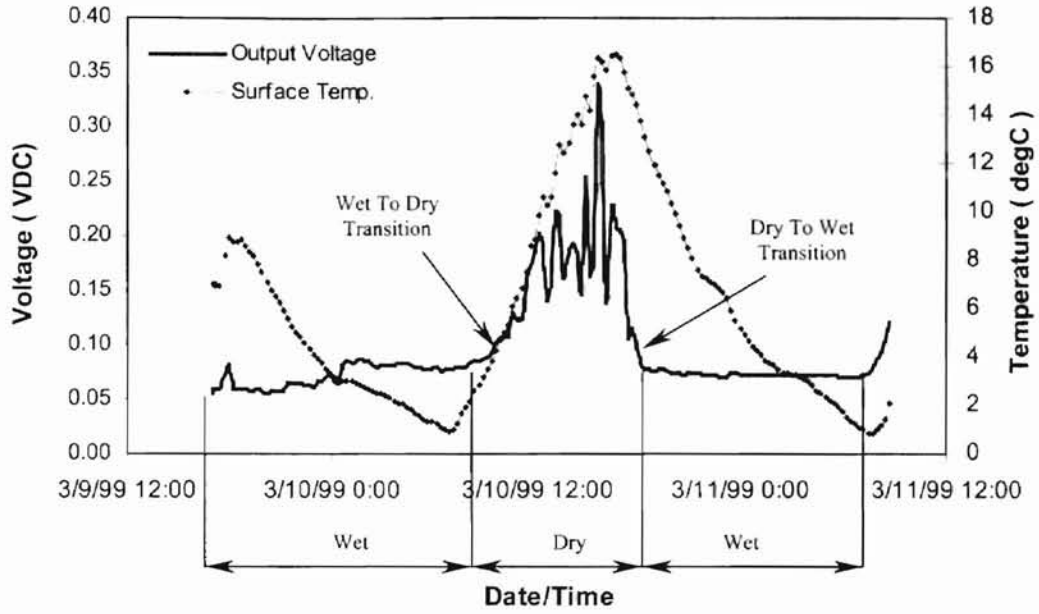

Figure 2-7. Data Logger Readings Over Three-Day Period

2.3. Operating Experience

The sensor type OPB-701, manufactured by "Optek Technologies, Inc." was used for the measurements described above. Exposed to outdoor conditions the first sensor lasted three weeks and the second lasted two weeks before complete failure. Obviously this represents a major drawback to the approach, even though results obtained in detection of surface conditions with this sensor were promising. One of the possible reasons for the equipment breakdown suggested by the manufacturer was condensation over photodiodes that may have lead to short circuit. The suggested remedy was to obtain a better sealed sensor that worked by the same principle. Sensor type OPB-704 from the same manufacturer was obtained and tested.

However, lenses of this sensor were covered with blue glass, which made this sensor sensitive to ambient light conditions, but not sensitive to the surface conditions. This is presented in the graph below, shown in Figure 2-8. As can be seen, for hours during the sunset and dawn output voltage varied even if the conditions of the surface did not change. During the night, there were no changes in voltage, whether or not moisture was present on the surface.

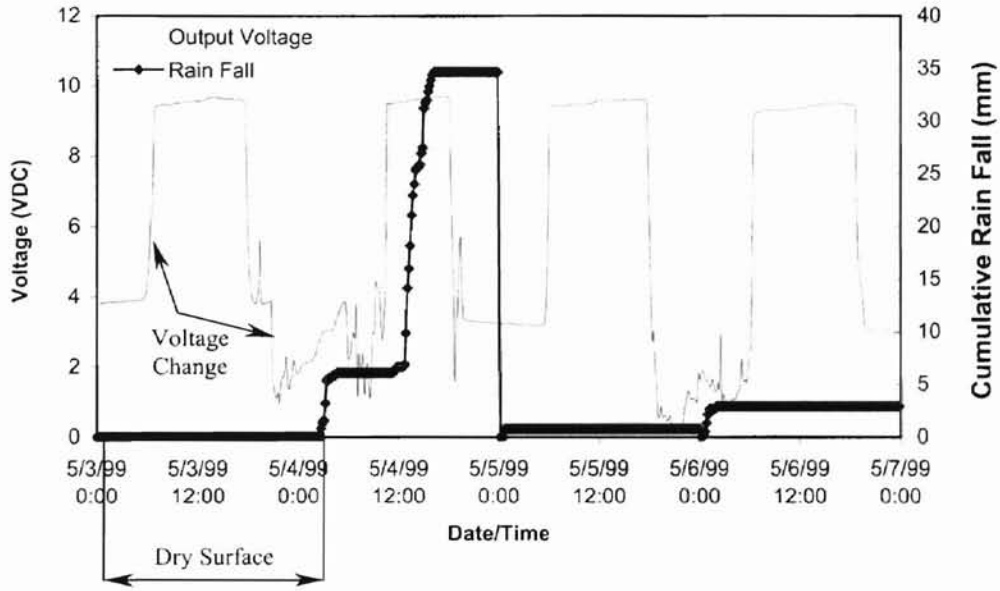

Figure 2-8. Output Voltage Given by OPB-704 Sensor

2.4. Conclusions

The first sensor evaluated, the Optek OPB-701, performed well under laboratory conditions, but failed under field conditions. The second sensor evaluated, the Optek OPB704, performed completely unsatisfactorily. Because of time constraints, a different approach was tried. This approach is described in Chapter 3.

CHAPTER III

HEATED RESISTANCE/TEMPERATURE SENSOR

This chapter presents the final design of the surrogate bridge freezing sensor. Due to the problems that occurred with infrared sensors, a different approach was considered. This approach is based on the conductivity/temperature device, described in the literature review.

3.1. Theory of Operation

The main principle for this device to function is the difference in resistance between ice and water. It is a well-known fact that water has a low electrical resistance whereas ice has a high one. To sense this difference, two sensors are used with the gap between each electrode. When freezing occurs, the unheated sensor has ice between its electrodes, providing high resistance. The heated sensor has water between its electrodes and gives a low resistance. Alternatively, conductance also can be observed. Thus, an icing signal can be generated when a resistive or conductive imbalance between two

sensors occurs. Once the ice on the unheated sensor melts, the resistive balance is restored.

As a conclusion one can say that ice formation or snow accumulation signal requires two input signals:

- Slab surface temperature of 0°C or below, and
- Resistive or conductive imbalance between two surface sensors

Frost detection cannot be directly made with this system. However, it can be inferred with additional information:

- Slab surface temperature should be lower than the dew point temperature, and the surface temperature should be close to or less than freezing point.

Dry surface will result in infinitely high resistance, the one that corresponds to an open circuit. When moisture occurs on the surface, it will result in low conductance on both sides, heated and unheated.

3.2. System Design: Surface Condition Detection

For testing purposes three systems were developed. Each system is composed of one instrumented concrete slab, two power supply batteries, two power back up photovoltaic units, control units, and a data logger. The following sections contain detailed explanations of the system components.

3.2.1. Instrumented Concrete Slab

The surrogate bridge freezing sensor is a small instrumented concrete slab, two feet in diameter and eight inches thick. The slab 8 inches thick was assembled from three layers, 2.5 inches thick, laid onto each other with the cement mix. Two sets of electrodes are embedded in the top layer. One side is heated with a regulated heating element in order to maintain the temperature on that side at 1°C or higher. The other side remains unheated. Two thermocouples measure surface temperature underneath the electrodes, while one thermocouple shows the actual temperature of the heater. The unheated side is supplied with one thermocouple that gives the temperature underneath the surface. The heated part of the sensor is given in Figure 3-1.

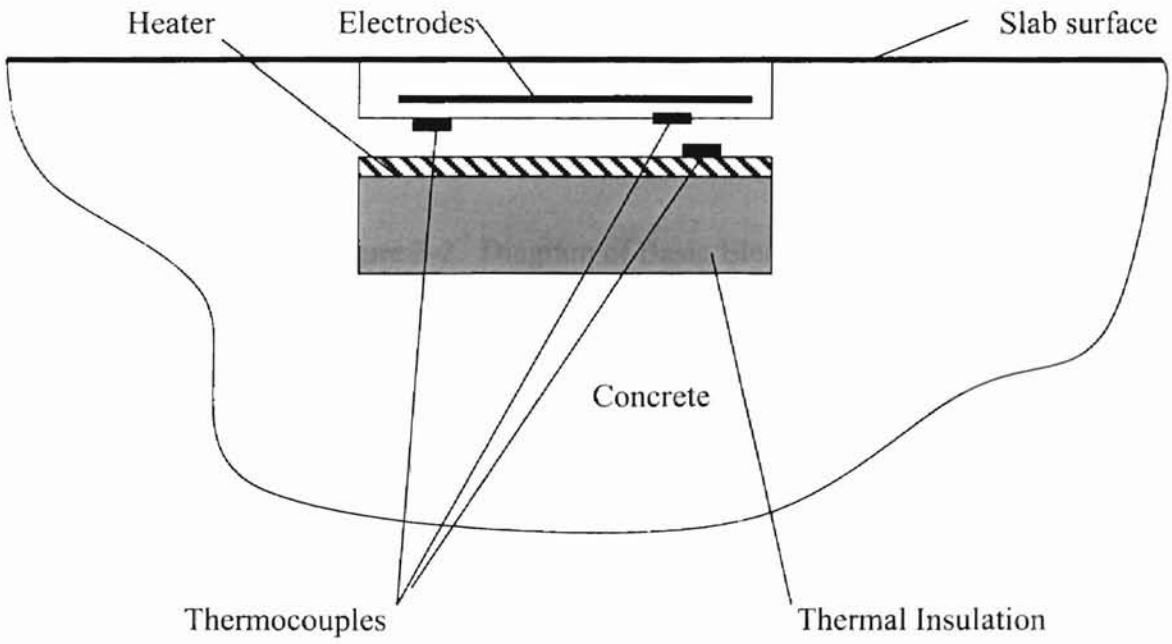

Figure 3-1. Heated Side of the Slab

The heater will be active whenever temperature drops below 1°C, resulting in change in the resistance of the thermistor embedded underneath the heated surface. It will go off as temperature rises over given set point of 1°C.

The electrodes are mounted flush with the surface and are placed in the rectangular indentations, called "active volumes". The size of the active volume is approximately 55x45x2mm. A diagram of the electrodes design is given in Figure 3-2.

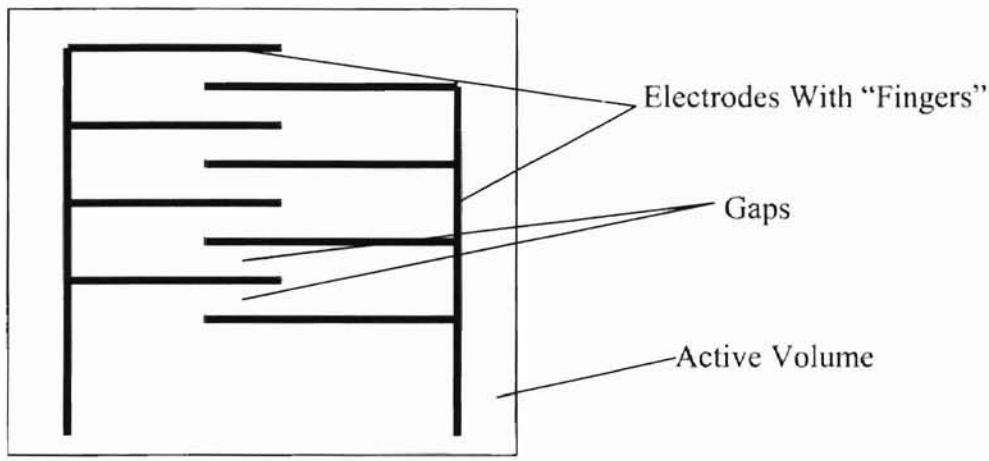

Figure 3-2. Diagram of Basic Electrodes Design

The electrodes are positioned to act as a resistance sensor, with the resistance across them changing as moisture formed between the fingers.

3.2.1.1. Heater Design

Power consumption for heated side is calculated for a design day, with the following design data from ASHRAE Fundamentals Handbook (1997):

- Place: Stillwater
- Winter dry bulb design temperature: $t_{d.b}$= -13.3 °C or $T_{d.b}$=259.85K

- Winter wet bulb design temperature: $t_{w.b.}$= -14.1°C
- For the dry and wet bulb temperatures relative humidity can be obtained from the psychrometric chart (Zimmerman and Levine, 1945): φ= 62%
- From Table 3 (Zimmerman and Levine, 1945) humidity ratio for the free stream condition of $t_{d.b}$= -13.3 °C and φ= 62% is: W_{∞}=0.000813
- W_{sat}=0.004, humidity ratio of a saturated mixture at the surface temperature of 1°C, obtained from the psychrometric chart (Zimmerman and Levine, 1945)
- Thermal conductivity of the concrete: k=2.0 W/m-K
- Design surface temperature: t_{surf}=1°C
- Dimensions of the active volume : 0.054 x 0.044 x 0.002m
- Area (A) of the active volume: 0.0024m^2

Calculated values for the conditions during the night- without solar radiation are based on the procedure given in McQuiston and Parker (1994) and Spitler (1999):

- Sky temperature can be approximated by (Swinbank,1963):

$$T_{sky} = 0.0552 \cdot T_{d.b}^{\ 1.5} = 0.0552 \cdot 259.85^{1.5} = 231.2\,\text{K} \qquad (3\text{-}1)$$

$$t_{sky} = T_{sky} - 273.15 = 231.2 - 273.15 = -41.9\,^{\circ}\text{C} \qquad (3\text{-}2)$$

- Convection coefficient calculated for the wind speed of 15m/s (Walton,1983):

$$h_c = 2.25 + 0.287 \cdot Windspeed = 5.355\ \text{W/m}^2\text{-K} \qquad (3\text{-}3)$$

- Coefficient h_{rs} calculated for the design surface temperature of 1°C:

$$h_{rs} = \sigma \cdot \varepsilon \cdot F_{ss} \cdot (T_{sky} + T_{surf}) \cdot (T_{sky}^{\ 2} + T_{surf}^{\ 2}) = 1.386\ \text{W/m}^2\text{-K} \qquad (3\text{-}4)$$

where,

F_{ss}=1, view factor to the sky

ε=0.9, emissivity

σ=5.673·10^{-8}W/m^2-K^4, Stefan-Boltzmann constant

- Heat flux due to convection:

$$q''_{conv} = h_c \cdot (t_{surf} - t_{d.b}) = 76.577 \text{ W/m}^2 \quad (3\text{-}5)$$

- Heat flux due to radiation:

$$q''_{rad} = h_{rs} \cdot (t_{surf} - t_{sky}) = 59.47 \text{ W/m}^2 \quad (3\text{-}6)$$

- *Add latent heat effects*, calculate the "film temperature":

$$t_{film} = \frac{t_{surf} + t_{d.b}}{2} = -6.15\,^{\circ}\text{C} \quad (3\text{-}7)$$

- Evaluate thermophysical properties at the "film temperature" for the values given in Table A-2b and B-4b of McQuiston and Parker (1994):

$k_{air-H_2O} \approx 0.0244$ W/m-K, thermal conductivity

$c_p \approx 1.006$ kJ/kg-K, specific heat of the air at the constant pressure

$\rho \approx 1.26$ kg/m^3, density of the air

- Thermal diffusivity (α) is calculated from:

$$\alpha = \frac{k_{air-H_2O}}{c_p \cdot \rho} = 1.925 \cdot 10^{-5} \text{ m}^2/\text{s} \quad (3\text{-}8)$$

- Diffusion coefficient (D_{AB}) can be obtained from the following empirical formula (Mills, 1995):

$$D_{ab} = 1.97 \cdot 10^{-5} \cdot (\frac{P}{P_0}) \cdot (\frac{T_{film}}{T_0})^{1.685} = 2.28 \cdot 10^{-5} \text{ m}^2/\text{s} \quad (3\text{-}9)$$

where,

P=1atm, pressure of the air

P_0=1atm, pressure

T_0=256K, temperature

- Lewis number is calculated from: $L_e = \frac{\alpha}{D_{AB}} = 0.844$ (3-10)

- Mass transfer coefficient (h_d) can be calculated from:

$$h_d = \frac{h_c}{c_p \cdot L_e^{2/3}} = 0.00596 \text{ kg/m}^2\text{-s} \quad (3\text{-}11)$$

- Mass transfer rate:

$$\dot{m}''_{evap} = h_d \cdot (W_{sat} - W_\infty) = 1.907 \cdot 10^{-5} \text{ kg/m}^3\text{-s} \quad (3\text{-}12)$$

- Latent heat flux:

$$q''_{evap} = \dot{m}''_{evap} \cdot h_{fg} = 47.717 \text{ W/m}^2 \quad (3\text{-}13)$$

where,

h_{fg}=2501.3kJ/kg, enthalpy for water at saturation at 1°C, obtained from Table A-1b of McQuiston and Parker (1994)

- Total heat flux from the surface:

$$q''_{surf} = q''_{conv} + q''_{rad} + q''_{evap} = 183.764 \text{ W/m}^2 \quad (3\text{-}14)$$

The same amount of the heat needs to be added to the surface from the heater.

- Temperature of the heater can be calculated from:

$$t_{heater} = q''_{surf} \cdot \frac{l}{k} + t_{surf} = 1.459 \text{ °C} \quad (3\text{-}15)$$

where,

l=0.005m, thickness of the concrete layer between the heater and the surface

- Heat flux due to conduction is from the heater downwards through the slab:

$$q''_{cond} = \frac{t_{heater} - t_{d.b}}{\sum_{i=1}^{2} \frac{l_i}{k_i}} \cdot A = \frac{1.459 - (-13.3)}{\frac{0.015}{0.9} + \frac{0.18}{2}} = 138.369\ \text{W/m}^2 \qquad (3\text{-}16)$$

where,

l_i [m], thickness of the layers throughout the slab, where thermal insulation forms first layer

k_i [W/m-K], corresponding thermal conductivities of styrofoam thermal insulation (k_1=0.9 W/m-K) and concrete

- Total power demand for the heater:

$$Q_{tot} = (q''_{surf} + q''_{cond}) \cdot A = 0.773\ \text{W} \qquad (3\text{-}17)$$

The design capacity should be about 1W in order to ensure nonfreezing conditions on the heated side of the slab and take in consideration any lateral heat loss from the heater. Unfortunately, the heater embedded in the slabs was oversized due to the mistake made in initial power demand calculation and it was built to provide 5W. For the modification of existing control circuit in order to provide capacity of calculated 1W refer to Appendix A.

Minimum electrical energy demands for calculated power consumption can be obtained from the following equation (Perez, 1985):

$$I = \frac{P}{V} \qquad (3\text{-}18)$$

where,

I = electrical current (Amps)

P = power consumption (Watts)

V = voltage (Volts)

For the 12VDC power supply, calculated electrical energy demand is 0.08A.

The heated element made of nickel chromium resistance wire was used as an energy source for the heated ice sensor. The wire was covered in epoxy over metal plate and placed under the surface that supposes to be heated. The resistance wire is a product of "Pelican Wire Company, Inc.". The product catalogue gives following procedure for heating element calculations.

The input parameters for the coil calculations are as follows:

- Voltage from the supply: 12 Volts
- Energy to be released by heater: 1 Watt
- Electrical current: 0.08 Amperes
- Total resistance of wire is calculated by Ohm's Law: 150Ω

Now length of the wire can be calculated by given formula:

$$L = \frac{R}{R_1} = \frac{150}{6.75} = 22.2\,ft. \tag{3-19}$$

where,

L = length (ft.)

R = total resistance (Ω)

R_1 = resistance per foot of wire (Ω/ft.)

The manufacturer as a function of wire diameter specifies resistance per foot of wire.

The heater that was actually embedded in the slab was made to provide 5W of power, thus the length of the wire was 4.26ft.

3.2.2. Data Acquisition

A "Fluke" model 2636A digital data logger with twenty one channel capacity was used to monitor and record necessary data readings. Using HYDRA, application software, the model 2636A data logger can interface with the personal computer through connecting cable to a RS-232 port.

Data logger was used for temperature, resistance and voltage measurements. For these measurements instrument's accuracy is shown in Table 3-1.

Table 3-1. Accuracy for a Different Measurements

Measurement	**Range**	**Accuracy**
Temperature	-150 to 120 °C	±0.69°C
DC Voltage	Up to 30 V DC	±0.024%
Resistance	Up to 10 MΩ	±0.169%

The different features of FLUKE 2636A series include universal input module, alarm outputs, digital I/O connectors, multidigit green led display, keypad for a operation setting, a real time clock and an RS-232 port. For the temporary storage of data memory cards of 4MB were used, where 90,000 scans of 10channels can be stored. The instrument can be connected to the computer and calibrated that way.

Application software translates stored data in the memory card to a comma-delimited file (*.csv) on PC that can be easily manipulated using a spreadsheet. Once data is uploaded to a PC, memory in the memory card can be cleared, thus full capacity is restored. More information about the FLUKE 2636A can be found in the user's manual (1997).

3.2.3. Thermocouples

For temperature measurements 24 AWG T-type copper/constantan thermocouple (0.0201in. wire diameter by Pelican Wire Company) wire was used. The thermocouple wire is rated as "special limits-of-error" to ±0.5°C. Therefore, the total expected accuracy of the temperature measurement might be found by adding the uncertainties in quadrature, by following formula:

$$A_t = \sqrt{A_1^{\,2} + A_2^{\,2}} \tag{3-20}$$

where,

A_t = total expected accuracy (°C)

A_1 = accuracy of the instrument (°C)

A_2 = rated accuracy of the thermocouple as "special limits of error" (°C)

Thus, rated accuracy is ±0.85°C. The thermocouples were calibrated in a constant temperature bath. A thermally insulated plastic container was used as a constant temperature bath. An antifreeze solution is used as a surrounding media for thermocouples, thus even when temperatures are below freezing point, the liquid phase is maintained. Ten sets of data were taken from –10 to 25°C at 2.5°C and 5°C increments. The result of the calibration showed an accuracy of ±0.25°C, when compared to reference temperatures on the mercury thermometer. Thus, the actual accuracy appears to be somewhat better than might be expected from the rated accuracy of the thermocouple and data logger. However, additional error might occur when the data logger is not maintained at room temperature, so the accuracy will be assumed to be ±0.85°C.

Sample readings for three thermocouples are given in Figure 3-3.

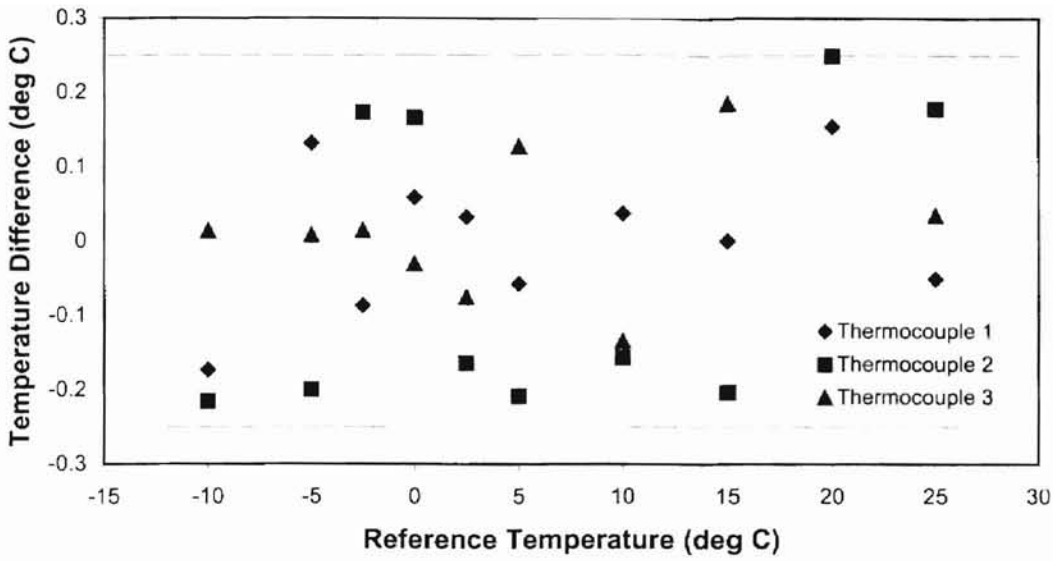

Figure 3-3. Deviations Between Thermocouple Readings and Reference Temperatures

3.2.4. Control Units for the On/Off Heater Operation

A simple switching device was designed to operate the heater embedded in the slab. Two of three systems were supplied with this control circuit, and one system had digital temperature controller to operate the heater. Since no frozen precipitation is desired on one side of the slab, the heater should be switched on when the surface temperature is below 1°C and switched off when the temperature is above 1°C.

The principle used to design a circuit was the change in resistance of a thermistor with change in temperature. With the increase in temperature, the resistance of the thermistor decreases. A calibrated NTC thermistor, rated for the resistance of 10kΩ at 25°C, was installed underneath the heated sensor's surface.

The thermistor was in series with a 100kΩ resistor, connected to a positive source of 12VDC battery. The voltage across the thermistor when the temperature was 1°C was

called the reference voltage. The voltage across the thermistor was fed to the non-inverting end of operational amplifier (op-amp). The same two 12VDC batteries previously installed in the system are used to feed power to operational amplifier. The negative side of one battery is connected to the positive side of the second battery, so that +12V and –12V can be provided. When the temperature is below 1°C the op-amp provides an output of 12 Volts, which biases the transistors, thereby energizing the relay. The relay is now in the normally open position, which means that it supplies 12 Volts to the heater. The heater is activated. When the temperature rises above 1°C the op-amp provides an output of –12 Volts, and thereby the relay is not energized. Thus no supply passes to the heater, and the heater is off. Specifications of the circuit components are enclosed in the Appendix A. A schematic diagram of the circuit is shown in Figure 3-4.

An "Omega" CN1632 series digital temperature controller was used to operate the heater of the third system installed. The features of this series include two alarm relay outputs, one DC pulse output and a universal input that accept seven thermocouple types. The reference point for the alarm mode was set to be 1°C; therefore when the thermocouple signals a temperature below the set point, relay passes power to the heater and activates it. When the temperature rises above 1°C, the alarm mode is off and the relay returns to its normally open state. For the T type thermocouple that was used as a source of input signal readable temperature range was from –128 to 400°C. Given in Figure 3-5 is circuitry for the controller application. The reader is referred to Appendix A for more details concerning temperature controller control setup.

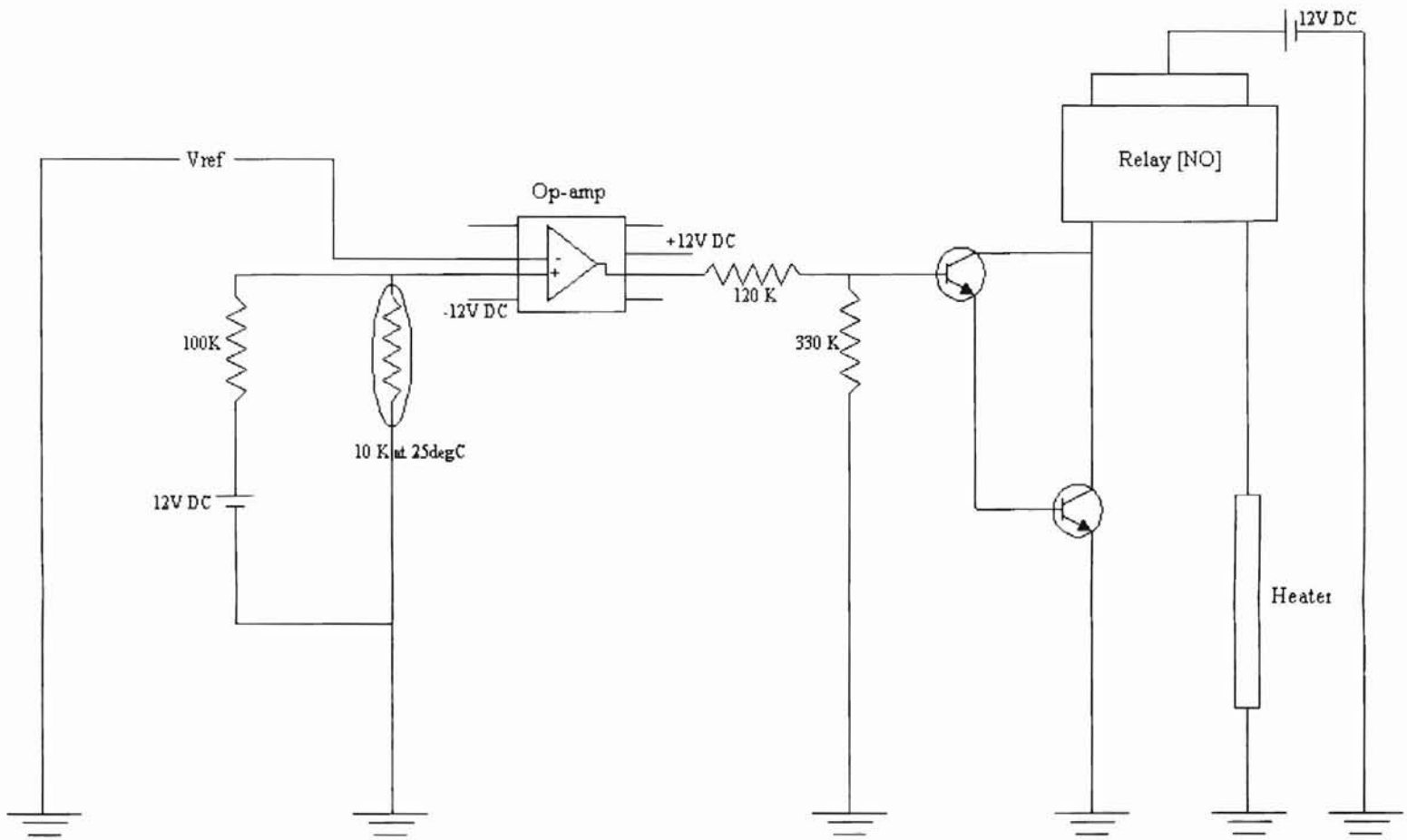

Figure 3-4. Schematic Diagram of the Circuit

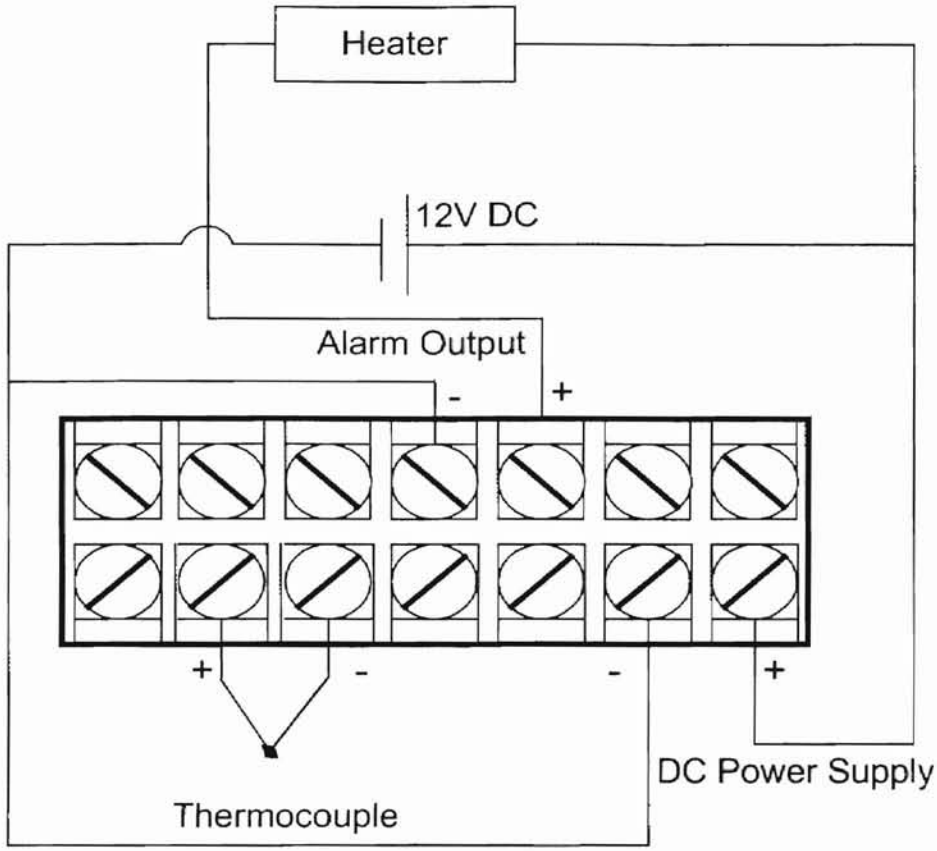

Figure 3-5. Rear Terminal Connections of Temperature Controller and Corresponding Circuitry

3.3. System Design: Photovoltaic Power Supply

3.3.1. Power Supply Battery Pack

Two batteries were required to supply the data logger and heater when necessary. In order to insure operation during cloudy weather they were sized to provide non-stop operation over at least five days without recharging.

An estimate of energy consumption is the first factor necessary for sizing a battery pack. The second factor is the number of days or hours the battery should provide energy without being recharged. The battery should be able to power most stand-alone alternative energy systems for at least five days without recharging. The amount of charging energy is highly dependent on the weather when solar panels are used as a source of a recharging energy. It must be decided how many days or hours of power one wishes to store.

The ampere-hour capacity required in the battery pack can be calculated by using the following formula (Perez, 1985):

$$C = (P_d)\,(D)\,(1.25) / V_b \qquad (3\text{-}21)$$

where,

C-capacity of the battery pack expressed in ampere-hours

P_d -estimated power consumption expressed in watt-hours per day

D -number of days between battery charges expressed in days

V_b -voltage of the battery pack expressed in volts

The factor of 1.25 in the equation compensates for the fact that the battery will only be cycled to a 20 percent state of charge before being refilled. Cycling the lead-acid battery below 20 percent of its rated capacity will result in premature battery discharge and reduced system efficiency. If the battery pack is cycled to other than 20 percent state of charge before refilling, the factor in the equation must be changed. For the heated sensor minimum required capacity of battery is as such:

$P_d = 1 * 24 = 24$ Watt-hours per day

$D = 5$ days

$V_b = 12$ V

$C = 24 * 5 * 1.25 / 12 = 12.5$ Ampere-hours

However, for the original design with the 5W heater, a 48 Ah battery was selected to ensure proper operation of the system over several days without recharging.

Power demands for data logger are specified to be from 9 VDC to 16 VDC, 235mA. The battery of 48Ah is chosen, providing data logger to run few weeks without recharging. Both batteries were deep cycle, non-spillable, lead-acid made by "Concorde Battery, co".

3.3.2. Photovoltaic System

Solid-state photovoltaic solar cells were used to transform sunlight directly into electricity in order to recharge the battery power supply pack. The desired charging profile for a battery depends on the size of solar module. The most common error made in using solar cells to charge batteries is undersizing the output power of the solar module. The total accumulated power output of a solar module might vary greatly with a number of factors. Solar modules can be expected to recharge with high efficiency only several hours during the day. In other words, the solar array will only provide its rated energy output about four hours per day and then only on sunny days.

According to Perez (1985) the solar array should be able to charge the battery at a rate of C/20 or greater where C is the ampere-hour capacity. If we consider cloudy days and the inefficiency of the cells during the early morning and late evening sun, output power should be higher when compared to that of the battery itself.

In order to recharge a 48Ah battery, output power from the solar module must be at least 2.35A. Photovoltaic modules PV40 manufactured by Kyocera Corporation were used as a charging system for the batteries. Rated characteristics are given as follows:

- Nominal maximum output: 40 Watts
- Nominal maximum current: 2.48 Amperes
- Open circuit maximum voltage: 16.9 Volts

Two metal frames were manufactured, and solar modules were placed on them. The tilt angle is adjusted to be equal the latitude plus 15 degrees from horizontal plane according to Kyocera Corporation user's manual (1998). For the three different sites in Oklahoma where systems were deployed, latitude is approximately 36 degrees which gives tilt angle of 51 degrees from horizontal plane. Solar module is shown in Figure 3-6.

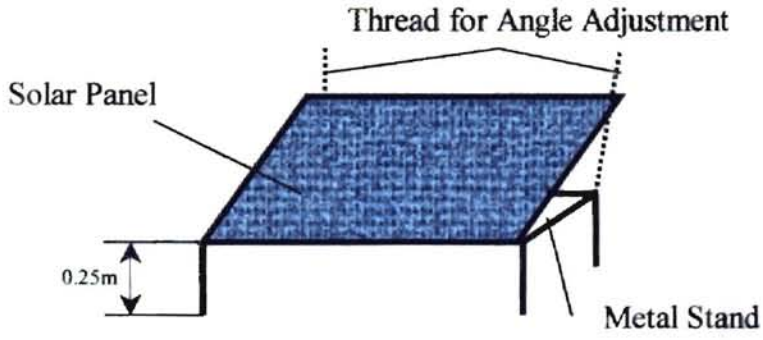

Figure 3-6. Solar Module Mounted on the Metal Stand

3.3.3. Charge Controller for Solar Modules

It is a common practice to use an output regulator on solar modules. In most cases, solar cells are inherently self-regulating. They will produce their rated output and no more. As such, if the module is properly sized to the battery, no further regulation is

necessary. However, charge regulators should be used if battery is charged daily, especially during days with high sunlight intensity (Lasnier and Ang, 1990). The charge controller provides constant voltage charging, thus prevents overcharging of the battery. It also prevents the battery from discharging through the solar panel at night. Therefore, there is no need to install a blocking diode for this purpose. For a 12 Volts system used in this project, a Morningstar Corporation Sunguard solar controller was installed. The device was solid-state, sealed for outdoor use, with the range of operation for ambient temperature from –40 to 60°C. The schematic of charge unit position in the system is shown in Figure 3-7.

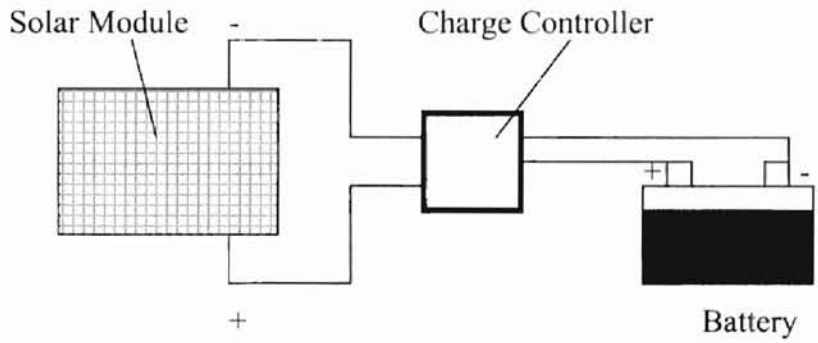

Figure 3-7. Schematic of Charge Unit Position

3.4. System Configuration for In-Situ Measurements

An instrumented circular concrete slab was insulated around the outer edge with Styrofoam in order to reduce lateral heat transfer. It was placed on a four foot high metal stand that was anchored to the ground. A lockable steel box holds batteries, control units and the data logger. The box was thermally insulated from the inside, preventing the influence of the very low temperatures on the system's efficiency by maintaining the heat produced by batteries during recharging. The solar panel frames were anchored to the ground and solar panels wired to the batteries, thus providing back up power for recharging. Schematic of the system design is shown in Figure 3-8. Figure 3-9 gives arrangement of the batteries, data logger and control unit inside the box.

Thermocouples and resistance electrodes embedded in the slab were wired to the channels of an input module for the data logger. The data were recorded in the following order:

- Channel 1-thermocouple: temperature on the unheated side
- Channel 2-thermocouple: temperature on the heated side
- Channel 3-thermocouple: temperature of the heater
- Channel 4: resistance over the electrodes on the unheated side
- Channel 5: resistance over the electrodes on the heated side
- Channel 6: voltage of the battery that powered the heater
- Channel 7: voltage of the battery that powered the data logger

Final arrangement of the system installed in Burbank, Oklahoma is shown in Figure 3-10.

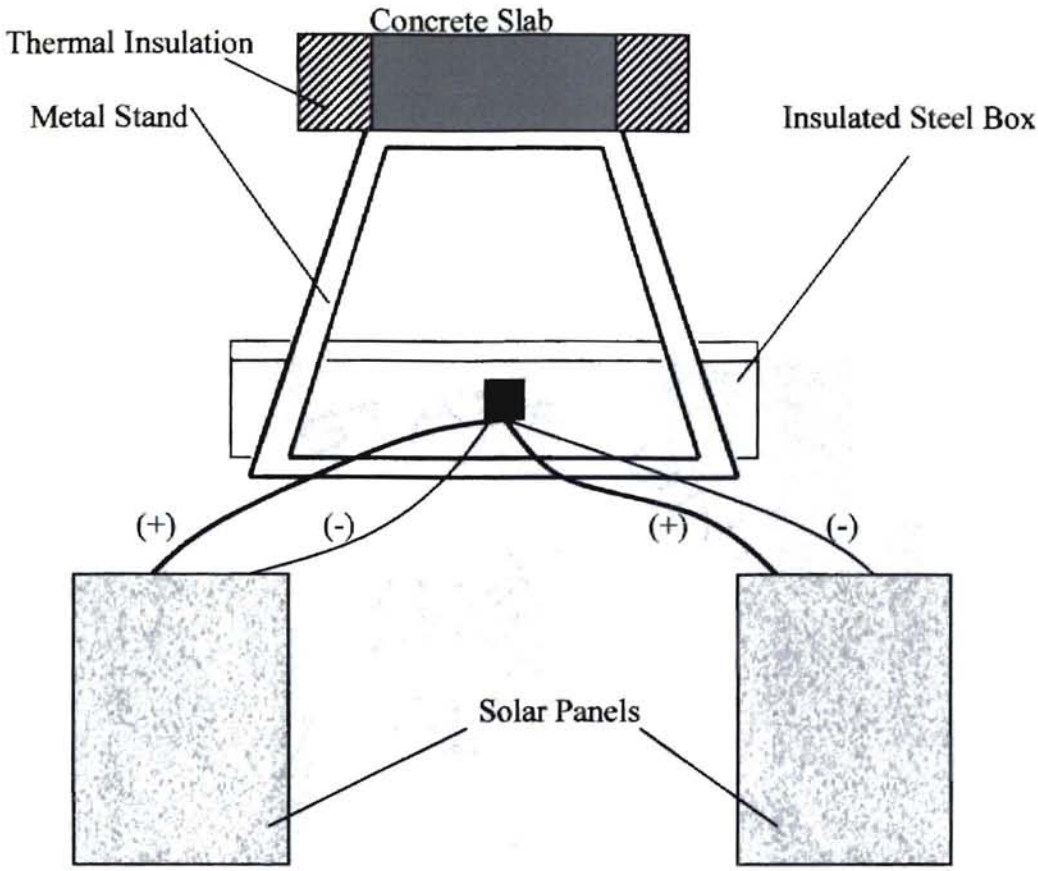

Figure 3-8. Schematic of the System

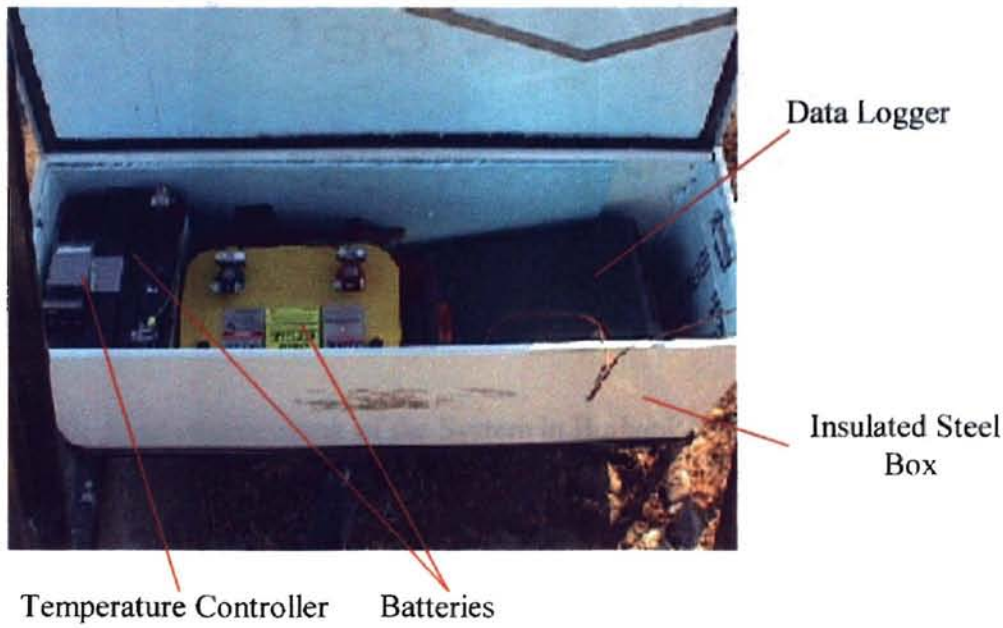

Figure 3-9. Arrangement of the Batteries, Data Logger and Control Unit

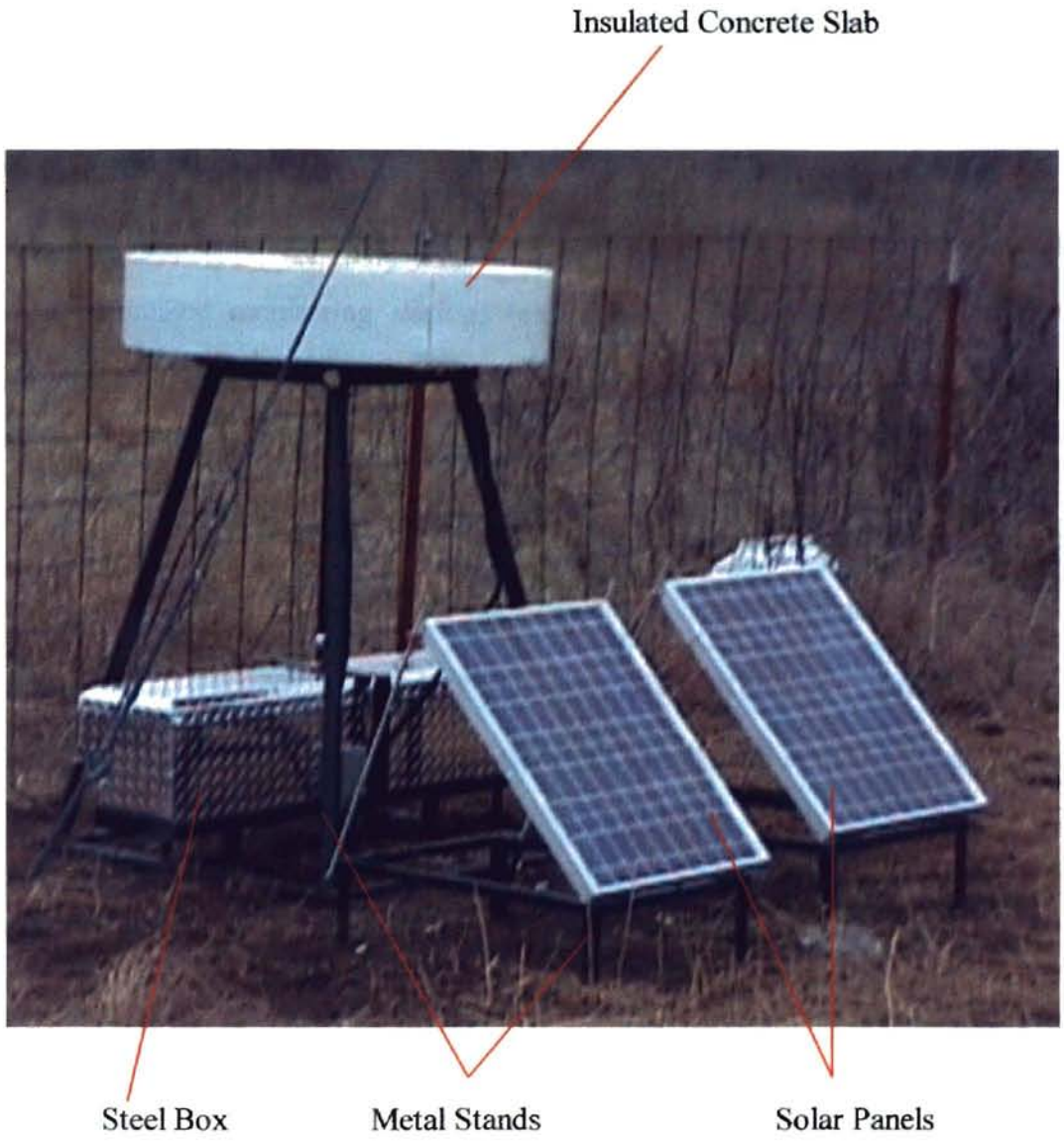

3-10. Final Arrangement of the System in Burbank, Oklahoma

3.5. Field Deployment

As mentioned before, systems should be installed at various locations throughout the state in order to cover the wide area where significantly different weather conditions might occur. One system was installed in Stillwater, at the OSU Petroleum Laboratory. Two systems were installed at Mesonet sites in Buffalo and Burbank, respectively.

The Oklahoma Mesonet (or Mesoscale Network) is a unique, statewide network of 115 automated monitoring stations (average station spacing is approximately 19 miles). At each site, a comprehensive set of weather and soil variables is measured by a set of instruments located on or near a 10-meter-tall tower. The measurements are packaged into "observations" every 5 minutes, and transmitted to a central facility every 15 minutes, using the Oklahoma Law Enforcement Telecommunications System. Within minutes after the observations are acquired, these Mesonet data are available and can be downloaded from the web. Chosen locations for the system deployment are shown on the map in Figure 3-11.

Freezing sensor system behavior was observed over several weeks and data were recorded. The complete results of the study will be presented and discussed in the Chapter 4.

Figure 3-11. Mesonet Weather Station Sites With Chosen Locations

CHAPTER IV

EXPERIMENTAL RESULTS

This chapter presents the experimental results obtained for different surface conditions observed on the bridge freezing sensor over time. Initially, tests were conducted under laboratory conditions. Secondly, sensors were deployed at the different sites throughout the state, and sequences of results were recorded during that field testing. Those results will be discussed in the following sections.

4.1. Laboratory Test Results

For the laboratory measurements the top layer of the concrete slab was used. Namely, the size was two feet in diameter and 2.5 inches in thickness. As it was explained in the previous chapter, the top layer of the slab carries the heated and unheated probes embedded in it.

4.1.1. Moisture and Ice Detection Experiments

Both probes were tested to a general reaction to moisture on the sensor. This test consisted of covering of electrodes with water. The amount of water is gradually increased over the electrodes. The concrete slab was placed in the freezer and resistance over electrodes was recorded and stored in data logger's memory. The idea was to observe transition from water to ice. A schematic of the apparatus is given in Figure 4-1. Thermocouples embedded underneath the electrodes, positioned at the middle of the active volume were used to measure the temperature of the inspected surface.

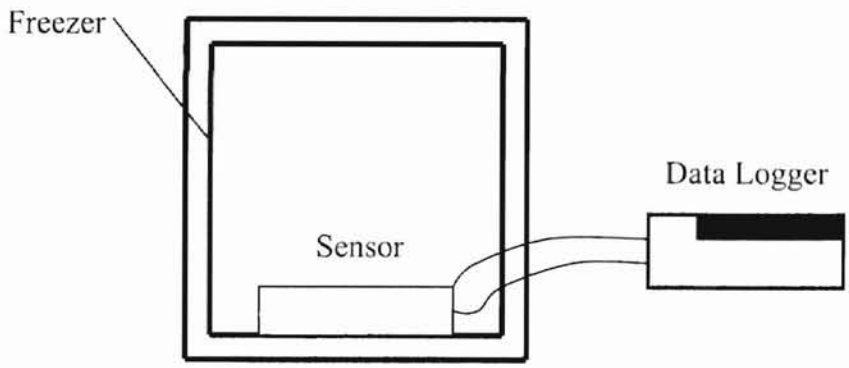

Figure 4-1. A Schematic of the Apparatus for the General Reaction to the Moisture and Ice

The following results are observed:

- Completely dry sensor behaved like an open circuit showing indefinitely high resistance, recorded on the instrument as 10^6kΩ.
- The sensor reached minimum resistance long before it was completely covered with moisture. Resistance that corresponded to the presence of the water on the surface was always less than 100kΩ, generally between 2 and 8kΩ.
- With the formation of first ice crystals, resistance gradually started to increase over 100kΩ. Finally, with 100% coverage of the electrodes with ice resistance reached values close to 6000kΩ. The transition from water to ice plotted versus time is shown in Figure 4-2. As can be seen there is no significant increase in resistance when temperature approached freezing point. The actual transition can be observed for the temperatures close to -1°C when the major percentage of water amount occupying active volume became ice. With the temperature decrease ice density increased resulting in increase of the resistance.

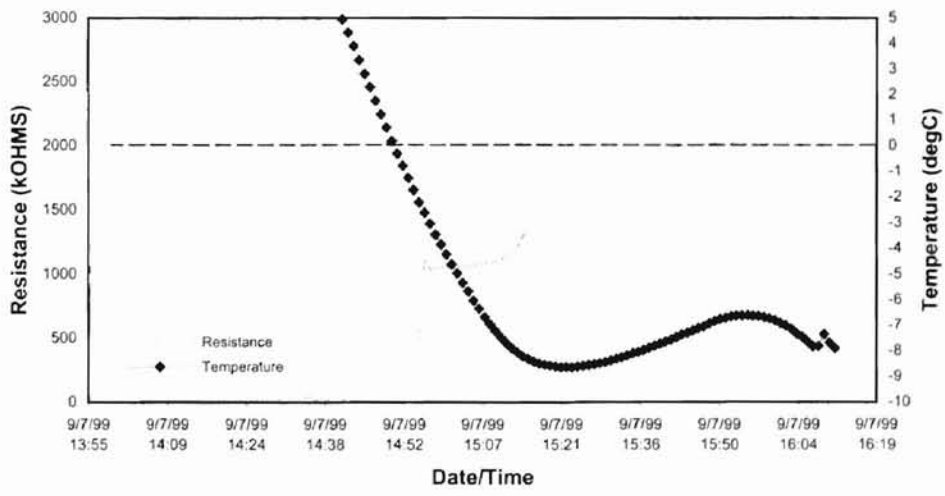

Figure 4-2. Transition From the Liquid Phase to the Ice

In the second part of the experiment, resistance over the electrodes is observed for the transition from ice to water. When the solid ice formation on the sensor is noted, it had been removed from the freezer, placed in the insulated box and exposed to the surrounding temperature of 25°C. Resistance that corresponds to presence of the ice over the electrodes at that point was around 5000kΩ. When the temperature underneath the sensor's surface started to increase above 0°C, the resistance decreased significantly. As the surface temperature reached approximately 5°C, almost all of the ice was melted, and resistance indicated values far below 100kΩ signifying wet conditions over the surface. This behavior is given in Figure 4-3.

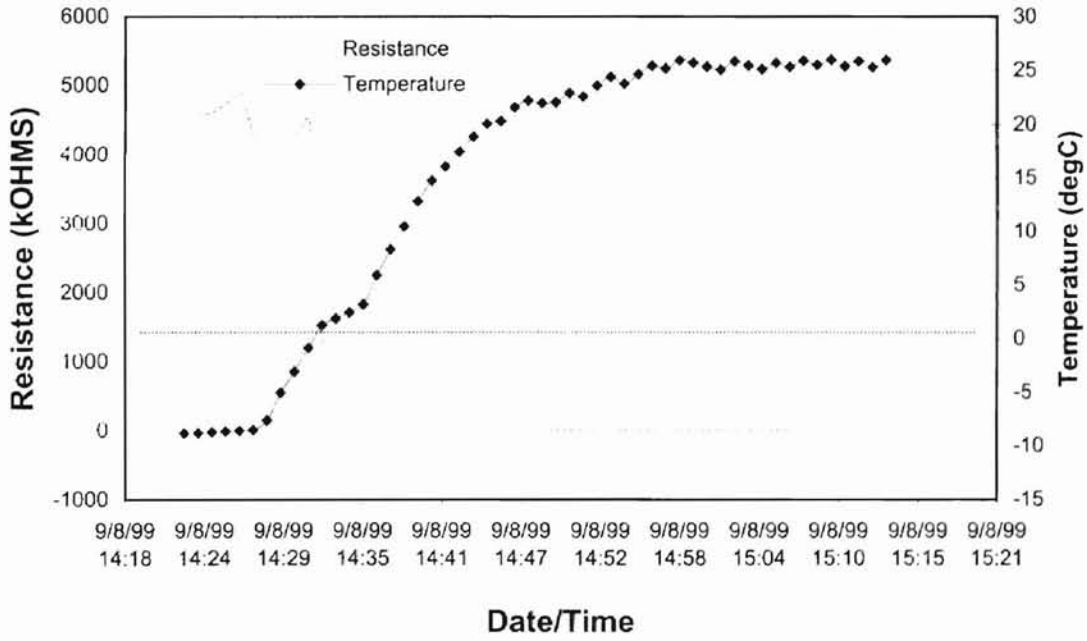

Figure 4-3. Transition From the Ice to the Liquid

4.1.2. Reaction of the Sensor to the Frost Formation

Evaluation of sensor's reaction to the frost formation required use of insulated box, previously shown in Figure 2-5. The same principle was applied as explained before, but instead of the infrared sensor, the instrumented concrete slab was used. The slab was precooled to the temperatures around -13°C, by the use of the dry ice blocks that were placed underneath the slab, and stored in the freezer over night.

As soon as the slab was placed into insulated box, the heater on the heated side was activated. The temperature on that side of the sensor was kept between 1 and 2°C. Mist was sprayed above the electrodes and the resistances for both the heated and unheated side were noted, as well as the corresponding temperatures. On the unheated side, formation of very small frost crystals did not show change in the resistance from the dry condition. The surface was sprayed over time resulting in the formation of the bigger frost crystals. Change in the resistance with the corresponding temperatures for both the heated and unheated side is shown in Figure 4-4.

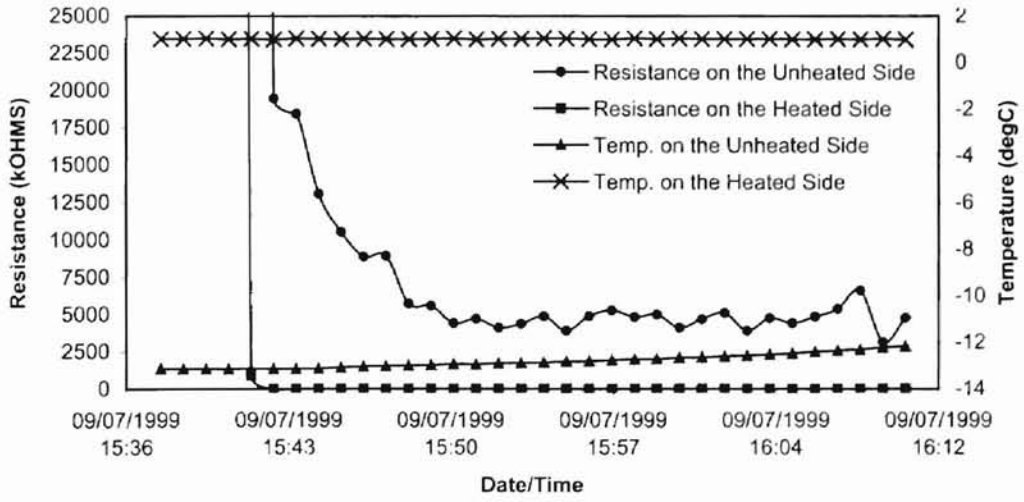

Figure 4-4. Reaction During the Frost Formation

It was observed that resistance on the unheated side decreased to the values in the range of 5000-10000kΩ, with the temperatures below freezing point. On the heated side resistance corresponded to one that indicates wet surface. The results show that with the significant amount of the frost built upon the electrodes, the system responded the same as under icy conditions. Since there was moisture detected on the heated side, real conditions when frost might occur were not simulated accurately. Mist was used in this experiment to significantly increase relative humidity of the surrounding air. Under real conditions, condensation on the heated side would not occur, since the temperature on that side is higher than dew point temperature of the surrounding air. The frost would form on the unheated side if the surface temperature approaches the dew point temperature. The useful information from this experiment is that with small frost crystals formed over the surface the resistance remains unchanged from dry conditions.

4.1.3. Snow Detection Experiments

Initial sensor's reaction on the presence of the snow is observed by placing the instrumented slab into a laboratory scale snowmaking machine (Longwill et al., 1999), the device that is capable of producing in excess of nine cubic feet of snow per hour, in a temperature range from -12°C to -6°C with densities ranging from 3 to 6 inches of snow per inch of water.

The snow machine consists of a control box, nozzle array, snow holder, snow tower, and exhaust tower used together with feed and transfer lines to deliver pressurized air and water along with liquid nitrogen. The control box contains two feed lines of 5/8" copper tubing, one for water and one for air as well as three transfer lines of a compressed air and water stream. The feed lines supply water and air under pressure,

passing the streams through pressure regulators to maintain a balanced flow. Three mixing tees produce three streams of air and atomized water and deliver them to the nozzle array through transfer lines made from 1/4" copper tubing. The control box can deliver air at a rate of up to 4.0 SCFM and water at a rate of up to 0.4 GPM.

The nozzle array delivers the air/water mix and nitrogen to the snow tower for the snow production. The array is constructed of 1/4" copper tubing and has a total of five nozzle lines, three of air/water and two for nitrogen. The three water/air lines are spaced symmetrically in the center of the snow holder and each line is bent upward. The lines are pointed at an apex about four inches above the nozzle tips to further atomize the streams and approximately cancel all horizontal velocity components, leaving a vertical stream of finely atomized water.

The snow holder is constructed of 3/4" plywood and stands two feet tall with an inside area of three feet by three feet. The interior is lined on the bottom with 3/4" styrofoam and along the sides with 1/2" foamboard to a height of 1 foot 6 inches. The box serves to support the nozzle array in the operating position as well as collect the snow formed.

The snow tower sits on top of the inner lining of the snow holder and serves as the mixing chamber for the air/water and nitrogen streams leaving the nozzle array. The snow tower is constructed of 1/2" foamboard with in inside area of three feet by three feet and a height of seven feet 11 1/2 inches. The snow tower is instrumented with two temperature sensors to monitor system performance. The exhaust tower is constructed of 1/2" foamboard, has a rough shape of two feet by two feet, and stands about eight feet tall. The exhaust tower connects with the snow tower by a 4.0-inch diameter plastic tube

approximately two feet long. The exhaust tower serves to pressurize the snow tower. The vent hole connecting the snow tower to the exhaust tower is cut in the side 2.5 feet above ground level. The exhaust tower serves to capture and collect all snow and water entrained with the nitrogen exhaust.

For this experiment the slab was previously precooled in order to prevent snow melting on its surface. The snow introduced to the surface was very wet, with the density of three inches of snow per inch of water. The sensor's response to snow accumulation is given in Figure 4-5.

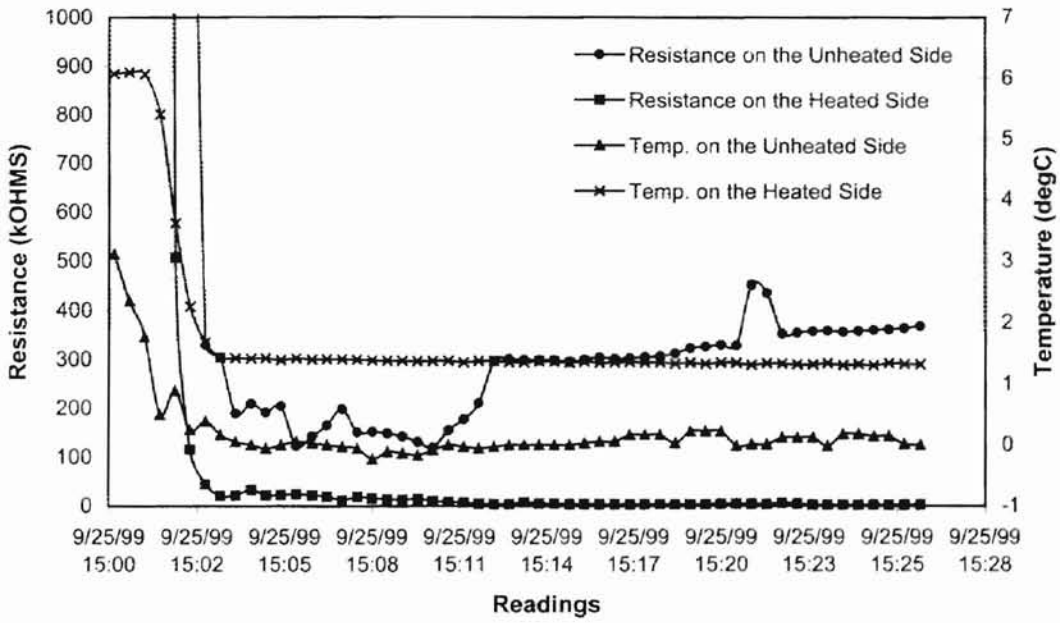

Figure 4-5. General Reaction to the Snow Accumulation

On the heated side, the heater was activated before the snow was introduced to the surface where snow melted immediately, while at the same time snow was gradually built up on the unheated side. As can be seen from Figure 4-5 resistance that corresponded to

the snow accumulation on the unheated side was in the range of 120-500kΩ. On the heated side, resistance was less then 100kΩ, with the majority of values less than 10kΩ signaling the presence of moisture and causing resistive imbalance between two probes, thus indicating snow on the surface. Temperature of the heated probe was kept around 1°C, while on the unheated side temperature decreased to approximately 0°C due to snow presence.

4.1.4. Conclusion

The laboratory tests lead to the conclusion that resistance/temperature sensors can be a potential to indicate different surface conditions. Next step was to deploy system in-situ, exposing sensors to the outdoor conditions. Results in brief for the field tests are given in the following section.

4.2. Field Test Results

Three systems were deployed for field testing purposes at different locations throughout the state. The first system was installed in Stillwater, at the OSU Petroleum Laboratory. The system was activated on November 19th 1999, and data were collected at 5 minute intervals. Data were recorded almost continuously until the beginning of April.

The second system was installed at the Mesonet weather station site in Buffalo, located 115 miles northwest from Stillwater. The system was activated on January 26th 2000, and data were recorded till mid March, when a power loss on the data logger battery occurred.

The third system was deployed and activated at the Mesonet weather station site

in Burbank, located 54 miles northeast of Stillwater. The system was run continuously from February 18th 2000 till the beginning of April.

4.2.1. Behavior of the System

One of the most important issues was to make sure that the system could run continuously without power loss. Each system was powered with two deep cycle batteries that were recharged on a daily basis by the photovoltaic arrays. In order to observe the behavior of the system, the voltage from the batteries was scanned and recorded. Also, the heater's operation was monitored by recording temperature on the heated side.

Weekly behavior of the system deployed at Stillwater experimental site is shown in Figure 4-6. As can be seen there is significant voltage increase during hours of the day when batteries were recharged with the photovoltaic array. For the proper operation, batteries used in the system should maintain over 100% of their capacity all the time (Lasnier and Ang, 1990). 100% capacity corresponds to the rated voltage, which is, for the 12V battery, 12VDC. However for the rated voltage of 12V, nominal operating voltage is usually between 12 and 13 VDC, providing a "capacity" over 100%. For the two systems deployed in Stillwater and Burbank no problems were noticed regarding loss in the battery capacity, i.e. both systems operated with capacity above 100% over the whole period of testing. The problem occurred at the Buffalo site, where loss in the battery capacity produced insufficient voltage for data logger's operation, which resulted in data loss. The reason for the power loss was the malfunction in the battery itself, which will be explained in brief later in Chapter 4.

In Figure 4-7 initial calibration of switching control device for the heater was

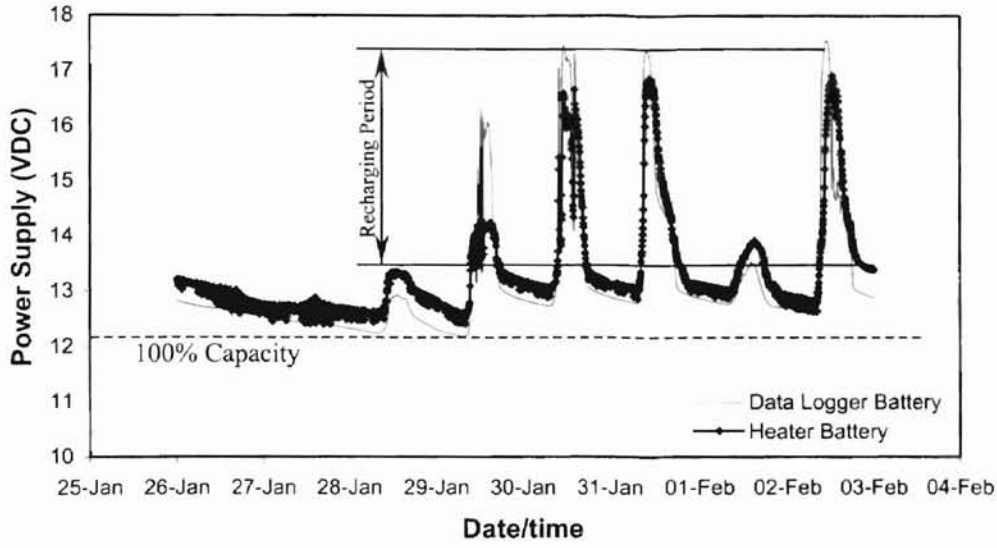

Figure 4-6. Voltage Increase During Recharging-Operation Above 100% Capacity

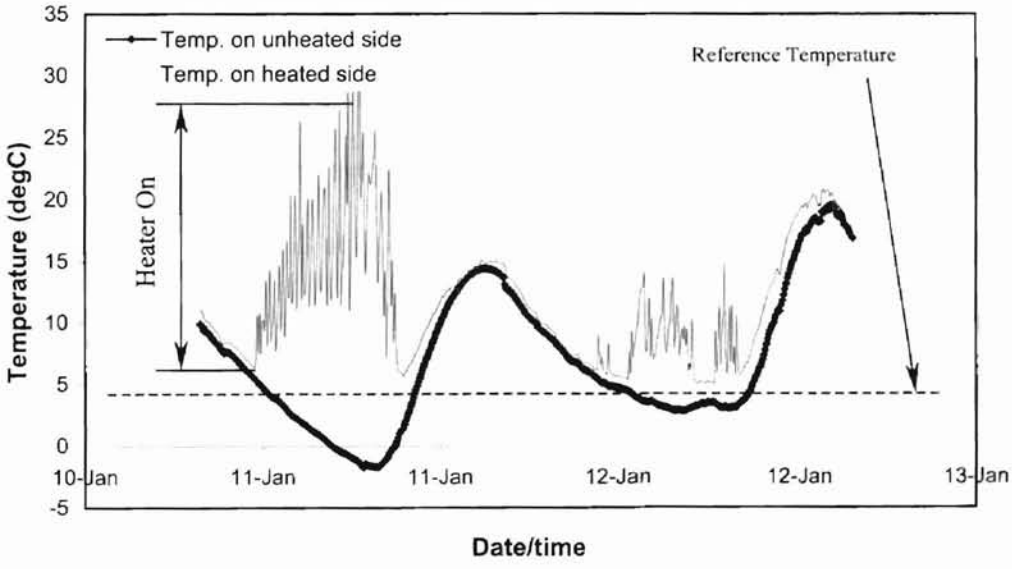

Figure 4-7. Initial Temperature Range Calibration During the Heater Operation

shown. The requirements were that the heater should be turned on once the temperature on the heated side drops below 1°C, and turned off when temperature of 1°C or higher is restored. Thermistor was used to signal the reference temperature of 1°C, and was connected to 10kΩ potentiometer. Thus, the resistance that corresponded to the temperatures higher than the reference one could be adjusted with the potentiometer. The initial calibration of the thermistor showed that temperatures on the heated side before the heater was turned off were unacceptable high, somewhere around 25°C, causing that if moisture is present on the heated side of the sensor it will evaporate much faster than from the unheated side, misrepresenting the real surface condition. Also, due to initial miscalculation of power consumption for the heater, the heater itself was oversized. In the later efforts, the resistance was successfully adjusted so the heater operated in the range of temperatures between 0.5 and 4°C(Figure 4-8). Readings were taken with 5 minute time intervals thus heater on/off operation in 5 minutes between two successive intervals cannot be seen in Figure 4-8. The adjusted temperature range for the heater operation almost equalized the evaporation time on both sides, heated and unheated.

The system deployed at Buffalo site had a digital temperature controller as a switching device for the heater. The relay output was set in alarm mode to turn on the heater when temperature drops below reference point of 1°C. As soon as the temperature increases over reference temperature, controller is no longer in alarm mode, turning off the heater. Unfortunately, heater was oversized by mistake, thus accumulated heat caused temperature to increase up to 5°C even when the heater was off. The temperature range for the system is given in Figure 4-9.

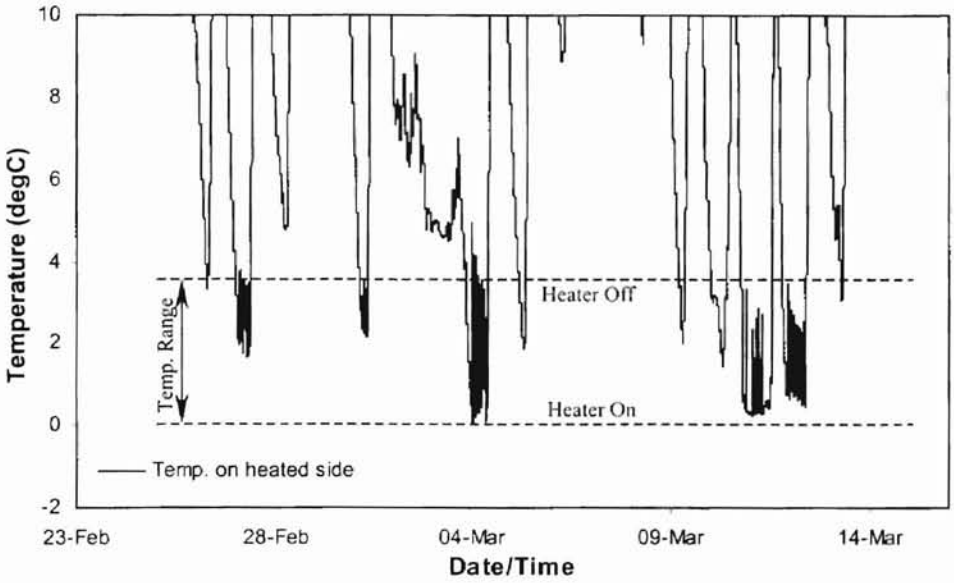

Figure 4-8. Adjusted Temperature Range for the Heater Operation

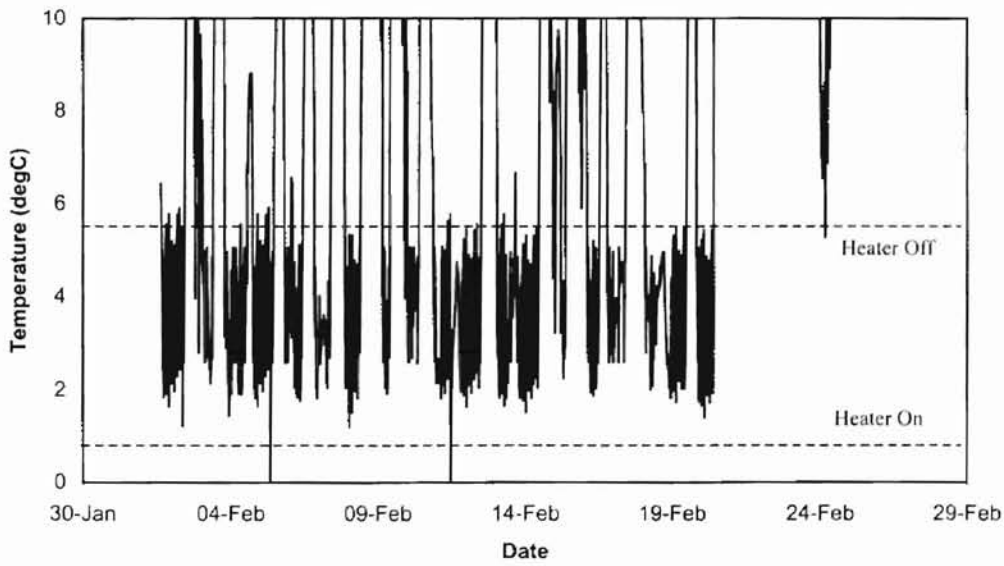

Figure 4-9. Temperature Controller On/Off Operation

4.2.2. Presence of Moisture

The response of the system exposed to the outdoor weather was recorded. General response to the moisture presence was observed during the days when rain occurred. The actual weather data were obtained by using an automated weather station network, named Mesonet. Hundreds of Mesonet weather files were downloaded through the Internet, in which the information about the air temperature, relative humidity, wind speed, rain fall etc. is obtained in five-minute segments.

Cumulative rain fall in millimeters is measured by rain gauge. The system dumps accumulated water, if any, at midnight every day. When the rain accumulation is plotted over time, horizontal lines represent amount of accumulated rain. Vertical lines heading downwards show when system dumps accumulated water. Actual precipitation is represented with an upward-heading line from one measurement to the next, and starts from the number that represents previously accumulated amount of water, if any. The sample plot of a cumulative rain fall is shown in Figure 4-10.

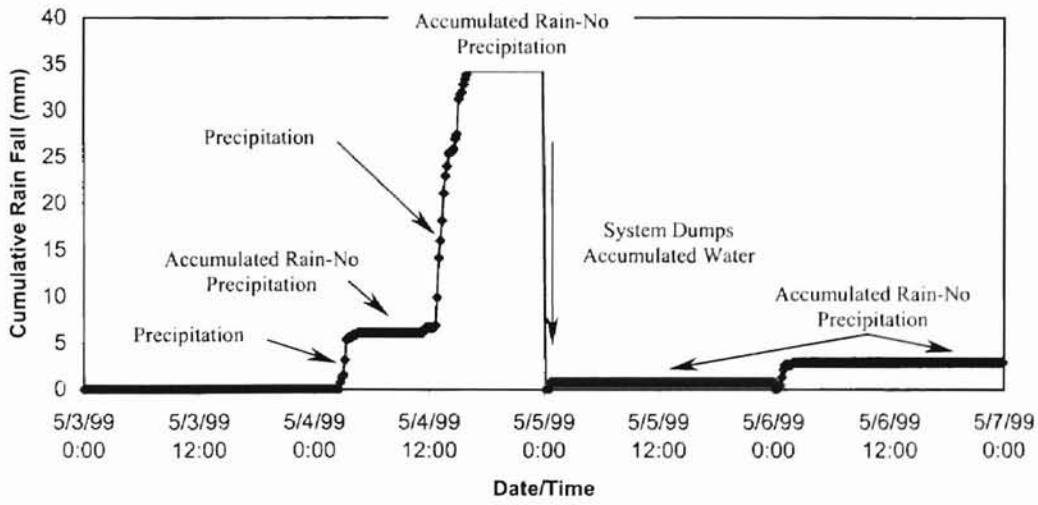

Figure 4-10. Cumulative Rain Fall Plotted Over Time

The system response to the presence of rain precipitation is shown in Figures 4-11, 4-12 and 4-13 for three different site locations.

Liquid precipitation is also measured by the rain gauge of the Mesonet weather station. Those data were used to plot rain fall over time, showing that sensors responded to moisture presence at the same time when the raining was detected by Mesonet instruments. As can be seen from figures very low resistance, generally less than 10kΩ on the both heated and unheated sides of the sensor corresponded to the presence of the moisture due to the rain precipitation. These results matched very well the results obtained in the lab when the slab was tested on the moisture presence.

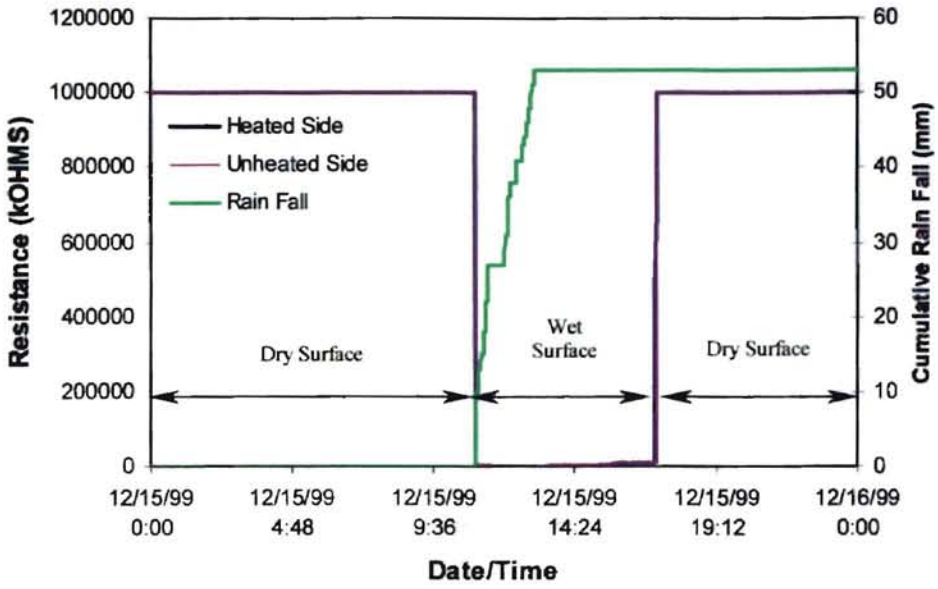

a) Sensors' Response to the Presence of Moisture

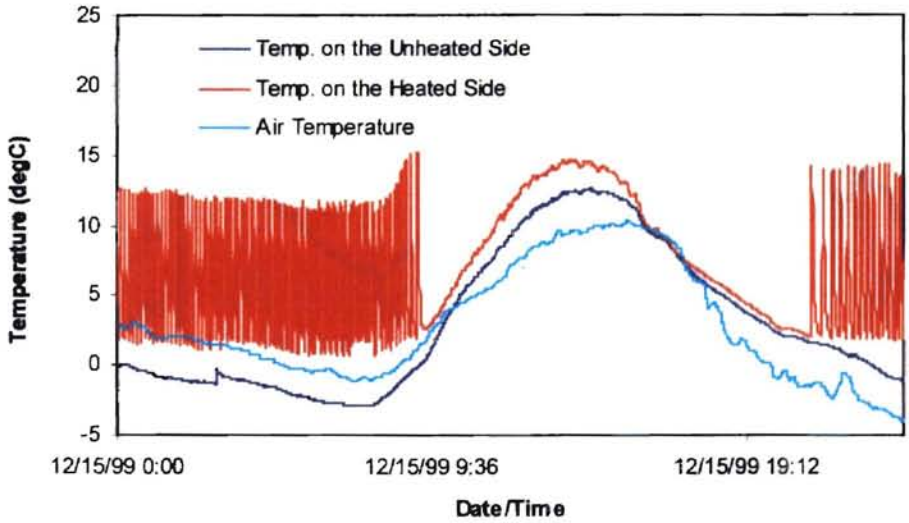

b) Corresponding Temperatures

Figure 4-11. General Response of the System to the Rain Precipitation at Stillwater Site

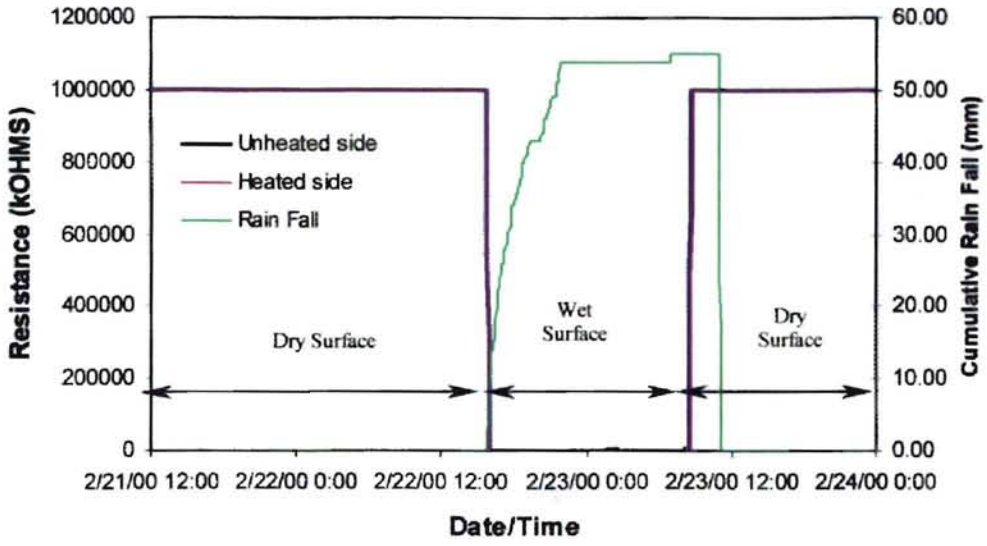

a) Sensors' Response to the Presence of Moisture

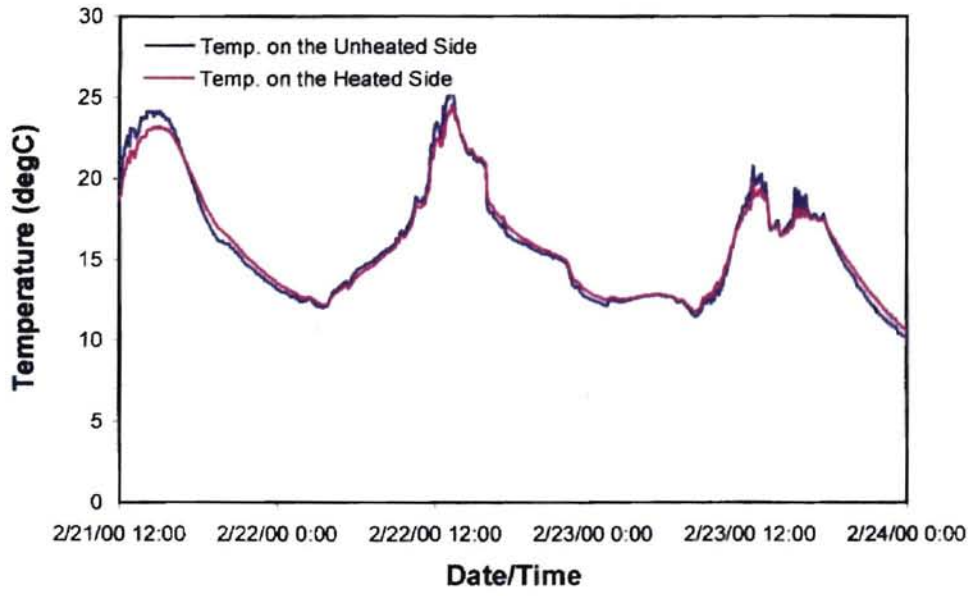

b) Corresponding Temperatures

Figure 4-12. General Response of the System to the Rain Precipitation at Burbank Site

4.2.3. Snow Accumulation Detection

Since there was no snow precipitation at the beginning of the winter season, sensors were initially tested with the snow made in the lab. First amount of snow was placed on the slab on December 20th 1999 around 23:00 hours. The snow layer over the slab was approximately 1.5 inches thick, packed powder; wet, with the density measured in the lab to be 4 inches of snow per 1 inch of water. Initially, the slab's surface was dry, with the temperature at approximately 0.5°C. The styrofoam insulation was placed on and around the snow layer, to prevent fast melting during the day when the temperatures were high. Conditions on the both heated and unheated side were checked for the different times of the day. Observations are shown in Table 4-1. On the December 21st, 1999 the amount of snow on the slab melted down to one inch. The surface on the unheated side was frozen (ice is observed over the electrodes), with the snow above the ice. The surface on the heated side was completely dry, with snow around it, but not over the electrodes. On the December 22nd the ice was still present over the electrodes on the unheated side, but this time snow above it melted completely. The heated side was wet, due to the presence of the melted snow.

The resistance obtained on the unheated surface under the wet snow varied between 200 and 700kΩ, while the heated surface responded to the wet conditions with the resistance generally less than 10kΩ. These results were similar to those obtained in the laboratory when the slab was treated with the artificial snow. Due to significant amount of heat radiated from the heater the heated side dried out in a short period of time, which was indicated by the resistance that corresponds to dry conditions. The spikes in

measured resistance represent the surface drying out, and being wetted again by the melting snow. Readings that represent these conditions are given in Figure 4-14.

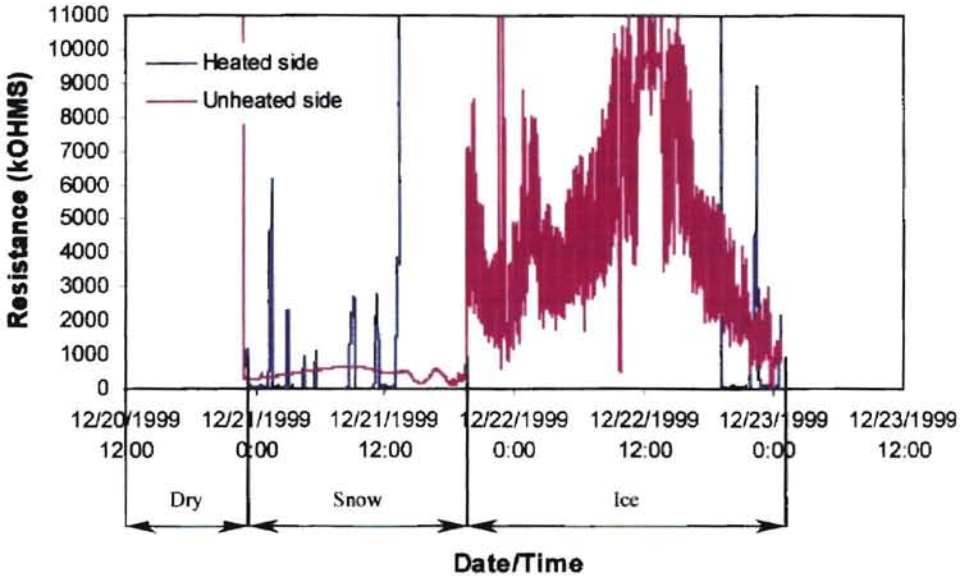

a) Sensor's Response to the Snow Accumulation

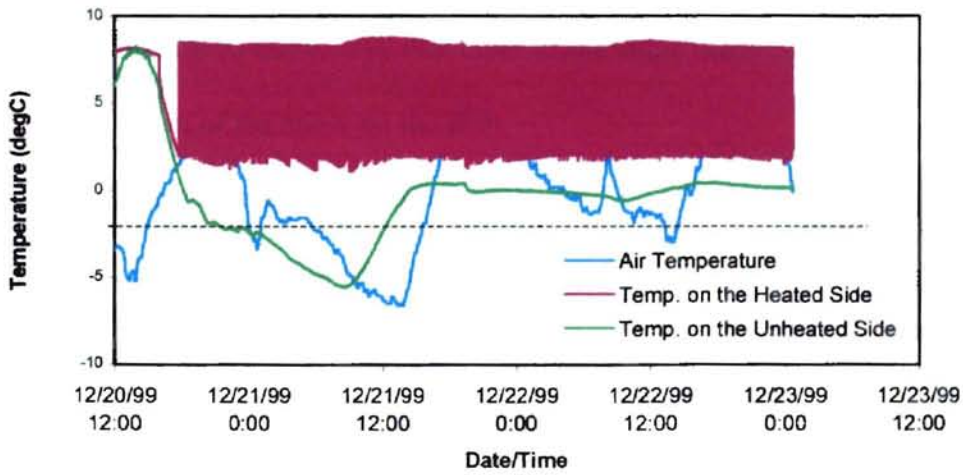

b) Corresponding Temperatures

Figure 4-14. General Response of the System to the Snow Accumulation at Stillwater Site (Artificial Snow Is Used Made in the Laboratory)

Table 4-1. Observations of the Surface Conditions

DATE/TIME	CONDITION OF THE SURFACE	
	Unheated Side	**Heated Side**
12/21/99, 2:30am	Wet snow	Wet
12/21/99, 11:30am	Wet snow	Wet
12/22/99, 1:00am	The ice under the snow	Dry
12/22/99, 1:30pm	The ice under the snow	Dry
12/22/99, 9:30pm	Ice	Wet

4.2.3.1. Snow Precipitation at Stillwater Experimental Site

On Wednesday, January 26th, 2000 it snowed at the Stillwater experimental site. The sequence of the events was noted and was as follows:

Wednesday, January 26th, 2000

- 9:00. Started to snow, very thin layer of the snow observed on the slab.
- 9:30. 5 mm of the snow on the slab.
- 10:15. 11 mm of the snow on the slab.
- 11:30. 17 mm of the snow on the slab.
- 14:45. 28 mm of the snow on the slab.
- 15:15. 28 mm of the snow on the slab.
- 17:30. 30 mm of the snow on the slab.
- 18:35. No precipitation, 30 mm of the snow on the slab.
- 19:55. 30 mm of snow on the slab, the heated side was wet.
- 22:30. 30 mm of snow on the slab, the heated side was wet.

Thursday, January 27th, 2000

- 00:15. 30 mm of the snow on the slab, the heated side was almost dry.
- 3:00. 30 mm of the snow on the slab, the heated side was wet, started to snow.
- 8:30. 62 mm of the snow on the slab.
- 9:30. 68 mm of the snow on the slab.
- 11:15. 81 mm of the snow on the slab.
- 13:05. 85 mm of the snow on the slab.
- 16:20. 86 mm of the snow on the slab.
- 23:50. 84 mm of the snow on slab, the heated side was wet.

Friday, January 28th, 2000

- 8:10. 80 mm of the snow on the slab, the heated side was dry.
- 11:55. 78 mm of the snow on the slab, the heated side was wet.
- 15:00. 73 mm of the snow on the slab, the heated side was wet
- 21:00. 72 mm of the snow on the slab, heated side was almost dry.
- *Saturday, January 29th, 2000*
- 2:30. Snowing, 77 mm of the snow on the slab, the heated side was wet.
- 12:00. 65 mm of the snow on the slab-no precipitation, the heated side was dry.

17:35. 50 mm of the snow on the slab, heated side was wet.

- 22:00. 50 mm of the snow on the slab, heated side was wet.

Monday, January 31st, 2000

- 9:00. 40 mm of the snow on the slab, heated surface was dry.
- 15:50. The slab was completely dry.

Snow accumulation and corresponding air temperature is shown in Figure 4-15.

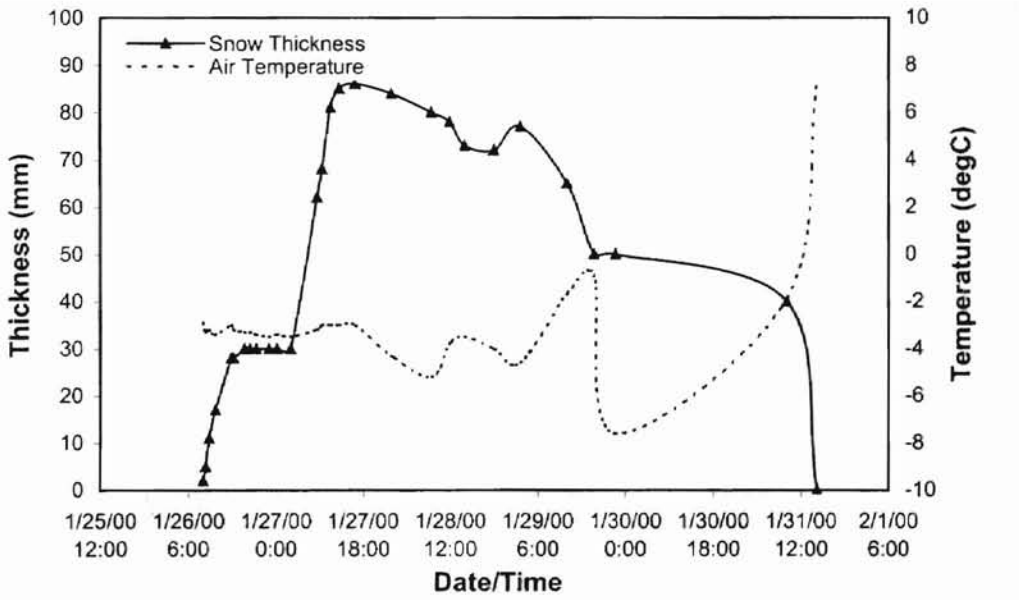

Figure 4-15. Snow Thickness on the Slab and Air temperature Over the Time of the Event

During the observations, series of photos were taken for the different surface conditions that occurred over the both heated and unheated side of the sensor. In Figure 4-16 can be seen that even the snow is present on the slab, heated side was dry over short periods of time due to the heating underneath the surface.

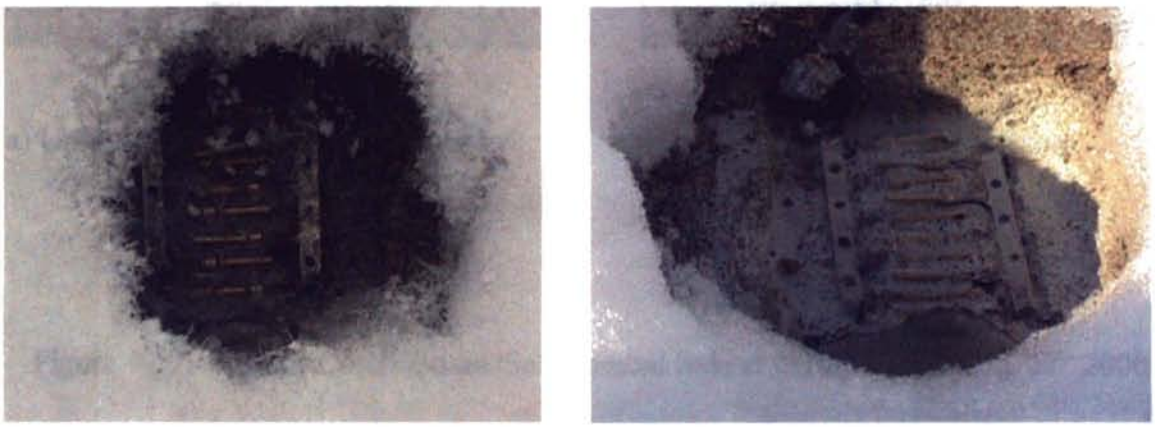

a) The Heated Surface Wet b) The Heated Surface Dry

Figure 4-16. Surface Conditions on the Heated Side

The unheated side under the snow remained dry during the whole period of time when snow precipitation occurred. The condition on the unheated side of the slab, at 8:30am on January 27th 2000 is shown in Figure 4-17.

a) Unheated Side Underneath the Snow Was Dry

b) Slab Under the Snow

Figure 4-17. Surface Condition on the Unheated Side at 8:30am on January 27th 2000

The electrical resistance over the electrodes on the unheated side of the sensor under the dry snow was the same as one that corresponds to an open circuit, i.e. it was infinitely high. For the heated side values of the electrical resistance corresponded to a wet surface condition due to the presence of moisture from melted snow. Sometimes, heated side was dry, even though the snow was present on the slab. As mentioned before, heater was initially oversized providing more power than necessary, and causing surface to dry out faster.

During the days of the snow precipitation, conditions on the experimental bridge deck located near the surrogate bridge freezing sensor were monitored. The bridge deck surface underneath the snow was also dry, being in the same condition as the surface of the slab underneath the snow.

Records of the event are given in Figures 4-18 and 4-19. As can be seen in Figure 4-18 the temperature on the heated side rose as high as 25°C. That was due to the fact that the control unit for the heater was out of calibration and needed to be recalibrated in order to control heater operation in the temperature range between 1 and 5°C.

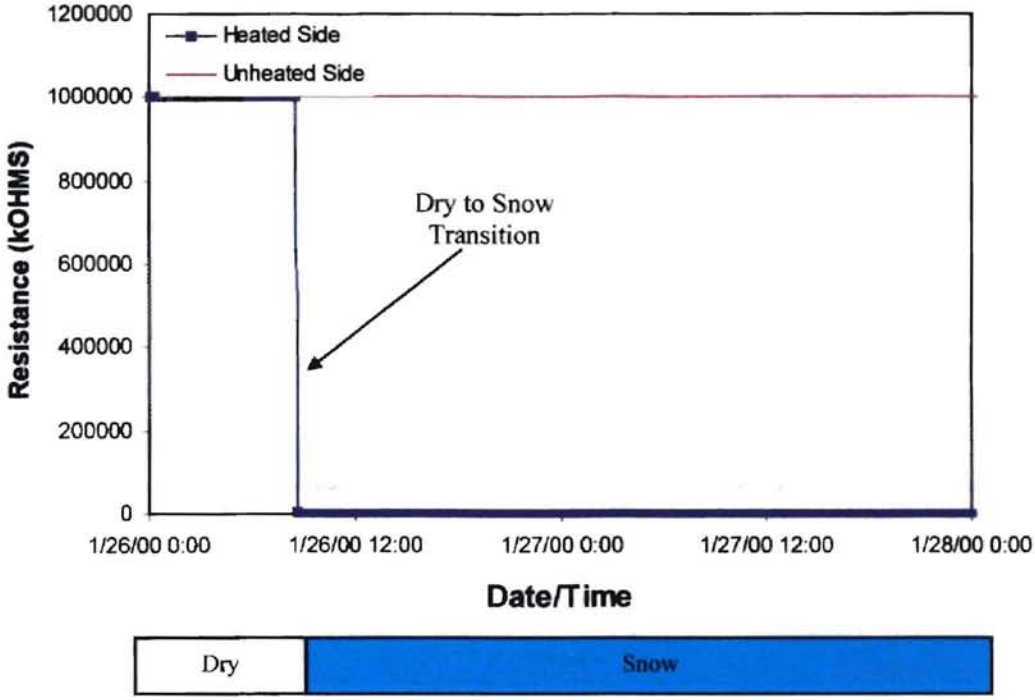

a) System's Response to the Snow Accumulation

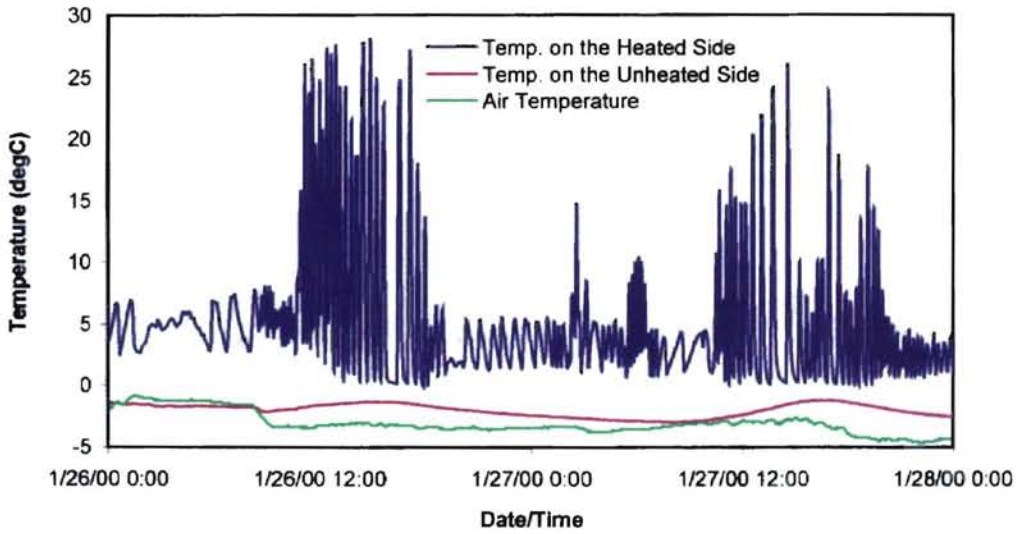

b) Corresponding Temperatures

Figure 4-18. General Response of the System to the Dry Snow at Stillwater Site Over Two-Day Period

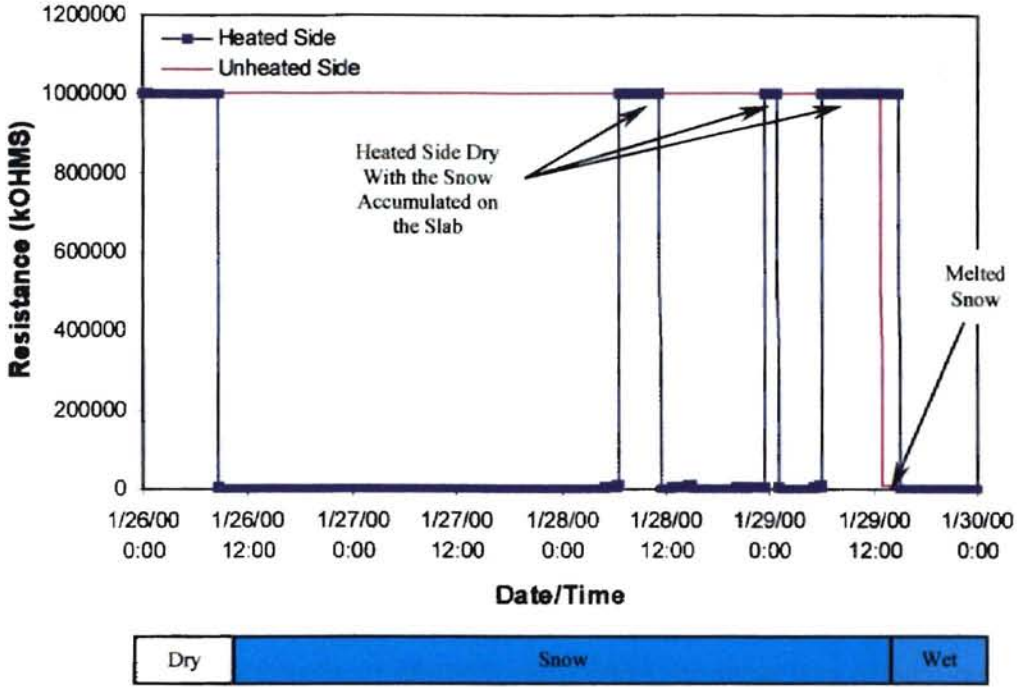

a) System's Response to the Snow Accumulation

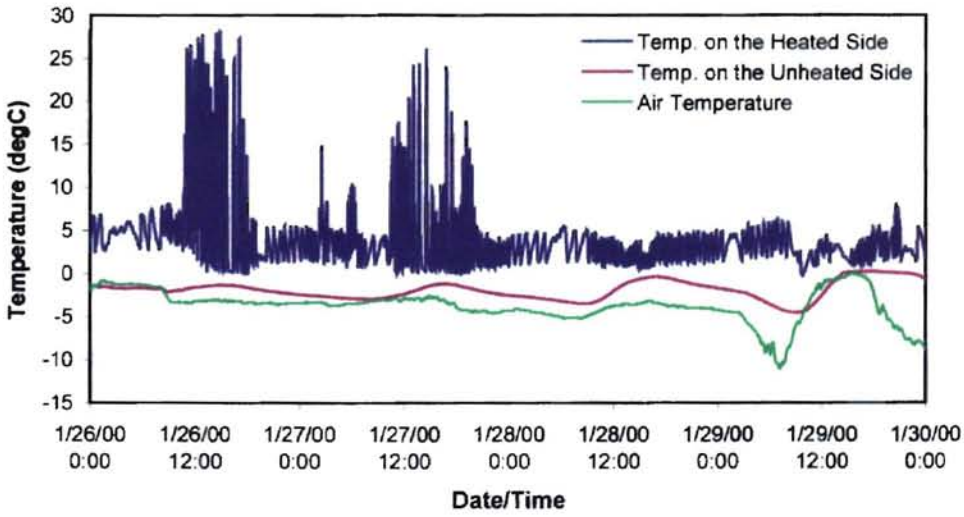

b) Corresponding Temperatures

Figure 4-19. General Response of the System to the Dry Snow at Stillwater Site Over Four-Day Period

4.2.3.2. Snow Precipitation at the Burbank Experimental Site

On March 10th 2000 there was an event where snow precipitation occurred at Burbank area. According to the information obtained (Muchmore, 2000) the snowfall started around 5:00pm and began to get fairly heavy early that evening. When it was over 4 to 7 inches were accumulated on the ground. The exact amount of the snow accumulated on the sensor remained unknown. The snow disappeared pretty quickly the following day since the weather warmed up and the temperature was between 10 and 20°C.

Looking at the results given in Figure 4-20 can be said that the system behaved differently than previously observed pattern when the snow was present on the surface at the Stillwater experimental site. There was no significant resistive imbalance observed. However, the presence of snow can still be inferred. It shows presence of the moisture on both heated and unheated side of the sensor. The likely explanation for such a behavior is that when it started to snow, the surface temperature of the slab was around 7°C, causing the snow to melt when it came in contact with the surface. Initial snow melting was recognized by Mesonet weather station rain gauge. However, no further liquid precipitation was detected until the accumulated snow started to melt. Later the temperature decreased, and snowfall intensified, covering the melted snow. However, the surface underneath the snow remained wet, due to initially formed water layer from the melted snow. Obviously water never changed its phase even though there was a snow accumulated above it. When the air temperature increased significantly, the remaining snow started to melt, turning into the water that was detected by the Mesonet instruments as an increase in liquid precipitation. Shown on the plot the process of melting started

around noon on March 11th 2000. From the readings can be seen that the snow melted down completely around 5pm.

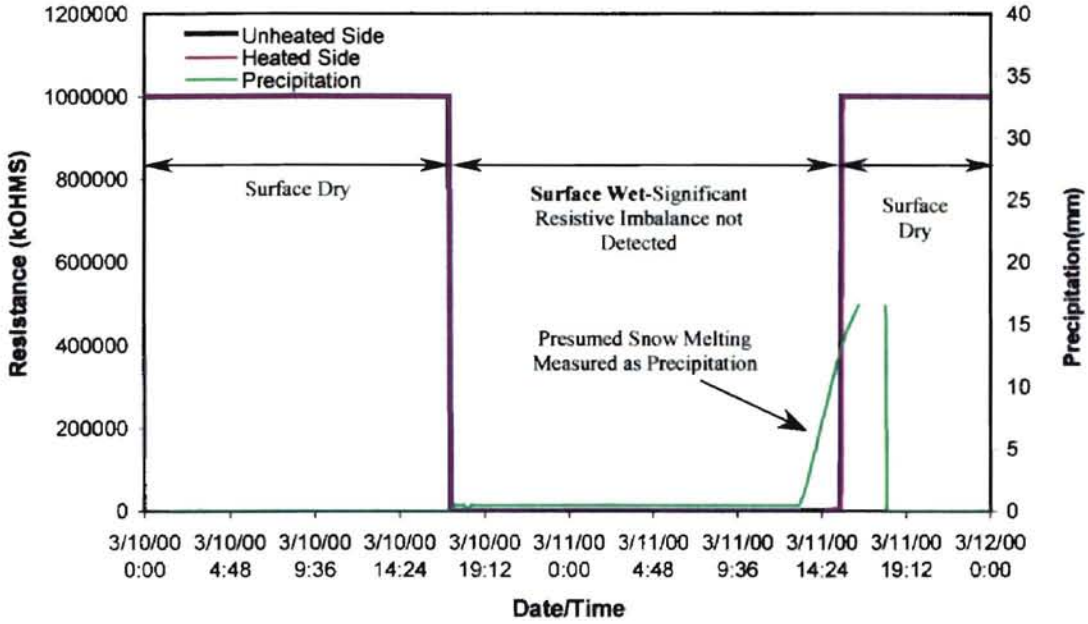

a) System's Response to the Frozen Precipitation

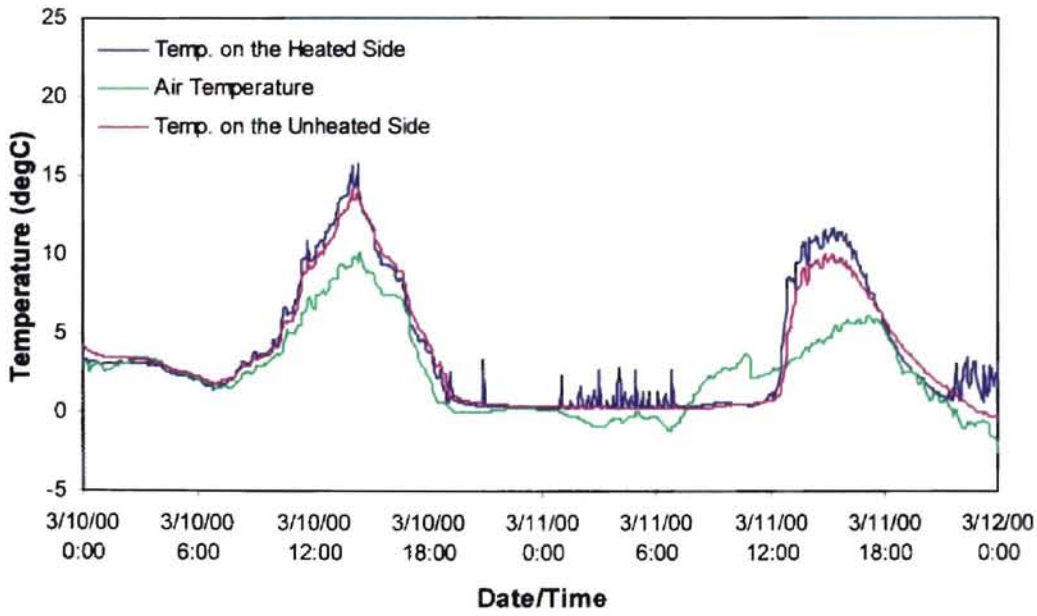

b) Corresponding Temperatures

Figure 4-20. Frozen Precipitation (Snow) Inferred by the System at Burbank Site

4.2.3.3. Snow Precipitation at the Buffalo Experimental Site

On March 16th 2000, there was an icing/snow event that struck Buffalo area. Frozen (snow) and liquid (rain) precipitation occurred at the same time. The temperatures at the surface during the event were around –5°C, causing a significant icing on it. Unfortunately, due to the malfunction of data logger power supply that occurred on March 13th 2000 the system failed to record this event.

4.2.4. Reaction of the Sensor to the Ice Formation

To simulate icing conditions, water was poured over both heated and unheated side of the slab on a night when the slab was likely to freeze. On the unheated side just enough water was added to cover the electrodes, while on the heated side the whole active volume of the sensor was filled with water in order to prevent fast evaporation due to heating. The experiment was conducted on November 29th and 30th 1999. The sensor was covered with water at 22:00 hours, when the air temperature was around 5°C. The idea behind this experiment was to wait until the temperature dropped below the freezing point and observe ice on the slab.

The condition on the surface observed on November 30th at 1:00 and 3:00 hours was solid ice over electrodes on the unheated side, and water on the heated side. Another check was done at 11:00 hours the same day, and complete slab was dry. Readings from the data logger clearly show the difference between distinct surface conditions observed during the experiment. Values of the electrical resistance that corresponded to an icy condition ranged from 1000 to 10000kΩ, and match pretty well those obtained from the similar experiment conducted in the laboratory. Results are shown in Figure 4-21. Again, problems with the temperature control can be seen.

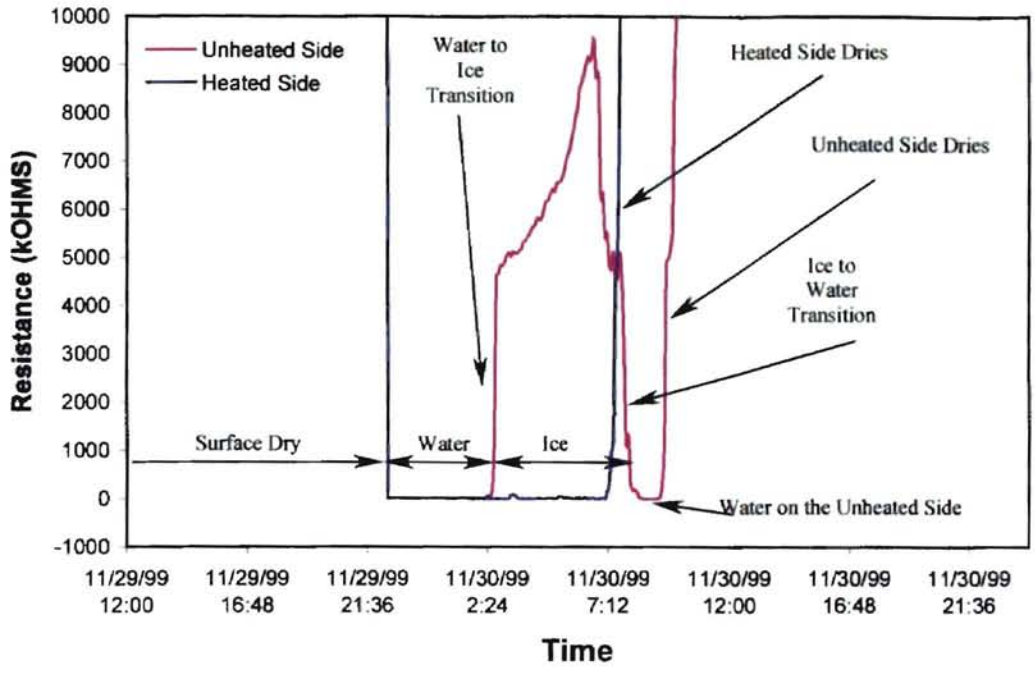

a) Sensor's Response to an Ice Formation

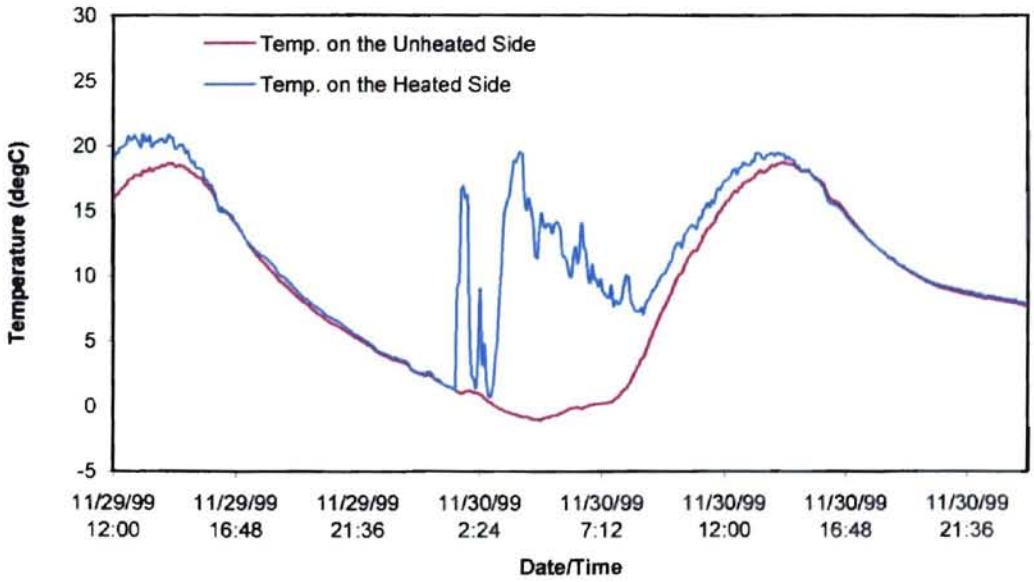

b) Corresponding Temperatures

Figure 4-21. System Response to Ice Formation at Stillwater Site

Another ice formation over the electrodes was observed when slab was tested with wet snow artificially made in the laboratory on December 21st 1999. After a certain period of time when the surface temperature reached freezing point accumulated water in the snow started to freeze forming an ice layer over the electrodes on the unheated side. Ice was observed on December 22nd 1999 at noon, underneath the snow, covering the whole slab's surface except the heated side that was dry. The results were previously shown in Figure 4-14.

The event where liquid precipitation (rain) changed phase to an ice, influenced by the temperatures being below freezing point did not occur at any of the experimental sites while the systems had run.

4.2.5. Frost Indication

As was discussed before, frost detection cannot be directly made with this system. However, it can be inferred with additional information obtained from Mesonet weather system. Based on the data for air temperature and relative humidity the dew point temperature can be calculated. If the dew point temperature of ambient air is higher than or equal to surface temperature and surface temperature is close to or below freezing point frost will occur.

The concrete slab was checked randomly for a frost formation over the surface. On February 9th 2000 at 5:30am a significant amount of frost was observed on the slab's surface and over the electrodes on the unheated side at Stillwater experimental site. Frost, of course, did not form on the heated side, and the heated side remained dry. Looking at the results shown in Figure 4-22 can be assumed that frost occurred when the surface temperature was below freezing and also below the dew point temperature.

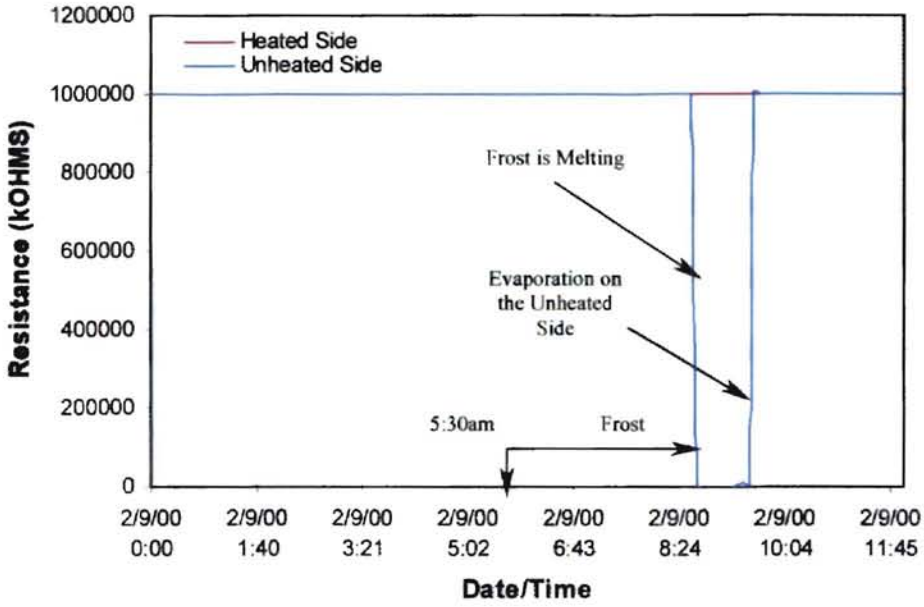

a) Sensor's Response to Frost Formation

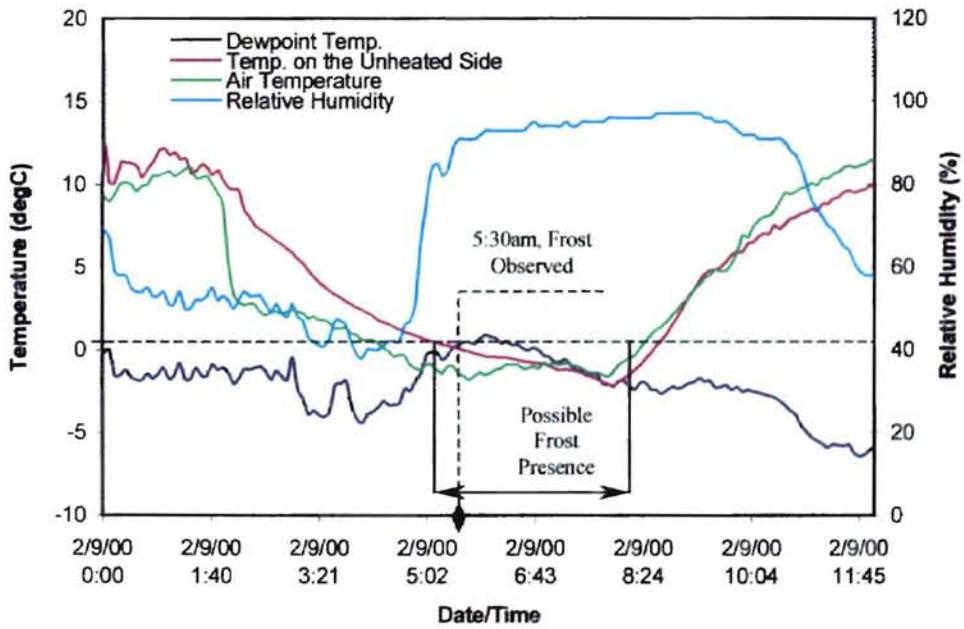

b) Corresponding Temperatures and Relative Humidity

Figure 4-22. System Response to Frost Formation at Stillwater Experimental Site

4.3. Analysis Based on Experimental Results

During the weeks of lab and in-situ testing values of electrical resistance and temperature were obtained from data logger scans for different surface conditions. A computer program can process those readings in order to declare surface condition for every set of scans. Based on the results, and observed surface conditions computer program will be developed based on following observations:

- *Icy surface*- resistance is high and it varies from $1x10^3$ to $2x10^4$ kΩ, while unheated surface temperature is below freezing point. On the heated side of the sensor, resistance is very low, and varies from 2 to 100 kΩ, corresponding to moisture present over the electrodes. Temperature on the heated side is maintained around 1°C, controlled by heater operation. Due to temperature sensor accuracy solid ice state might occur even for temperature around 0.85°C. However, the change in resistance that describes solid ice state did not occur for such high limits of inaccuracy, but it was more consistent with the readings close to freezing point meaning that inaccuracy of temperature sensors was less than outer margins for established range of ±0.85°C.
- *Dry*-resistances on both heated and unheated side show values that correspond to those of an open circuit, namely greater than 20000kΩ.
- *Damp, less than 100% coverage of electrodes with water*- readings for the resistance can vary, but always are greater than 100kΩ both sides of sensor, with temperature of the surface above freezing point. After

certain period of time water will evaporate, if no further precipitation occurs. The condition of surface drying out can be detected by observing sequence of readings over time where resistance raises and temperature is still above freezing point. When resistance reaches values greater than 20000kΩ, the surface is dry. However, due to heater operation, heated surface can dry out even when the unheated side is still wet, snow coated or ice coated.

- *Wet (100% coverage of electrodes with water)*-values for the resistance can vary, but always are less than 100kΩ, with the majority of values less then 10 kΩ. The temperature of the slab is above freezing point, and in order to separate wet conditions from phase change temperatures and to incorporate temperature sensors accuracy, temperature of the slab should be above 1.5°C, else it might be considered as phase change.
- *Frost*-it can be inferred for the electrical resistance on the unheated side being equal to that of an open circuit (>20000kΩ), when the temperature on the same side is less than freezing and also the dew point temperature of the surrounding air. As the temperature on the unheated side raises above 0°C, resistance should indicate wet conditions, due to melted frost crystals. The heated side remains dry, with temperatures around 1°C.
- *Wet snow*-values for the electrical resistance on the unheated side are between 100 and 1000 kΩ, with the majority of values in the range of 100 to 300 kΩ. Electrical resistance on the unheated side reflected values for the wet conditions, caused by melted snow. Temperature on

the unheated side is always close to 0°C or below, with the temperature on the heated side maintained above 1°C. To account for error of the temperature sensors, monitored temperatures on the unheated side should be less than 1°C on the instrument. Wet snow that occurs at higher temperatures is treated below as *snow-possible* condition.

- *Dry snow*- electrical resistance on the unheated side should be equal to that of an open circuit (>20000kΩ), while the heated side gives values signaling wet conditions due to the melted snow. Temperature on the unheated side must be equal or less than the freezing point.
- *Water-Ice transition*-when measured temperatures start to decrease below 1.5°C, to between -0.5°C and 1.5°C (accounting for the accuracy of temperature sensors), and there is water over electrodes, resistance will start to increase, thus for a sequence of readings with temperature decreasing and resistance increasing, transition from water to ice can be identified.
- *Ice –Water transition*- principle is the same as explained before, but this time temperature increases, between -0.5°C and 1.5°C (again, accounting for the accuracy of temperature sensors), while resistance values descend.
- *Snow-possible*-if the snowfall occurs when the air temperature is relatively high (assume higher than measured 2°C), the sensors will indicate wet conditions on both sides due to melted snow. With the fast snow accumulation over the wet surface, the temperature on the

unheated side will decrease and stay between –0.5 and 1.5°C (accounting for the accuracy of temperature sensors).

Temperature on the heated side is above 1°C due to heater operation. Resistances on both sides, heated and unheated are <100 kΩ, still signaling wet conditions.

A computer program was developed that, for given electrical resistances and temperatures, can determine the surface conditions. Input values obtained from the data logger scans for an actual surface condition can be used. The program should determine the surface condition that matches the actual one observed in the field.

Information that is required for the inputs consist of temperatures and resistances on the heated and unheated side as well as the relative humidity and temperature of the surrounding air. Using the procedure described in ASHRAE (1997), the program is able to calculate the dew point temperature of the ambient air. For the calculations of the dew point temperature following equations were used in the program:

$$\alpha = A \cdot T^2 + B \cdot T + C + D \cdot T^{-1} \tag{4-1}$$

$$p_{WS} = 1000^{\alpha} \tag{4-2}$$

$$p_w = \phi \cdot p_{WS} \tag{4-3}$$

$$\beta = \ln(p_{WS}) \tag{4-4}$$

$$t_{dew} = E \cdot \beta^4 + F \cdot \beta^3 + G \cdot \beta^2 + H \cdot \beta + K \tag{4-5}$$

where,

T = absolute temperature of the ambient air, K,

p_{ws} = saturation vapor pressure, Pa,

p_w = water vapor pressure, Pa,

ϕ = relative humidity of the ambient air,

t_{dew} = dew point temperature, °C,

α,β = coefficients feature temperatures in K and pressure in Pa

A, B, C, D, E, F, G, H, K are constants that are for the different temperature and pressure range tabulated in ASHRAE (1997).

The program is able to determine surface condition for each of the readings obtained from data logger.

The basic algorithm that describes process of determination of surface conditions for different input values is shown in Figure 4-23. In the following section sample readings from data logger with determined surface condition for the specific cases are given. In addition, complete code listing written in VBA is enclosed in Appendix B.

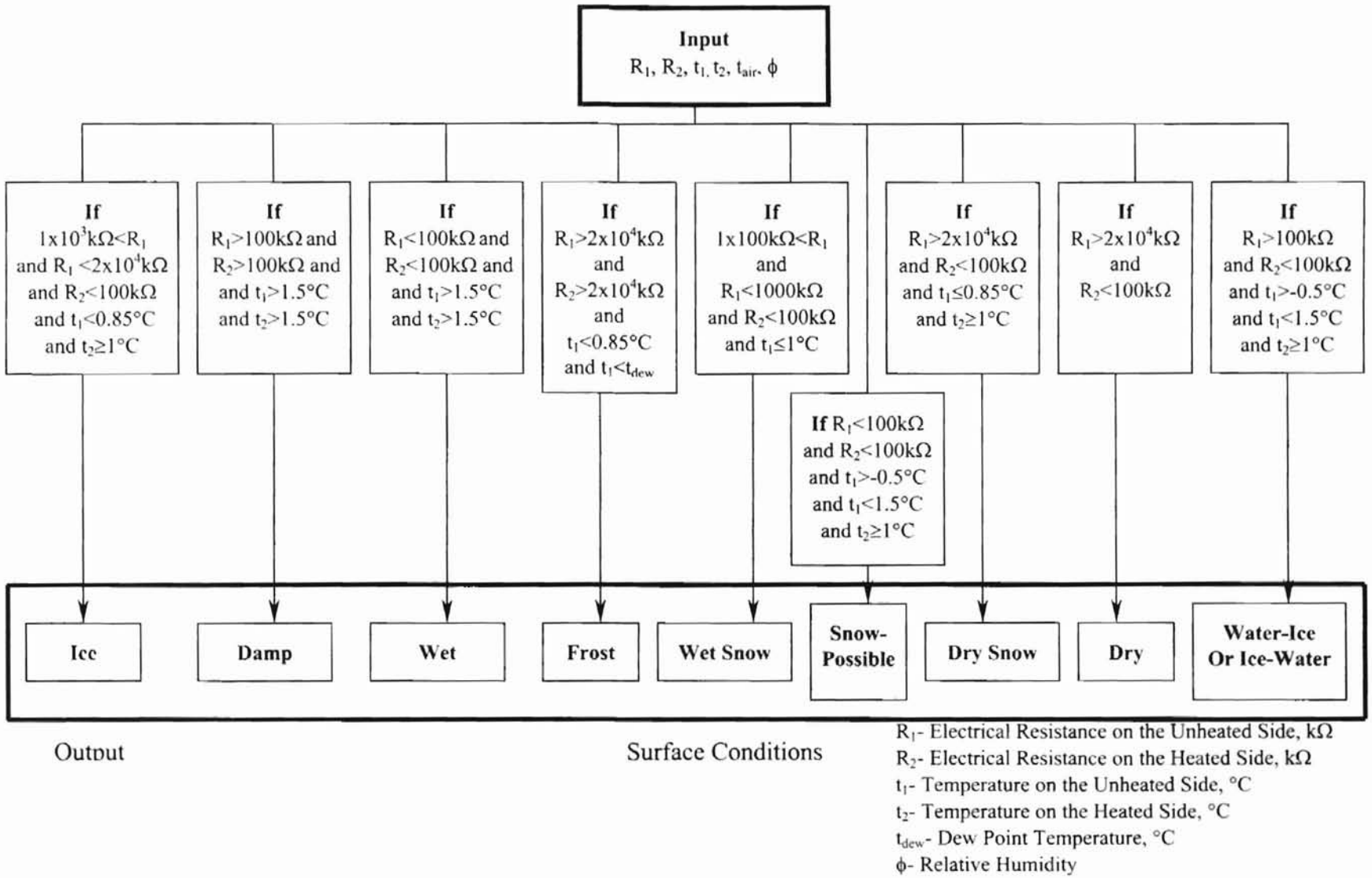

Figure 4-23. Basic Algorithm for Surface Condition Determination

4.3.1. Sample Readings and Surface Conditions Determined by the Program

Three examples of sample readings from the data logger are extracted from Excel files. The first example, given in Figure 4-24 shows recordings from January 26th 2000, when the snow occurred at the Stillwater experimental site. Highlighted are surface conditions determined by the program.

Microsoft Excel - Sysck12

File Edit View Insert Format Tools Data Window Help

Times New Roman 12

H95

	A	B	C	D	E	F	G	H
95		Temp on Unheated Side	Temp on Heated Side	Air Temp	Resistance-Unheated Side	Resistance-Heated Side	Rel Humidity	
96	TIME	(degC)	(degC)	(degC)	(kOHMS)	(kOHMS)	/	Condition
97	01/26/2000 7:49	-1.732	3.537	-1.500	1000000	1000000	0.53	Dry
98	01/26/2000 7:54	-1.721	3.310	-1.500	1000000	1000000	0.53	Dry
99	01/26/2000 7:59	-1.711	2.821	-1.500	1000000	1000000	0.53	Dry
100	01/26/2000 8:04	-1.693	2.839	-1.500	1000000	1000000	0.54	Dry
101	01/26/2000 8:09	-1.731	4.338	-1.500	1000000	1000000	0.54	Dry
102	01/26/2000 8:14	-1.724	6.650	-1.600	1000000	1000000	0.58	Dry
103	01/26/2000 8:19	-1.735	7.755	-1.800	1000000	1000000	0.62	Dry
104	01/26/2000 8:24	-1.793	6.969	-1.900	1000000	1000000	0.67	Dry
105	01/26/2000 8:29	-1.827	5.624	-2.100	1000000	1000000	0.72	Dry
106	01/26/2000 8:34	-1.907	4.467	-2.200	1000000	1000000	0.74	Dry
107	01/26/2000 8:39	-1.979	5.086	-2.400	1000000	3121	0.77	Dry snow
108	01/26/2000 8:44	-2.044	7.282	-2.500	1000000	1557	0.79	Dry snow
109	01/26/2000 8:49	-2.060	4.985	-2.600	1000000	961	0.82	Dry snow
110	01/26/2000 8:54	-2.092	7.964	-2.700	1000000	731	0.84	Dry snow
111	01/26/2000 8:59	-2.089	6.636	-2.900	1000000	362	0.85	Dry snow
112	01/26/2000 9:04	-2.089	4.028	-3.000	1000000	278	0.86	Dry snow
113	01/26/2000 9:09	-2.077	8.043	-3.100	1000000	90	0.87	Dry snow
114	01/26/2000 9:14	-2.075	4.754	-3.200	1000000	79	0.88	Dry snow
115	01/26/2000 9:19	-2.044	7.539	-3.300	1000000	36	0.89	Dry snow
116	01/26/2000 9:24	-2.002	3.919	-3.300	1000000	71	0.9	Dry snow
117	01/26/2000 9:29	-2.004	6.160	-3.300	1000000	22	0.91	Dry snow
118	01/26/2000 9:33	-1.972	4.727	-3.300	1000000	16	0.92	Dry snow
119	01/26/2000 9:38	-1.990	5.981	-3.300	1000000	13	0.92	Dry snow
120	01/26/2000 9:43	-1.958	4.978	-3.300	1000000	13	0.92	Dry snow
121	01/26/2000 9:48	-1.957	6.078	-3.300	1000000	11	0.92	Dry snow
122	01/26/2000 9:53	-1.939	3.311	-3.300	1000000	15	0.93	Dry snow

SYSCK12 / Weather / Snow / SnowThickness / Test /

Figure 4-24. Sample Readings From the Data Logger with the Corresponding Surface Conditions Determined by the Program in the Case when Dry Snow Occurred

Example given in Figure 4-25 shows recordings from November 30th 1999, when the ice over the surface was formed at the Stillwater experimental site. Highlighted are surface conditions determined by the program.

Microsoft Excel - sysck2

File Edit View Insert Format Tools Data Window Help

L1057

	A	B	C	D	E	F	G	H
1049		Temp. on Unheated Side	Temp. on Heated Side	Air Temp	Resistance-Unheated Side	Resistance-Heated Side	Rel. Humidity	
1050	TIME	(degC)	(degC)	(degC)	(kOHMS)	(kOHMS)	/	Condition
1051	11/30/1999 2:16	1.064	1.443	1.5	10	2	0.64	Wet
1052	11/30/1999 2:21	1.0214	4.4	1.5	7	43	0.58	Wet
1053	11/30/1999 2:26	0.9228	9.029	1.4	3	58	0.48	Wet
1054	11/30/1999 2:31	0.83537	3.376	1.3	19	9	0.48	Wet
1055	11/30/1999 2:36	0.63091	4.798	1.1	190	6	0.45	Wet/Ice
1056	11/30/1999 2:41	0.49507	1.952	1.0	1234	6	0.45	Wet/Ice
1057	11/30/1999 2:46	0.36009	0.808	0.8	4631	6	0.45	Wet/Ice
1058	11/30/1999 2:51	0.30569	0.779	0.8	4676	7	0.43	Wet/Ice
1059	11/30/1999 2:56	0.14196	1.556	0.6	4848	5	0.41	Wet/Ice
1060	11/30/1999 3:01	0.034811	3.423	0.5	4838	5	0.38	Wet/Ice
1061	11/30/1999 3:06	-0.056657	5.082	0.4	4932	5	0.35	Ice
1062	11/30/1999 3:11	-0.15513	7.975	0.3	5050	6	0.33	Ice
1063	11/30/1999 3:16	-0.20513	10.508	0.3	5104	7	0.34	Ice
1064	11/30/1999 3:21	-0.28751	13.676	0.2	5027	76	0.33	Ice
1065	11/30/1999 3:26	-0.38235	15.244	0.1	5116	89	0.34	Ice
1066	11/30/1999 3:31	-0.408	15.777	0.1	5091	68	0.33	Ice
1067	11/30/1999 3:36	-0.48222	16.421	0.0	5098	17	0.3	Ice
1068	11/30/1999 3:41	-0.54142	17.726	-0.1	5151	7	0.29	Ice
1069	11/30/1999 3:46	-0.59684	18.861	-0.1	5189	8	0.3	Ice
1070	11/30/1999 3:51	-0.62171	18.782	-0.2	5330	8	0.31	Ice
1071	11/30/1999 3:56	-0.69363	19.253	-0.2	5350	6	0.3	Ice
1072	11/30/1999 4:01	-0.7317	19.524	-0.3	5443	8	0.31	Ice
1073	11/30/1999 4:06	-0.79069	19.378	-0.3	5487	7	0.32	Ice
1074	11/30/1999 4:11	-0.77695	16.221	-0.3	5605	9	0.33	Ice
1075	11/30/1999 4:16	-0.78275	15.104	-0.3	5643	9	0.33	Ice
1076	11/30/1999 4:21	-0.85951	15.976	-0.4	5729	8	0.32	Ice

SYSCK2 / Ice / Test /

Figure 4-25. Sample Readings From the Data Logger with the Corresponding Surface Conditions Determined by the Program in the Case When Ice Occurred

Example given in Figure 4-26 shows recordings from December 21st 1999, when the sensor is tested on the presence of the wet snow made in the laboratory at the Stillwater experimental site. Highlighted are surface conditions determined by the program.

Microsoft Excel - Sysck5

File Edit View Insert Format Tools Data Window Help

H2135 Wet snow

	A	B	C	D	E	F	G	H
2108		Temp. on Unheated Side	Temp. on Heated Side	Air Temp	Resistance-Unheated Side	Resistance-Heated Side	Rel. Humidity	
2109	TIME	(degC)	(degC)	(degC)	(kOHMS)	(kOHMS)	/	Condition
2110	12/21/1999 3:02	-3.464	10.240	-4.8	415	12	0.67	Wet snow
2111	12/21/1999 3:03	-3.483	7.592	-4.8	417	23	0.67	Wet snow
2112	12/21/1999 3:04	-3.478	5.641	-4.8	418	22	0.67	Wet snow
2113	12/21/1999 3:05	-3.497	4.177	-4.8	417	24	0.67	Wet snow
2114	12/21/1999 3:06	-3.519	3.095	-4.9	419	12	0.68	Wet snow
2115	12/21/1999 3:07	-3.509	2.281	-4.9	420	24	0.68	Wet snow
2116	12/21/1999 3:08	-3.526	1.678	-4.9	421	12	0.68	Wet snow
2117	12/21/1999 3:09	-3.545	11.886	-4.9	422	24	0.68	Wet snow
2118	12/21/1999 3:10	-3.545	13.455	-4.9	423	13	0.68	Wet snow
2119	12/21/1999 3:11	-3.563	10.145	-4.9	424	24	0.66	Wet snow
2120	12/21/1999 3:12	-3.556	7.499	-4.9	424	22	0.66	Wet snow
2121	12/21/1999 3:13	-3.573	5.591	-4.9	424	23	0.66	Wet snow
2122	12/21/1999 3:14	-3.590	4.085	-4.9	426	8	0.66	Wet snow
2123	12/21/1999 3:15	-3.610	3.027	-4.9	426	25	0.66	Wet snow
2124	12/21/1999 3:16	-3.632	2.202	-5	427	7	0.66	Wet snow
2125	12/21/1999 3:17	-3.627	1.578	-5	427	25	0.66	Wet snow
2126	12/21/1999 3:18	-3.649	11.806	-5	428	7	0.66	Wet snow
2127	12/21/1999 3:19	-3.671	13.376	-5	428	25	0.66	Wet snow
2128	12/21/1999 3:20	-3.670	10.061	-5	429	21	0.66	Wet snow
2129	12/21/1999 3:21	-3.691	7.410	-5.1	429	25	0.69	Wet snow
2130	12/21/1999 3:22	-3.690	5.476	-5.1	431	13	0.69	Wet snow
2131	12/21/1999 3:23	-3.705	3.994	-5.1	432	26	0.69	Wet snow
2132	12/21/1999 3:24	-3.726	2.912	-5.1	434	12	0.69	Wet snow
2133	12/21/1999 3:25	-3.720	2.116	-5.1	436	25	0.69	Wet snow
2134	12/21/1999 3:26	-3.746	1.482	-5.2	437	6	0.77	Wet snow
2135	12/21/1999 3:27	-3.767	11.734	-5.2	438	17	0.77	Wet snow

SYSCK5 / Weather / Test /

Figure 4-26. Sample Readings From the Data Logger with the Corresponding Surface Conditions Determined by the Program in the Case When Wet Snow Occurred

Example given in Figure 4-27 shows recordings from March 11th 2000, when the snow occurred at the Burbank experimental site. Highlighted are surface conditions determined by the program.

Microsoft Excel - burb2

File Edit View Insert Format Tools Data Window Help

F4426 = 86.573

	A	B	C	D	E	F	G	H
4416		Temp. on Unheated Side	Temp. on Heated Side	Air Temp.	Resistance-Unheated Side	Resistance-Heated Side	Rel. Humidity	
4417	TIME	(degC)	(degC)	(degC)	(kOHMS)	(kOHMS)	/	Condition
4418	03/10/2000 18:32	2.954	2.170	0.700	2	12	0.84	Wet
4419	03/10/2000 18:37	3.088	2.414	0.700	8	11	0.83	Wet
4420	03/10/2000 18:42	3.199	2.633	0.600	11	11	0.82	Wet
4421	03/10/2000 18:47	2.872	2.175	0.600	12	8	0.82	Wet
4422	03/10/2000 18:52	2.489	1.399	0.600	7	26	0.82	Wet
4423	03/10/2000 18:57	2.357	1.223	0.500	6	34	0.82	Wet
4424	03/10/2000 19:02	1.949	0.967	0.500	11	28	0.81	Wet
4425	03/10/2000 19:07	1.430	0.621	0.400	31	16	0.81	Wet
4426	03/10/2000 19:12	0.940	2.532	0.200	23	87	0.8	Wet
4427	03/10/2000 19:17	0.837	0.925	0.100	11	22	0.79	Snow possible
4428	03/10/2000 19:22	0.841	0.792	0.000	25	17	0.78	Snow possible
4429	03/10/2000 19:27	0.882	0.751	0.000	19	21	0.78	Snow possible
4430	03/10/2000 19:32	0.876	0.713	0.000	21	79	0.77	Snow possible
4431	03/10/2000 19:37	0.931	0.691	0.000	21	95	0.76	Snow possible
4432	03/10/2000 19:42	0.845	0.670	0.000	21	30	0.75	Snow possible
4433	03/10/2000 19:47	0.804	0.608	0.000	19	31	0.75	Snow possible
4434	03/10/2000 19:52	0.798	0.579	0.000	19	40	0.75	Snow possible
4435	03/10/2000 19:57	0.769	0.551	0.000	18	39	0.76	Snow possible
4436	03/10/2000 20:02	0.786	0.480	0.000	18	46	0.76	Snow possible
4437	03/10/2000 20:07	0.750	0.487	0.000	18	35	0.76	Snow possible
4438	03/10/2000 20:12	0.689	0.493	0.000	18	35	0.76	Snow possible
4439	03/10/2000 20:17	0.677	0.458	0.000	17	35	0.74	Snow possible
4440	03/10/2000 20:22	0.670	0.452	0.000	16	37	0.73	Snow possible
4441	03/10/2000 20:27	0.669	0.450	0.000	15	35	0.73	Snow possible
4442	03/10/2000 20:32	0.649	0.430	0.000	15	36	0.73	Snow possible
4443	03/10/2000 20:37	0.606	0.431	0.000	15	37	0.72	Snow possible
4444	03/10/2000 20:42	0.618	0.421	0.000	14	31	0.73	Snow possible
4445	03/10/2000 20:47	0.623	0.426	0.000	13	31	0.73	Snow possible
4446	03/10/2000 20:52	0.610	0.413	0.000	12	38	0.74	Snow possible
4447	03/10/2000 20:57	0.576	3.344	0.000	12	44	0.74	Snow possible
4448	03/10/2000 21:02	0.572	0.725	0.000	15	39	0.74	Snow possible
4449	03/10/2000 21:07	0.543	0.412	0.000	13	38	0.74	Snow possible
4450	03/10/2000 21:12	0.537	0.384	0.000	12	37	0.73	Snow possible

Burb2 / Snow / Test /

Figure 4-27. Sample Readings From the Data Logger with the Corresponding Surface Conditions Determined by the Program in the Case When Snow Occurred at the Burbank Experimental Site

4.4. Field Operating Experience

The systems installed at Stillwater and Burbank experimental sites did not experience any difficulties in the operation. Power supply from the batteries was always above 100% capacity, providing proper operation of the system. However, after six weeks of operation, on March 7th 2000, the system at the Buffalo experimental site experienced power loss on the data logger' side. Figure 4-28 shows that battery operated with decreased capacity even though it was charged on a daily basis.

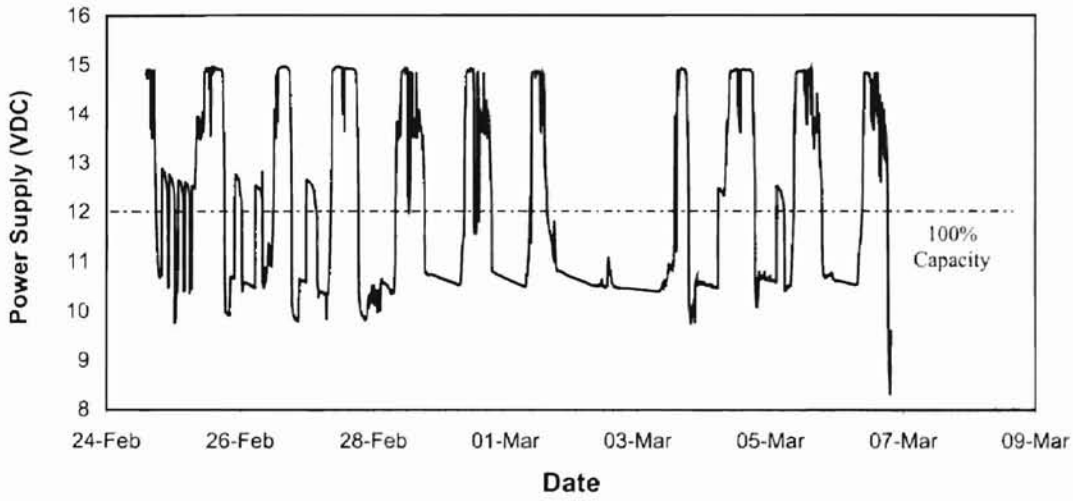

Figure 4-28. Decreased Capacity Operation

The type of the battery that was used at Buffalo site was deep cycle, lead-acid battery, with the sulfuric acid as an electrolyte. According to Lasnier and Ang (1990) a lead acid battery storage capacity decreases about 1% for every 1°C drop in temperature. 100% rated capacity is usually for the temperatures of 25°C or higher. Lead-acid capacity as a function of temperature is given in the Figure 4-29.

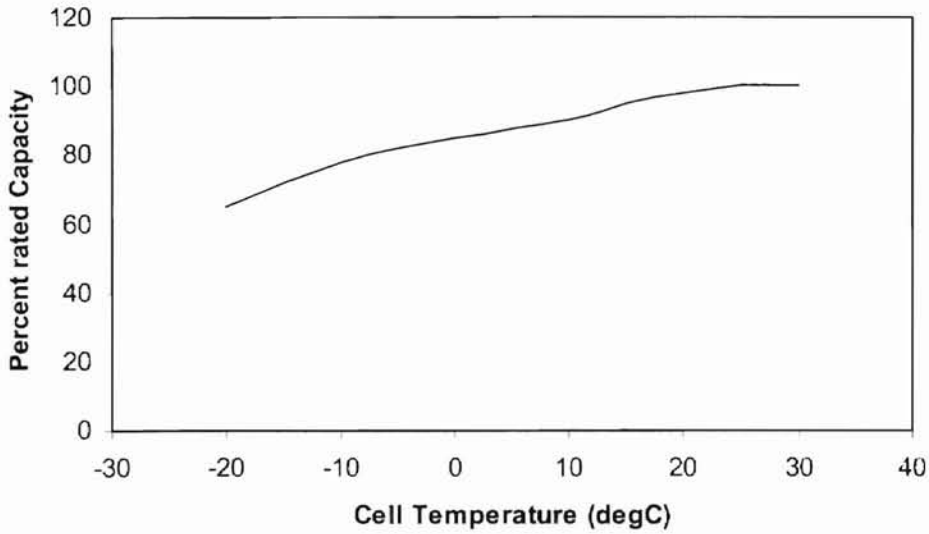

Figure 4-29. Lead-Acid Battery Capacity as a Function of the Temperature (Lasnier and Ang, 1990)

If the battery is recharged under the state of decreased storage capacity, lead sulphate sediment is deposited at the bottom of the cells. This is one of the most common causes of buckling of the battery plates. This is due to the strain on the plates because the lead sulphate occupies more space than the original active material does on the plates. In addition, excess accumulation of sediment at the bottom of the cells can cause short circuits within the battery. Evidences of short circuits within the battery are (1) continued low readings of specific gravity even though the battery is receiving the normal amount of charge and (2) rapid loss of capacity after a full charge or low battery open-circuit voltage.

In order to determine the problem, the battery was tested for the capacity. Suggested by "JFM Engineering, Inc."(2000) the most comprehensive of battery tests is the deep cycle/capacity test. In this test, the battery must be discharged at a specific rate.

Different rate of discharge requires different time period for the test duration. The suggested discharge rate is C/1 for one hour or C/20 for 20 hours, where C is battery capacity. During this test the total battery voltage must not fall below 12 V, or capacity must maintain above 100%, otherwise the battery failed capacity test and must be replaced. For the capacity test two batteries were chosen, good one and the one that failed at Buffalo experimental site. To begin with the test both batteries were fully recharged in the laboratory. The batteries were of the same capacity and manufacturer. Both were connected to the same load of 3.25Amps and tested over 14 hours. It was noted that sudden decrease in supply voltage occurred as soon as the bad battery was connected to the heater. The normal operating range for a fully charged battery is between 12 and 13 VDC. The tested battery showed oscillation of the voltage between 7.5 and 10 VDC, which brought to the conclusion that even fully recharged, battery capacity decreases suddenly, when battery was under load. According to the theory of the battery chemistry and possible problems with it, it can be concluded that one or more of the battery cells were buckled, or lead sulphate sediment was deposited at the bottom of the cells, causing them to produce less voltage than rated. The good battery maintained its capacity higher than 100% for the whole duration of the test (Figure 4-30).

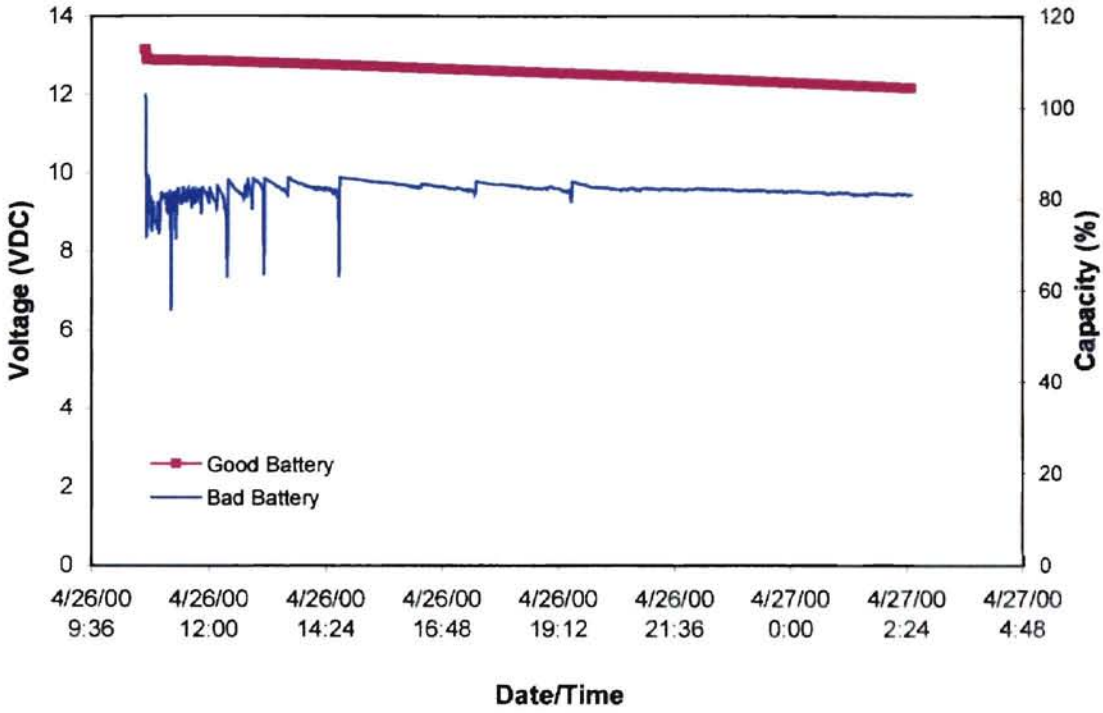

Figure 4-30. Discharge Curve for the Good and the Bad Battery

CHAPTER V

SUMMARY, CONCLUSIONS AND RECOMMENDATIONS

5.1. Summary

5.1.1. Optical Sensors

The main objective of this project, as stated earlier, was to design, test and fabricate surrogate bridge freezing sensors in order to provide training data for advanced control strategies.

In the initial stage of this project, over the course of several months optical sensors were tested in the laboratory and in the field. The first sensor evaluated was an "Optek Technologies, Inc." company product, type Reflective Object Sensor-OPB701. Exposed to outdoor conditions two sensors were tested. The first sensor lasted three weeks and the second lasted two weeks before complete failure. As laid out in Chapter 2, one of the possible reasons for equipment breakdown was condensation over photodiodes that may have lead to short circuit. The second type of the infrared sensor evaluated, the Optek OPB704, performed completely unsatisfactorily. This represented the major

disappointment to the approach, even though results obtained in detection of surface conditions with infrared sensors were promising.

Overall, operating experience with the optical sensors can be summarized as follows:

1) The sensor type OPB701 performed very well under laboratory conditions and was able to determine distinct surface conditions.
2) The same sensor failed under field operating conditions.
3) Field tests showed that the sensor type OPB704 was sensitive to ambient light conditions, but not sensitive to the surface conditions, as laid out in Chapter 2.

5.1.2. Heated Resistance/Temperature Sensors

Because of time constraints, a different approach was applied where three heated resistance/temperature sensors were designed, tested and fabricated. The first system was deployed at OSU Petroleum laboratory site in Stillwater. Two other systems were installed at Mesonet weather station sites, in Buffalo and Burbank, respectively. The air temperature and relative humidity, along with other data obtained from the sensor itself gave a useful input for the surface condition prediction. Systems were monitored over the winter and data were recorded.

Results provided by the systems and operating experience are summarized in the two following sections.

5.1.2.1. System Reliability

To provide continuous system operation over the winter, power supply batteries used in it should maintain over 100% of their capacity all the time.

1) For the two systems installed at Stillwater and Burbank experimental sites no problems were experienced regarding loss in the battery capacity.
2) A problem occurred at the Buffalo experimental site on March 7th 2000, where decreased battery capacity produced insufficient voltage for data logger's operation, which resulted in a loss of data. Due to this problem, the snow/ice event was not recorded. The reason for the power failure was the malfunction in the battery itself, which was explained in Chapter 4.

5.1.2.2. System Accuracy

In an attempt to find out how reliable this system was, visual surface condition observations were noted and compared to those recorded by the system. However, visual inspection of surface conditions was conducted only at the Stillwater experimental site since it was close enough to be monitored every day. Results obtained from two remote sites in Buffalo and Burbank were evaluated based on the information obtained from Mesonet weather stations and training data provided by the first system.

1) In cases where moisture, ice, snow or frost were observed on the slab's surface at the Stillwater site, data analysis matched visual observations.
2) For the two other systems, data analysis showed that the systems were able to detect any liquid precipitation that occurred.
3) Frozen precipitation (snow, freezing rain) did not occur at Buffalo site while system was operational.
4) During the snow event that occurred at Burbank site on March 10th 2000 a significant resistive imbalance was not detected. The system detected liquid precipitation while there was a significant snow accumulation over the slab.

However, it can be inferred from the results that was possible snow accumulation on the surface. The program algorithm showed those scans as a snow-possible condition.

The next section is devoted to the conclusions reached by this experimental study.

5.2. Conclusions

1) Over the course of this experimental study, optical sensors that could have met the research objectives satisfactorily were not found.
2) The desired result from the surrogate bridge freezing sensor was to provide information from which distinct surface conditions can be recognized. In this respect, and with due consideration given to the design and duration of testing of the detection device involved in this project, the accuracy and therefore the effectiveness of the system as a whole could be regarded as satisfactory. This evaluation was based on the detectors responses to the various types of precipitation encountered during one winter season.
3) The system reliability could be regarded generally as good, except on one occasion where the battery malfunction occurred.

With the further effort, the system accuracy and reliability can be further improved, making the surrogate bridge freezing sensor very valuable innovation in surface condition prediction. The following section outlines some recommendations for future work.

5.3. Recommendations

1) *Insure system reliability:*

- Before installation perform deep cycle/capacity test explained in Chapter 4 for every battery to be used.
- Perform capacity test in-situ to check if there is a rapid decrease in battery capacity after load is applied. If so, replace the battery.

2) *Improve system accuracy:*
   - Use heater with lower capacity in order to improve controllability and prevent early evaporation on the heated side.
   - Install additional electrodes on the slab, placing them 0.5-1 inches above the slab's surface in order to detect fast snow accumulation when temperatures are above freezing point.
   - Adjust control units for the heater in order to be switched on and off in a 1°C temperature range.
3) *Test all systems continuously from late fall till early spring.*
4) *Design and test detection systems that are based on a different principles of operation in order to obtain the most accurate surface condition detection:*
   - Capacitive electrodes should be investigated to show whether different values for capacitance itself can predict distinct surface conditions.
   - The device based on a radiometer that measures spectral temperature should be tested. Spectral temperature is the product of actual temperature and surface emissivity. For the dry pavement surface emissivity is around 0.8, that of water 0.1, and that of ice around 0.4, thus different spectral temperatures should be obtained for different surface conditions.

REFERENCES

ASHRAE, (1997), Handbook-Fundamentals, ASHRAE, Atlanta.

ASHRAE, (1997), Psychrometrics-Theory and Practice, ASHRAE, Atlanta.

Besant, R.W., Rezkallah, K.S., Mao, Y., Falk, J. (1994), "Measurement of Frost Thickness Using a Laser Beam and Light Meter", ASHRAE Transactions, Vol. 78, Part 2, pp. 519-522.

Brinkman, C.P. (1977), "Highway Ice Detection", Transportation Engineering, Vol. 11, pp. 34-36.

Chiasson, A., Spitler, J.D. (2000), "A Modeling Approach to Design of a Ground-Source Heat Pump Bridge Deck Heating System", Accepted for Publication in Proceedings of the 5th International Symposium on Snow Removal and Ice Control Technology. Roanoke, VA. September 5-8, 2000.

Ciamberlini, C., Innocenti, G., Longobardi, G. (1995), "An Optoelectronic Prototype for the Detection of Road Surface Conditions", Rev. Sci. Instrum., Vol. 66, No. 3, pp. 2684-2689.

Ciemochowski, M.F. (1969), "A Detection System for Frost, Snow, and Ice on Bridges and Highways", Highway Research, Vol.8, pp. 17-24.

Electronics Plus, Inc. (2000), Resistors, Online. Available: http://www.Electronics-plus.com/.

Feely, R. (1994), "Enhancing Aircraft Flight Safety With Primary Ice Detection Sensors", Sensors, Vol. 11, No. 6, pp. 28-30.

Finkele, R. (1997), "Detection of Ice Layers on Road Surfaces Using a Polarimetric Millimeter Wave Sensor at 76GHz", Electronic Letters, Vol. 33, No. 13, pp. 1153-1154.

FLUKE, (1997), Hydra Series II User's Manual, FLUKE Corporation, Everett, WA

Holzwarth, F. and Eichhorn, U. (1993), "Non-Contact Sensors For Road Conditions", Sensors and Actuators, Vol. 37, pp. 121-127.

JFM Engineering (2000), Deep Cycle/Capacity Test, Online. Available: http://www.jfmeng.com/.

Kyocera, (1998) KC-Type Series Installation Manual, Kyocera Co., San Diego, CA.

Lasnier, F. and Ang, T.M. (1990), Photovoltaic Engineering Handbook, Adam Higler, Bristol and New York.

Longwill M., Schultz B., Thompson D. (1999), Snow Machine, Senior Design Project Report, Oklahoma State university, Department of Mechanical and Aerospace Engineering, Stillwater, Oklahoma

Mawhinney, R.C. and McCone A.I. (1974), "Snow and Ice Detection and Warning Systems", Report No. MB-R-74/105, Department of Transportation, Federal Highway Administration, Washington, D.C.

McQuiston, F.C. and Parker, J.D. (1994), Heating, Ventilating, and Air Conditioning Analysis and Design, John Wiley & Sons, Inc., New York.

Mills, A.F. (1995), Basic Heat and Mass Transfer, Chicago-Irwin, Chicago, IL.

Muchmore, T. (2000), Personal Communication. Tom Muchmore, an employee of Ponca City News, available via e-mail: tmuch@poncacitynews.com.

Perez, R.A. (1985), The Complete Battery Book, Tab Books Inc., Pennsylvania.

Pruzan, L.M. (1993), "Smart Skin technology Development for Measuring Ice Accretion, Stall and high AOA aircraft performance. Part 1, Capacitative Ice Detector Development", Final Technical Report, NASA, Springfield, VA.

Ringer, T.R. and Stallabrass, J.R. (1978), "The Dynamic Ice Detector For Helicopters", AGARD Conference Proceedings, Vol. 51, No. 236, pp. 8.1-8.8.

Spitler, J.D. (1999), Class Notes for MAE 5873, Department of Mechanical and Aerospace Engineering, Oklahoma State University.

Swinbank, W.C. (1963), "Long-Wave Radiation From Clear Skies", Quarterly Journal of Royal Meteorological Society, Vol. 89, pp. 339-348.

Walton, G. (1983), Thermal Analysis Research Program Reference Manual, Bureau of Standards, NBSIR 83-2655.

Zimmerman, O.T. and Lavine, I. (1945) Psychrometric Tables and Charts, Industrial Research Service, Dover, New Hampshire.

Zweibel, K. (1990), Harnessing Solar Power, Plenum Press, New York and London.

APPENDIX A

SPECIFICATIONS

A.1. Control Circuit Components

An on/off switching device is designed to control heater operation. Specifications of the circuit components are given as follows:

1) Resistors: 100K, 55K, 120 K, 330 K
2) Transistor MPS3904 (NPN Silicon)
   - h_{FE} (min)=100
   - V_{CBO}=60V
   - V_{CEO}=40V
   - V_{EBO}=6V
   - I_C=200Ma
   - F_T=300MHz
   - Dissipation=350mW
3) Relay-PC relay 12VDC coil, rated 5A at 240VAC/24VDC, type OMI-SS-212D.

- Expected life: 100,000 cycles at rated voltage and current
- Operating temperature range: -30-55°C at 60% relative humidity
- V_{nom}=12VDC
- V_{max}=15.6VDC
- I_{nom}=60mA
- Coil resistance: 200 ohms ± 10%
- Pickup/dropout voltage: 9.6/6.0VDC

4) Op-Amp, model LM741CN-ND, 8 pin IC requiring +12 and –12VDC

5) NTC thermistor, model C100F103G, resistance ratio 10KΩ ± 2% at 25°C

The complete circuit diagram for the control unit is given in Figure A-1, with all pin connections on the relay, op-amp, potentiometer and transistor side.

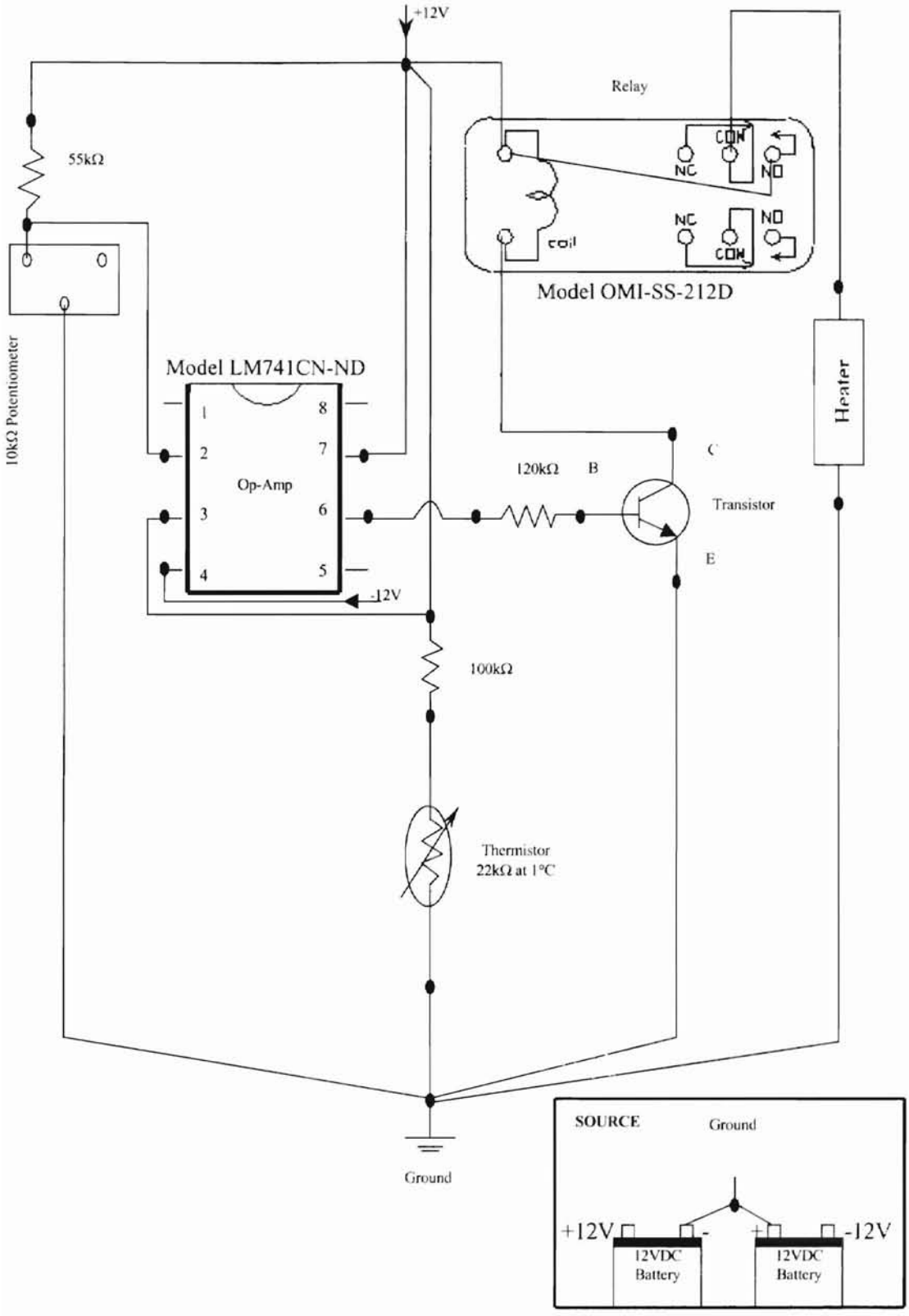

Figure A-1. Circuit Diagram

A.2. Temperature Controller Control Setup

An "Omega" CN1632 series digital temperature controller was used to operate heater of the system installed at Buffalo experimental Site. Control setup mode that ensures on/off operation should be set as follows:

1) Setpoint value- set it to be at the chosen reference temperature at which heater should be turned on or off
2) ON/OFF hysteresis value- 0.1% of input span
3) Alarm level-process low, ensures that heater is turned on when temperature drops below reference point
4) Alarm value-should equals the setpoint value

A.3. Control Circuit Modification

In order to derate existing heaters in order to provide 1W capacity instead of 5W, an additional resistor can be installed in circuit, on the positive side of power supply. The schematic of the circuit is given in Figure A-2, and corresponding calculations were done according to Perez (1985).

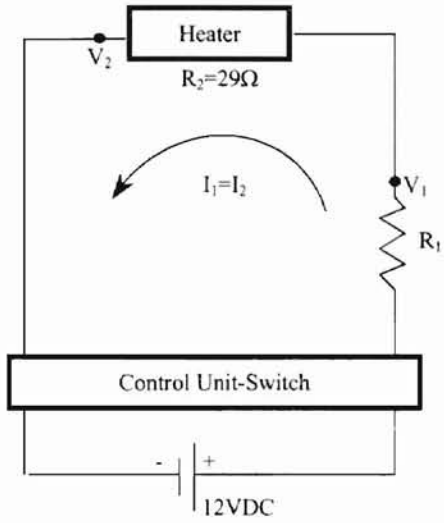

Figure A-2. Control Circuitry Modification

According to Ohm's Law:

$$P = \frac{(V_1^2 - V_2^2)}{R_2} = 1W \qquad \text{(A-1)}$$

From A-1, the necessary voltage for the heater to provide 1W is 5.36V. The voltage difference across the resistor R_1 is 6.64V. Current through the circuit is, for resistors in series:

$$I_2 = I_1 = \frac{V_2}{R_2} = 0.185A \qquad \text{(A-2)}$$

Thus, desired resistance is: $R_1 = V_1/I_1 = 35.89\Omega$ (A-3)

The resistor must be capable of dissipating:

$$P = \frac{(6.64)^2}{35.81} = 1.23\ \text{W} \qquad \text{(A-4)}$$

The resistor rated for 2W, 36Ω, and 2% tolerance available through "Electronics Plus, Inc." (2000) can be recommended for this application. The part number is 2W036.

APPENDIX B

COMPUTER PROGRAM

A relatively simple computer program was developed that for given values of electrical resistances over electrodes and temperatures can determine condition on the slab's surface. As mentioned before, program takes readings from data logger as well as data from Mesonet weather stations to determine surface condition for every scan. Input values consist of a following parameters:

- Electrical resistance and temperature on the heated side of the slab
- Electrical resistance and temperature on the unheated side of the slab
- Air temperature
- Relative humidity

The program was written in Visual Basic for Applications but can be easily translated to some other programming language such as Fortran. The computer codes are given in the following sections.

B.1 Program Source Code

```
Function Surf_condition(Res1, Res2, T1, T2, Tair_C, Relhum)

'*************************************************************************

'Main function that calls the functions that calculate dew point
'temperature and determine surface conditions

'PROGRAM INFORMATION:
'        AUTHOR                          Srdjan Jankovic
'        LANGUAGE                        VBA
'        DATE WRITTEN                    January, 2000
'        MODIFIED                        June, 2000

'PURPOSE:
'      To determine slab's surface condition for a readings obtained
'      from the data-logger

'*************************************************************************

'FUNCTIONS CALLED:
'                Dewpoint1
'                Determine1

'*************************************************************************

'INPUT VARIABLES
'               Res1[kOHMS]-Resistance on the unheated side
'                          of the sensor
'                Res2[kOHMS]-Resistance on the hetedside
'                          the sensor
'                Tair_C[C]-Outdoor air temperature
'                          (ambient temperature)
'                Relhum[/]-Relative humidity of the air
'                T1[C]-Temperature of the surface on the
'                      unheated side of the sensor
'                T2[C]-Temperature of the surface on the
'                      heated side of the sensor

'*************************************************************************

'INTERNAL VARIABLES
'                tdew_C[C]-Dew point temperature

'*************************************************************************

    tdew_c = Dewpoint1(Tair_C, Relhum)
    Surf_condition = Determine1(Res1, Res2, T1, T2, tdew_c)

End Function
Function Determine1(Res1, Res2, T1, T2, tdew_c)

'*************************************************************************

'Function that compares readings for electrical resistances 'and
temperatures for both heated and unheated side of the 'sensor and gives
back the corresponding surface condition

'*************************************************************************
```

```
'INPUT VARIABLES
'               Res1[kOHMS]-Resistance on the unheated side
'                          of the sensor
'               Res2[kOHMS]-Resistance on the heated side of
'                          the sensor
'               T1[C]-Temperature of the surface on the
'                     unheated side of the sensor
'               T2[C]-Temperature of the surface on the
'                     heated side of the sensor

'*************************************************************************

'INTERNAL VARIABLES
'               tdew_C[C]-Dew point temperature

'*************************************************************************

'REFERENCES
'          Implemented procedure is based on the algorithm
'          developed and explained in
'          Chapter 4 of this thesis

'*************************************************************************

'Take the values and compare to determine surface condition

 If Res1 > 20000 And Res2 > 20000 Then
       x = "Dry"
    ElseIf Res1 < 100 And Res2 < 100 And T1 => 1.5 And T2 => 1.5 Then
       x = "Wet"
    ElseIf Res1 > 100 And Res2 < 100 And T1 < 1.5 And T1 => -0.5 And T2
         > 0 Then
       x = "Water-Ice"
    ElseIf Res1 > 1000 And Res1 < 20000 And Res2 < 100 And T1 <= 0.85
         And T2 > 0 Then
       x = "Ice"
    ElseIf Res1 > 100 And Res2 > 100 And T1 => 1.5 And T2 => 1.5 Then
       x = "Damp"
    ElseIf Res1 < 100 And Res2 > 100 And T1 > 0 And T2 > 0 Then
       x = "Damp"
    ElseIf Res1 < 100 And Res2 < 100 And T1 < 1.5 And T1 => 0.5 And T2 >
         0 Then
       x = "Snow possible"
    ElseIf Res1 > 20000 And Res2 < 20000 And T1 <= 0.85 And T2 > 0 Then
       x = "Dry snow"
    ElseIf Res1 > 100 And Res1 < 1000 And Res2 < 100 And T1 <= 1 And T2
         > 0 Then
       x = "Wet snow"
    ElseIf Res1 > 20000 And Res2 > 20000 And T1 <= 0.85 And T1 < tdew_c
         And T2 > 0     Then
       x = "Frost"
    Else: x = "Indeterminable"
   End If

    Determine1 = x


End Function

Function Dewpoint1(Tair_C, Relhum)

'*************************************************************************

'PURPOSE:
```

```
'        To calculate dew point temperature taking  the
'        temperature and relative humidity of the air

'*************************************************************************

'INPUT VARIABLES
'               Tair_c[C]-Outdoor air temperature
'                        (ambient temperature)
'               Relhum[/]-Relative humidity of the air

'*************************************************************************

'INTERNAL VARIABLES
'               Tair_K[K]-Outdoor air temperature
'                        (ambient temperature)
'               P_water_sat[Pa]-Water vapor saturation
'                         pressure over ice or liquid water
'               P_water_vap[Pa]-Water vapor pressure
'               alpha, beta-Dimensionless coefficients
'               tdew_C[C]-Dewpoint temperature of the air
'               tdew_K[K]-Dewpoint temperature of the air

'*************************************************************************

'REFERENCES
'               Calculations based on the procedure given in
'               ASHRAE, (1997), Psychrometrics-Theory and
'               Practice,pages 56 and 59

'*************************************************************************

'Calculate the absolute temperature of the air

Tair_K = 273.15 + Tair_C

'Use coefficients for the temperature in the different range

 If Tair_K < 273.15 Then
       a = -0.7297593707 * 10 ^ -5
       B = 0.5397420727 * 10 ^ -2
       C = 0.206988062 * 10 ^ 2
       D = -0.6042275128 * 10 ^ 4
    Else
       a = 0.1255001965 * 10 ^ -4
       B = -0.1923595289 * 10 ^ -1
       C = 0.2705101899 * 10 ^ 2
       D = -0.6344011577 * 10 ^ 4
    End If

'Calculate  dimensionless  coefficient  alpha,  water  vapor  'saturation
pressure
'and water wapor pressure

   alpha = a * Tair_K ^ 2 + B * Tair_K + C + D * Tair_K ^ -1
    P_water_sat = 1000 ^ alpha
    P_water_vap = Relhum * P_water_sat

'Use coefficients for the water vapor pressure in the 'different range

    If P_water_vap < 611 Then
       E = 0.1004926534 * 10 ^ -2
       F = 0.1392917633 * 10 ^ -2
       G = 0.2815151574
       H = 0.7311621119 * 10 ^ 1
```

```
        K = 0.2125893734 * 10 ^ 3
    ElseIf P_water_vap >= 611 And P_water_vap < 12350 Then
        E = 0.5031002503 * 10 ^ -2
        F = -0.882677938 * 10 ^ -1
        G = 0.1243688446 * 10 ^ 1
        H = 0.3388534296 * 10 ^ 1
        K = 0.2150077993 * 10 ^ 3
    ElseIf P_water_vap >= 12350 And P_water_vap < 101420 Then
        E = 0.1209512517 * 10 ^ -4
        F = -0.3545542105 * 10 ^ 0
        G = 0.2125893734 * 10 ^ 3
        H = -0.205030105 * 10 ^ 2
        K = 0.2718585432 * 10 ^ 3
    ElseIf P_water_vap >= 101420 And P_water_vap < 476207 Then
        E = 0.2467291016 * 10 ^ -1
        F = -0.9367112883 * 10 ^ 0
        G = 0.1514142334 * 10 ^ 2
        H = -0.9882417501 * 10 ^ 2
        K = 0.4995092948 * 10 ^ 3
    Else
        E = 0.2748 * 10 ^ -1
        F = -0.1068661307 * 10 ^ 1
        G = 0.1742964962 * 10 ^ 2
        H = -0.1161208532 * 10 ^ 3
        K = 0.547261812 * 10 ^ 3
    End If

'Calculate dimensionless coefficient alpha, dew point 'temperature in
degrees Kelvin and degrees Celsius

    beta = Log(P_water_vap)
    Tdew_K = E * beta ^ 4 + F * beta ^ 3 + G * beta ^ 2 + H * beta + K
    tdew_c = Tdew_K - 273.15

    Dewpoint1 = tdew_c

End Function
```

VITA

Srdjan Jankovic

Candidate for the Degree of

Master of Science

Thesis: SURROGATE BRIDGE FREEZING SENSORS

Major field: Mechanical Engineering

Bibliographical:

Education: Graduated from University of Belgrade, Belgrade, Yugoslavia in December 1996 with the Bachelor of Science degree. Completed the requirements for Master of Science degree with major in Mechanical Engineering from Oklahoma State University, Stillwater, Oklahoma in December 2000.

Experience: Employed as Teaching Assistant and research Assistant at Oklahoma state University from August 1998 to present.

Professional Membership: American Society of Heating, Refrigeration and Air-Conditioning Engineers, Inc. (ASHRAE).